Executive Summary

In December 2009, the U.S.EPA issued the new national discharge and monitoring standards for stormwater runoff from construction sites, known as the C&G Rule. The new C&G rules established a numeric Effluent Limitation Guideline (ELG) which required all construction sites disturbing 20 or more acres of land must sample to stormwater discharge, and the daily average turbidity must not exceed 280 NTU. The numeric limitation was subsequently vacated in the final rule in 2014 as a part of a settlement of industry lawsuit. Currently, the Wisconsin Department of Transportation (WisDOT) does not document any actual turbidity level of stormwater runoff from construction project sites. Therefore there is a need to determine the limits of this measure and other measurable water quality parameters from WisDOT construction sites.

This research designed and conducted field sampling experiments to measure and monitor the turbidity of stormwater runoff from WisDOT construction sites. Five ongoing WisDOT projects were identified for this study. Field grab samples were collected from four of the five sites at various locations where water was drained from disturbed soil, and at the major outfall locations. Measured parameters include: the turbidity level in NTU, the mass concentration of total suspended solids, pH value and the conductivity.

Measured turbidity in grab samples during or after storms ranged from 20 to 2,300 NTU, representing a typical range of turbidity reading of construction sites effluent with conventional Best Management Practice (BMP) implementations. Sampling results also showed that conventional BMP controls are not able to significantly reduce the turbidity, although they are effective to reduce soil erosion, runoff volume and speed, thus reducing the total sediment load into receiving waters. No correlations exist among the pH value, conductivity and turbidity in grab samples.

An automated turbidity sampling device was developed and deployed at outfalls of four selected sites to monitor the time series of turbidity. Thirty rainfall-turbidity runoff events were recorded by these automated sampling devices. Unit runoff turbidity functions, which represent response functions of turbidity with respect to a unit precipitation depth, were reconstructed with the observed time series at each site following a least-square fit approach. All reconstructed response functions showed a rapid increase of turbidity to its peak followed by a gradual decrease to the background level. A secondary turbidity peak was also observed, which might be attributed to the subsurface interflow, while the first peak is due to the surface runoff. The second peak can also be observed from other field monitoring studies and the laboratory modeled runoff time series.

Both the peak turbidity and the daily maximum were found to be linearly correlated with the total precipitation depth for all sampling sites, while they are not

correlated with either the average or the peak rainfall intensity. Although a power law can also explain their correlations, it is not statistically better than the linear correlation, and the exponent varied between 0.6 and 1.6. Turbidity averaged over the entire runoff period, however, did not seem to be correlated with any precipitation statistics.

Reconstruction of the turbidity response function and the observed statistical correlations suggest that it is possible to develop models to predict the daily maximum turbidity and the total turbidity load of effluent from construction site for designed storm events. Models of this kind are valuable for future BMP managements of WisDOT construction projects as well as for U.S. EPA to evaluate new regulation policies.

DISCLAIMER

This research was funded through the Wisconsin Highway Research Program by the Wisconsin Department of Transportation and the Federal Highway Administration under Project 0092-13-03. The contents of this report reflect the views of the authors, who are responsible for the facts and accuracy of the data presented herein. The contents do not necessarily reflect the official views of the Wisconsin Department of Transportation or the Federal Highway Administration at the time of publication.

This document is disseminated under the sponsorship of the Department of Transportation in the interest of information exchange. The United States Government assumes no liability for its contents or use thereof. This report does not constitute a standard, specification or regulation.

The United States Government does not endorse products or manufacturers. Trade and manufacturers' names appear in this report only because they are considered essential to the object of the document.

Technical Report Documentation Page

1. **Report No.** WHRP	2. **Government Accession No**	3. **Recipient's Catalog No**
4. **Title and Subtitle** Understanding and Complying with New Storm Water Mitigation Requirements from the EPA		5. **Report Date** November 2015
		6. **Performing Organization Code** Wisconsin Highway Research Program
7. **Authors** Qian Liao, Hani H. Titi, Jin Li, Jonathan Steinbach, Chunqi Shen, Jyotsna Shrestha, and Jin Tong		8. **Performing Organization Report:** No.
9. **Performing Organization Name and Address** Department of Civil and Environmental Engineering University of Wisconsin-Milwaukee 3200 N. Cramer St. Milwaukee, WI 53211		10. **Work Unit No. (TRAIS)**
		11. **Contract or Grant No.** WHRP 0092-13-03
12. **Sponsoring Agency Name and Address** Wisconsin Highway Research Program Wisconsin Department of Transportation WisDOT Research & Library Unit 4805 Sheboygan Avenue, Room 104 P.O. Box 7915 Madison, WI 53707		13. **Type of Report and Period Covered** Final Report, 10/2012 – 12/2015
		14. **Sponsoring Agency Code**
15. **Supplementary Notes**		

16. **Abstract**

The objective of this research is to examine the range of turbidity levels in stormwater runoff from WisDOT construction sites. Knowing the limits of this measure and other measurable water quality parameters can help WisDOT to better understand and comply with the EPA's new C&D rules.

Field and laboratory experiments were conducted to acquire grab samples from 5 selected WisDOT construction sites. Measured turbidity in grab samples varied from 20 to 2,300 NTU, representing a typical range of turbidity of construction sites effluent with conventional BMP implementations. Field experiments demonstrated that conventional BMP controls are generally not effective at reducing the turbidity. However, BMP measures can help to reduce soil erosion, runoff volume and speed, thus reducing the total sediment load into receiving waters. No correlations exist among the pH value, conductivity and turbidity measured in this study.

Automatic turbidity sampling devices were developed and deployed at 4 construction sites. Recorded time series of effluent turbidity were used to reconstruct a unit rainfall-turbidity response function. Statistical analysis indicated that both the peak and the daily maximum turbidity are linearly correlated with the total precipitation depth for all 4 sampling sites.

17. **Key Words** Turbidity, EPA C&G rules, Construction projects, Total suspended solids, BMP, turbidity-precipitation relation	18. **Distribution Statement** No restriction. This document is available to the public through the National Technical Information Service 5285 Port Royal Road Springfield VA 22161		
19. **Security Classif.(of this report)** Unclassified	19. **Security Classif. (of this page)** Unclassified	20. **No. of Pages** 127	21. **Price**

Form DOT F 1700.7 (8-72)   Reproduction of completed page authorized

Acknowledgements

Table of Contents

List of Figures

List of Tables

Chapter 1
Introduction

1.1   Background

As a result of the National Environmental Policy Act of 1969 and the Clean Water Act of 1972, numerous state and federal regulations governing land disturbing activities were developed. At the National level, stormwater discharge associated with construction activities has been regulated through the Environmental Protection Agency's (EPA) National Pollutant Discharge Elimination System (NPDES). The NPDES regulations provide two options for obtaining authorization to discharge or ''permit coverage'': General permits and individual permits. Since 1992, EPA has issued a series of ''national'' Construction General Permits (CGP) that cover areas where EPA is the NPDES permitting authority. For the most part, other state-issued permits for stormwater discharge associated with construction activities have followed EPA's CGP format and contents, although some components of the permit have been changed to address specific conditions. The key components of EPA's CGP have been non-numeric effluent limitations and "Best Management Practices" (BMPs) that require the permittee to minimize discharge of pollutant in stormwater using appropriate erosion and sediment controls. Furthermore, the 2008 EPA CGP requires dischargers to develop and implement a stormwater pollution prevention plan (SWPPP) to document the steps they will take to comply with the terms, conditions, and effluent limitations of the permit.

For years EPA has considered that a numeric limitation for sediment discharges from construction sites not feasible until recently that more data and information became available indicating the numeric limit is technically available and appropriate for some sites. On December 1, 2009, EPA published the final Effluent Limitations Guidelines (ELGs) and New Source Performance Standards (NSPS) to control the discharge of pollutants from construction sites. The new guidelines consist of a series of non-numeric limitations, as well as a numeric limitation for the pollutant turbidity. In summary:

- After the effective date of February 1, 2010, all permits issued by EPA or states must incorporate the final rule requirements.

- All construction sites required to obtain permit coverage must implement a range of erosion and sediment controls and pollution prevention measures.

- Beginning on August 1, 2011 all sites that disturb 20 or more acres of land at one time are required to comply with the turbidity limitation.

- Beginning on February 2, 2014 the limitation applies to all construction sites disturbing

10 or more acres of land at one time.

- These sites must sample stormwater discharges and comply with a numeric limitation for turbidity. The limitation is 280 NTU (nephelometric turbidity units)

Since the publication of the final ELGs, EPA has subsequently withdrawn the limit to correct a calculation error. Effective on January 4, 2011, EPA has kept the numeric limitation of 280 NTU but requests additional data from construction and development sites. EPA plans to use data and information submitted by public to propose a revised limit in a future rulemaking.

The EPA has estimated that the benefit from improved water quality may reach a total of $369 million, the new requirement comes with a hefty price tag. Compliance with the new requirements will impact more than 82,000 construction firms, 96 percent of which are small businesses. Cost to the construction industry will be about $1 billion per year, according to EPA's estimation. Possible negative consequences may include job lossesand firm closures, as well as difficulties in obtaining new-home financing approvals due to the increasing construction cost associated with the compliance.

EPA's 2009 Rule came under immediate attack, including a lawsuit brought by industry groups and a petition for administrative review by the Small Business Administration (SBA) Office of Advocacy. The new rule, published in the Federal Register on March 6, 2014 (New Rule), which is part of a settlement of the industry lawsuit, removes the numeric turbidity limits and changes several non-numeric provisions of the 2009 Rule. However, EPA iterated that it reserves the right to consider additional effluent limits and monitoring requirement in future regulation rules.

1.2   Problem Statement

, The EPA delegated to the Wisconsin Department of Natural Resources (WDNR) the responsibility to administer the requirements of the NPDES for the state of Wisconsin. Under WDNR's authority, these regulations are known as the Wisconsin Pollutant Discharge Elimination System (WPDES) requirements and are authorized under Chapter 283 of the State Statues. The WPDES requirements are designed to regulate, through a permitting process, the quality of storm water being discharged. WPDES storm water discharge permits are issued by the WDNR under Wisconsin Administrative Code Chapter NR 216. Although the Wisconsin Department of Transportation (WisDOT) is exempt from regulatory requirements, WisDOT and WDNR have a Cooperative Agreement that addresses construction site erosion control on WisDOT construction projects. The Cooperative Agreement, along with Section Trans 401 of the Wisconsin Administrative Code, meets the substantive WPDES requirements for WisDOT construction sites. Trans 401 establishes and implements erosion control and storm water management standards for projects administered by WisDOT. Trans 401 also establishes

minimum performance standards, which all projects administered by WisDOT need to meet. WisDOT, acting jointly with the WDNR, developed the *Wisconsin Erosion Control Product Acceptability List* (http://www.dot.state.wi.us/business/engrserv/pal.htm) and Section 10, *Erosion Control and Stormwater Quality*, of the *Facilities Development Manual* (http://roadwaystandards.dot.wi.gov/standards/fdm/10-00toc.pdf) to meet the performance standards of Trans 401 and NR 216.

Major components of the Erosion Control Plan (ECP) documented in Trans 401 are non-numeric BMPs to reduce the amount of sediment erosion and transport from construction projects. Currently, WisDOT does not document any turbidity level of stormwater runoff from construction project sites. Therefore there is a need to determine the limits of this measure and other measurable water quality parameters from WisDOT construction sites. Although the final ELGs have removed the numeric limitations of the runoff turbidity, it may subject to future reconsiderations. Collecting and documenting these data is still important for WisDOT to better understand EPA ELGs and potential impacts on future construction practices.

1.3   Research Objectives

The overall objective of the research was to design and conduct field sampling experiments to monitor the concentration of sediment, turbidity and other associated pollutant in stormwater runoff at selected WisDOT constructions sites representing different stormwater runoff characteristics. The research also evaluated the effectiveness of various BMPs that control erosion and sediment discharge based on quantitative measures, i.e., the turbidity level. Data collected and analyzed could be applied to establish appropriate stormwater runoff monitoring protocols for WisDOT construction projects that can comply with the recently established Effluent Limitation Guidelines by EPA. Specifically, the conducted study addressed the following objectives.

- We reviewed the technical details of the EPA ELGs, designed sample collection and measurement procedures.

- We identified active WisDOT construction sites with significant earth disturbance for monitoring and testing.

- For each construction site, sampling frequencies based on the magnitude (return period) and duration of precipitation events were determined. Field grab samples were collected and measured *in situ*. Sampling locations were selected where water enters the construction site, at pre-treatment, at post-treatment and leaving the construction site (discharging points).

- Automatic turbidity sampling devices were developed and deployed at the outfall locations of selected sampling sites to monitor the change of turbidity level of the receiving water bodies, including streams and rivers or stormwater drainage systems.

- Collected turbidity data was analyzed and statistical analyses were conducted to investigate the relation with the characteristic parameters of precipitation events.

1.4　Organization of the Report

This report is organized in seven chapters. Chapter One introduces the problem statement and objective of the research. The background information and literature review is presented in Chapter Two, and the research methodology is discussed in Chapter Three. Chapter Four presents the information of five selected sampling WisDOT construction sites, and field grab sampling results during storm events. The relation between the suspended solids concentration and the turbidity is analyzed with samples collected in the field and lab simulated runoff samples, the result and discussion are described in Chapter Five. Statistical analysis on the relation between runoff turbidity and precipitation is detailed in Chapter Six. The conclusions are provided in Chapter Seven.

Chapter 2
Background and Literature Review

This chapter presents background information of construction site stormwater runoff problems, particularly the impact of sediment in the effluent on the natural environment. A brief history of the recent EPA Construction and Development (C&D) rule is also given, particularly of the establishment of a numerical limitation on turbidity and how it was abandoned from the final rules. The definition of turbidity, measurement methods and its relation with total suspended sediment are discussed. Typical BMPs applied in WisDOT projects are also reviewed and the effects on turbidity reduction are discussed. This chapter ends with a short introduction on recent research projects and findings that are closely related to this study.

2.1 Environmental Impact of Sediment Discharge from Construction Activities

Construction activities include cleaning, grading and excavating soil in which vegetation and other natural soil stabilizing materials are removed. Disturbed soil is then exposed to wind, rainfall and other erosive forces. If the stormwater discharge from a construction site is not controlled properly, large amounts of sediment, turbidity, nutrients and pollutants can be entrained and introduced to receiving surface waters. In United States, sediment (both suspended and deposited) and turbidity are the most commonly documented pollutants in construction site discharges. Dramatic increases in sediment loadings downstream of construction sites have been documented by dozens of studies over the past four decades. As an early study, Wolman and Schick (1967) found that the concentration of suspended sediment in streams that receive discharge from construction sites in Baltimore, MD were between 2 and 200 times greater than those in streams in rural or wooded areas. Another early study by Vice et al. (1969) found that highway construction areas constituting from 1 to 10 percent of a watershed contributed 85 percent of that watershed's total sediment yield. Reed (1980) monitored a highway construction site in central Pennsylvania before, during, and after construction activity. He finds that sediment discharge increased two- to four-fold during the active construction period over pre-construction levels, even in the presence of sediment abatement practices. A comprehensive list of studies that documented the impact of construction projects (a large portion of case studies are highway construction) on the sediment levels in surface waters can be found in the EPA document titled "*Environmental Impact and Benefits Assessment for Proposed Effluent Guidelines and Standards for the Construction and Development Category*" published in 2008.
(http://water.epa.gov/scitech/wastetech/guide/construction/upload/2008_11_25_guide_construction_proposed_proposed-env-20081120.pdf)

Stormwater discharge with entrained sediment from construction sites can cause an array of physical, chemical and biological impacts to surface waters. Pollutant loadings to the receiving water body can be significantly increased. The three major water quality parameters that impair the aquatic environment are: total suspended solids (TSS), turbidity and total dissolved solids (TDS). Studies show that high levels of sediment and turbidity can have profound impacts on the aquatic ecosystem, impairing photosynthetic activity, reducing available food, smothering fish eggs, and burying or severing benthic communities, thereby forcing fish and other organisms to relocate or risk death. Increased sediment deposition and high level of suspended turbidity also adversely affect the direct human use and management of water resources, e.g., navigation channels and reservoirs; municipal, industrial and agricultural water supplies; flood control; and recreational uses.

In addition to sediment and turbidity, other pollutants can be entrained due to runoff from construction sites, including heavy metals, oils, organic compounds and nutrients. Construction activities involve the use of many materials and equipment have the potential to produce a variety of toxic pollutants, such as: wood treated with creosote and chromated copper arsenate, paint, adhesives, solvents, vehicle oils, fuel, and grease. Asphalt and concrete pavement and building materials contain chemicals that can alter water pH or have toxic effects in aquatic environments. Concrete wastes have an elevated pH due to the lime they contain. Asphalt and tar used in road construction and repair contain a variety of organic compounds, including polycyclic aromatic hydrocarbons (PAHs) (Ohio EPA 1998a, 1998b, 1999). Many of these pollutants, including PAHs, can leach into the soil on construction sites due to rainfall, subsequently become attached to sediment particles and discharge with sediment during runoff. Eventually they settle together with sediment on the beds of the receiving water body. They may then be ingested by benthic dwelling organisms, facilitating PAH transfer up the food chain (USEPA 2004). Higher levels of nutrient (nitrogen and phosphorus) loading were also found to correlate with sediment runoff from construction sites (Daniel et al., 1979; Harbor et al., 1995), which increases the potential for algae growth. Materials for landscaping such as fertilizer, mulch, lime, and pesticides can also wash from construction sites, contributing to elevated level of nutrients, oxygen-demanding material and toxic pollutants. Recent studies show that bacteria (such as *E. Coli*) have also been found in stormwater runoff from construction sites, which are usually attached to and transported with small soil particles (silt or clay) (Sawyer, 2009; Trempel, 2011).

Sediment loadings in construction sites runoff are highly dependent on the type of soil, characteristics of rainfall events, presence and effectiveness of sediment abatement practices, along with many other factors. Episodic precipitation events are the primary cause of construction site sediment discharge, and dewatering and irrigation are other possible causes. Most sediment discharge takes place during or shortly after precipitation events. Once a precipitation event ceases, discharges from construction sites generally cease within a relatively short time period. Environmental impacts due to high levels of sediment loading are usually

temporary, and conditions eventually return to preconstruction levels. Pollutants other than sediments and turbidity have not been widely documented. Due to the fact that many of the pollutants described above adsorb and travel with sediment discharge, TSS and turbidity could be used as indicators for other possible toxic pollutants form construction activities. It should be noted that there has been relatively less evidence that normal construction activities contribute significant increase of toxic materials in receiving water bodies. However, many pollutants such as PAHs are persistent chemicals that can remain in the aquatic environment for a very long period of time. Little is known about the chronic toxicity that might result from bioaccumulation of metals or other toxic materials resulting from construction runoff.

2.2   A Brief History of the EPA's new C&D Rules

In December 2009, US EPA has issued the new national discharge and monitoring standards for stormwater runoff from construction site, known as the Construction and Development (C&D) Rule, which is detailed in the Federal Register 40 CFR Part 450 (US EPA, 2009) titled "Effluent Limitations Guidelines and Standards for the Construction and Development Point Source Category; Final Rule". The new C&D rules specified that owners and operators of permitted construction activities must

- Implement erosion and sediment controls
- Stabilize soils
- Manage dewatering activities
- Implement pollution prevention measures
- Prohibit certain discharges
- Utilize surface outlets for discharges from basins and impoundments

The new C&D rule also established a numeric Effluent Limitation Guidelines in addition to various non-numeric limitations. Specifically, all construction sites disturbing 20 or more acres of land at one time must sample to stormwater discharge, and the daily averaged turbidity must not exceed 280 NTU, with the following details:

- Turbidity limit does not apply to stormwater discharges from precipitation events that exceed the magnitude of the local two-year, 24-hour storm.
- On construction sites where the numeric limit applies, the rule requires contractors to collect numerous stormwater runoff samples from all discharge points during every rain event and measure the NTU levels.
- If the average NTU level of the sample taken over the course of a day exceeds the "daily maximum limit" of 280 NTU on any given day, then the site is in violation of the federal limitation requirement.

Following promulgation of the C&D rule, the Wisconsin Builders Association, the National Association of Home Builders (NAHB) and the Utility Water Act Group (UWAG) filed petitions for review in the U.S. Circuit Courts of Appeals for the Fifth, Seventh, and D.C. Circuits. The petitions were consolidated in the Seventh Circuit on July 8, 2010. The brief history of the petitions and the final settlement are summarized below

- In April 2010, the Small Business Administration (SBA) filed with EPA a petition for administrative reconsideration of several technical aspects of the C&D rule. The SBA identified potential errors with the dataset and in the calculation that EPA used to support its decision to adopt the 280 NTU numeric turbidity limit. In June 2010, the NAHB also filed a petition for administrative reconsideration with EPA incorporating by reference SBA's argument regarding the potential deficiencies in the data.
- On August 12, 2010, EPA filed an unopposed motion with the Court seeking to hold the litigation in abeyance until February 15, 2012, and asked the Court to remand the record to EPA and vacate the numeric limitation portion of the rule. In addition, EPA agreed to reconsider the numeric limitation and to solicit site-specific information regarding the applicability of the numeric effluent limitation to cold weather sites and to small sites that are part of a larger project.
- On August 24, 2010, the Court issued an order remanding the matter to the Agency but without vacating the numeric limitation. Subsequently on September 9, 2010, the petitioners filed an unopposed motion for clarification or reconsideration of the Court's August 24, 2010 order, asking the Court again to vacate the numeric limitation. On September 20, 2010, the Court remanded the administrative record to EPA and ordered the case to be held in abeyance until February 15, 2012, but did not vacate the numeric limitation. During this period, EPA provided additional information in the docket to supplement the administrative record for the C&D rule and an updated response to comment on the document.
- In November 2010, EPA issued a direct final regulation and a companion proposed regulation to stay the numeric limitation at 40 CFR 450.22 indefinitely. The proposed rule solicited comment due no later than December 6, 2010. On January 4, 2011, the EPA acknowledged the error in calculating the 280 NTU effluent limits. As of this date, neither states nor EPA were required to incorporate the numeric turbidity limitation and monitoring requirements found in § 450.22(a) and § 450.22(b) into NPDES permits because the numeric limitation was stayed. However, the remainder of the C&D rule was still in effect and had to be incorporated into newly issued NPDES permits.
- After issuing the stay of the numeric turbidity limitation, EPA continued to consult with stakeholders regarding next steps with respect to numeric discharge standards. EPA published a Federal Register notice (77 FR 112, January 3, 2012) seeking data on the

effectiveness of technologies in controlling turbidity in discharges from construction sites and information on other related issues.

- EPA also continued to meet with the petitioners in an effort to settle the litigation over the C&D rule. On December 10, 2012, EPA entered into a settlement agreement with petitioners to resolve the litigation in Wisconsin Builders Association, et al. v. EPA, Case Nos. 09-4113, 10-1247, and 10-1876 (7th Cir.). The settlement agreement provides for EPA to propose for public comment certain changes specific to the non-numeric portions of the C&D rule, as well as withdrawal of the numeric limitation, and take final action on the proposal. Under the terms of the settlement agreement, by April 15, 2013 EPA was to sign for publication in the Federal Register a notice of proposed rulemaking, with at least a 30-day comment period, to amend the C&D rule in a manner substantially similar to Exhibit A which is attached to the settlement agreement. The settlement then stipulates that by February 28, 2014, EPA will take final action on the proposed rule. Under the settlement, if EPA takes the above actions by the specified dates, and EPA's final action on the proposed rule amends the C rule in any manner, then Petitioners and EPA will promptly file a joint request with the Court asking it to dismiss the C litigation. In addition, if EPA's final action amends the C rule in a manner substantially similar to Exhibit A, Petitioners will not seek judicial review of those amendments. Finally, the settlement provides that within 60 days after EPA signs the proposal mentioned above, NAHB and EPA will file a joint request with the Court to dismiss NAHB's challenge to the 2012 Construction General Permit (CGP), which EPA issued on February 29, 2012.
- EPA proposed a rule on April 1, 2013, which vacated the numeric standard and added provisions to improve the flexibility of the best management practices. For the flexibility of a BMP control, EPA has added a definition for "infeasible" which has two part focus: (1) whether a control is "technologically possible"; or (2) whether it is "economically practicable and achievable in light of best industry practices". Today's final rule satisfies EPA's commitments under the settlement agreement.

However, EPA also stated that it reserves the right to propose additional effluent limits and monitoring requirements, although it is removing the language establishing numeric turbidity limits and requiring turbidity monitoring that was part of the 2009 rule. EPA also reiterated that it was continuing to collect data on turbidity in stormwater.

2.3 Understanding Turbidity and its Measurement Methods

Turbidity, as explained by EPA, is a measure of water clarity, i.e., how much the material suspended in water decreases the passage of light through the water (EPA, 2012). Suspended materials mainly include soil particles, algae, microbes and other substances. Turbidity is an important parameter in assessing the environmental health of water bodies. For example, high turbidity will reduce the amount of light penetrating the water body, which will affect the

photosynthesis and the production of dissolved oxygen to a large extent. Turbidity can be also very useful as an indicator of the effects of the runoff from construction, agricultural practices, industrial discharges and other resources.

2.3.1   Turbidity Measurement and Turbidimiters

Since turbidity is an optical property of water which carries suspended solids, it is measured by the scattering light by these fine particles. Today, there are several methods available to measure turbidity and different units have been defined to standardize turbidity levels and allow comparison based on these measurement methods. Several units for turbidity exist depending on the method of measurements. Since Formazin (a polymer produced when hydrazine sulfate and hexamethylenetetramine as reacted) solution is widely used for the calibration of turbidity measurement, the most widely measured unit is the Formazin Turbibity Unit (FTU), while ISO refers it to as the Formazin Nephelometric Units (FNU). If attenuation of light as it travels through the column of the water sample is used to determine turbidity, for example in the Jackson Candle method, then the Jackson Turbidity Unit (JTU) can be used. More recently, measuring light scattering from the side of the light beam(s) is considered as a more meaningful measure of turbidity. The device that measures this scattering is usually called a Nephelometer, and the units of a calibrated nephelometer are called the Nephelometric Turbidity Units (NTU). As of today, this is no standard method to convert between various turbidity units (e.g. NTU vs. FNU) (Campbell Scientific, Inc. 2014).

For the evaluation of water quality, eight turbidity standards have been approved by the U.S. EPA for monitoring drinking water. They are: USEPA Method 180.1, Standard Method 2130B, Great Lakes Instrument Method 2 (GLI 2), Hach Method 10133, Mitchell Method M5271 and M5331, Orion AQ4500 and AMI Turbiwell (EPA, 2012, 2009). Besides the first three methods approved by the EPA, the United States Geological Survey (USGS) uses the International Organization for Standardization (ISO) 7027 to measure turbidity since it appears to be more accurate at high turbidity levels. However, EPA-approved methods must be followed when the methods are applied to measure drinking water. The comparison among these measurement methods is summarized in table 2.1.

Table 2.1: Comparison of different turbidity measurement methods

Methods	EPA Approval	Light Source	Degree of scattered light
EPA Method180.1	YES	broadband Tungsten lamp	90
ISO 7027	NO	830-890nm LED or	90
GLI 2	YES	860 nm LEDs	90
HACH Method 10133	YES	630-690nm laser light	90
Standard Method 2013B	YES	broadband Tungsten lamp	90
Mitchell Method M5271	YES	620-680nm laser light	90
Mitchell Method M5331	YES	510-540 nm LEDs	90
Orion Method AQ4500	YES	Broadband LED	90
AMI Turbiwell	YES	Broadband LED	90

Continue- Table 2.1

Methods	Multiple	Non-contact	Range (NTU)	UNIT
EPA Method 180.1	NO	NO	0-40	NTU
ISO 7027	NO	NO	0-1000(0-4000 if	FNU(FNRU if
GLI 2	YES	NO	0-100	FNMU
HACH Method 10133	NO	NO	0-5	mNTU
Standard Method	NO	NO	0-1000	NTU
Mitchell Method	NO	NO	0-40	NTU
Mitchell Method	NO	NO	0-40	NTU
Orion Method AQ4500	NO	NO	0.06-40	NTU
AMI Turbiwell	NO	YES	0-40	NTU

Of all the methods listed above, none are completely comprehensive. Each method has advantages and limitations. Generally, the EPA method 180.1 and the ISO 7027 are the most well-known guidelines and are internationally recognized for verifying turbidity meter and turbidity sensor performance and method compliance (Battelle, 1999). The two methods are summarized as the following:

EPA Method 180.1:

Method 180.1 is based upon a comparison of the intensity of light scattered by the sample under defined conditions with the intensity of light scattered by a standard reference suspension (usually Formazin); the appropriate unit of measurement is the Nephelometric Turbidity Unit (NTU), since this method uses nephelometric technology which measures light scatter at 90-degree angle from the initial light path (Figure 2.1).
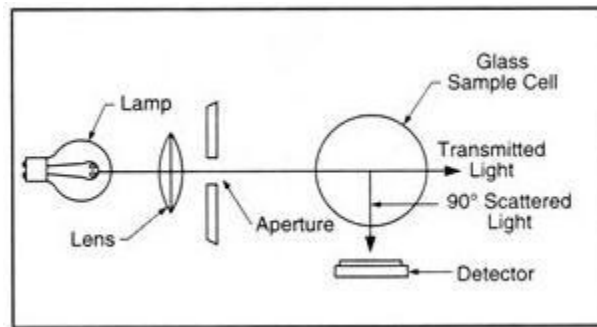
Figure 2.1: Nephelometry measures scattered light

This method also specifies that the detector must be centered at that angle and cannot extend more than 30 degrees from the center point. In addition, the maximum light travel distance from the source to the detector is specified as 10 cm to minimize differences in light scatter measurements (O'Dell, J.W. 1993). The tungsten lamp with a color temperature between 2000 K and 3000 K is chosen to be the light source. Instruments in compliance with this method are accurate in measuring the turbidity levels between 0-40 NTU; accuracy will decrease if the turbidity of certain sample is above 40 NTU, since it is believed that the relationship between light scatter and turbidity becomes non-linear at higher levels. However, high levels of turbidity still can be measured by diluting the samples below 40 NTU according to the EPA's manual.

The general procedure the 180.1 method is cited from EPA's publication as the following:

o   Turbidities less than 40 units: If possible, allow samples to come to room temperature before analysis. Mix the sample to thoroughly disperse the solids. Wait until air bubbles disappear then pour the sample into the turbidimeter tube. Read the turbidity directly from the instrument scale or from the appropriate calibration curve.

o   Turbidities exceeding 40 units: Dilute the sample with one or more volumes of turbidity-free water until the turbidity falls below 40 units. The turbidity of the original sample is then computed from the turbidity of the diluted sample and the dilution factor. For example, if 5 volumes of turbidity-free water were added to 1 volume of sample, and the diluted sample showed a turbidity of 30 units, then the turbidity of the original sample was 180 units.

> o   Some turbidimeters are equipped with several separate scales. The higher scales are to be used only as indicators of required dilution volumes to reduce readings to less than 40 NTU

ISO 7027:

This method is essentially the same as the EPA180.1, with the exception of some minor changes. ISO 7027 requires a monochromatic light source (mainly LEDs) at a wavelength of 860 nm, with a light source range of 830-890 nm while 180.1's light source is broadband in spectrum. So for samples with colored particles and molecules, ISO 7027 should have a relatively more accurate measurement because near-infrared light is rarely absorbed by them, however, the EPA180.1 method is recommended if finer particle samples are provided since longer wavelengths are less sensitive to small particles (Sadar, M 1999). The ISO 7027 method requires a primary detector angle of 90 degrees +/- 2.5 degrees, and the acceptance angle of the detector should extend 20-30 degrees. Moreover, the unit usedin ISO 7027 is the Formazin Nephelometric Unit (FNU). And as suggested by the USGS, the range of this method can be up to 1000 NTU with one detector, or up to 4000 NTU if multiple detectors are used. Units should be Formazin Nephelometric Ratio Units (FNRU).

Bench-top turbidimeters are considered as a standard method for turbidity measurements in laboratory settings. A wide variety of meters are available on the market, under brand names such as Hach, Oakton, HF Scientific, LaMotte, etc. most of these bench-top meters claim compliance with EPA's standard method. There are also portable, handheld turbidimeters that can be applied in the field for grab sample measurements. Some field sensors can be connected to dataloggers allowing long term continuous sampling of water quality. Many of these *in situ* turbidimeters use backscattering for turbidity measurements, such as the Campbell Scientific's OBS series, Turner Designs' Cyclops turbidity sensor, etc. Near infrared lights are usually selected as the light source for these sensors, which can minimize the effects of particle size and water color on the turbidity level readings (Jastram et al., 2009). The measurement range can exceed the 40 NTU limits (up to 4000 NTU), although it is not clear if the results at higher turbitdity levels will agree with that of the EPA standard method when diluted to low levels. Since the turbidity of runoff from construction sites with large area of disturbed land is usually very high and the daily average values need to be reported according to EPA's vacated C&D rule, it appears that field deployable turbidity sensors is the only viable method for site monitoring purposes.

2.3.2   Variability of Turbidity Readings

Many factors can affect the level of turbidity measured by the scatting method. Perkins et al. (2014) summarized that these factors can be categorized into two groups: (1) factors related to the sample itself, such as particle size, particle shape, particle color, water color and organic matter; (2) factors related to the measurement devices, such as the angle of detection, type of photodetector, light source wavelength, etc.

Scattering patterns from particles of different sizes differ substantially. Suspended soil particles from stormwater runoff have a wide size distribution and a variety of scattering patterns. This may create significant variation when reading the sample with a turbidimeter. Moreover, spherical particles produce more predictable light scattering patterns compared to irregularly shaped particles such as suspended soil particles (Omega Engineering, 2001). Light scatter from irregularly shaped particles differs in intensity compared to spherical particles, even if the "equivalent" diameters of those irregular particles are the same as the spherical ones. This can cause unpredictable effects on turbidity measurement in stormwater runoff.

Calibration of a turbidimiter usually uses the Formazin suspension. Formazin particles have varying shapes and the average particle size is 1.5 ± 0.6 μm (cf figure 2.2). As a result, turbidity reading of the Formazin standard may vary by 2% (Downing, 2005) from lot to lot. This may cause variability for turbidimeters calibrated with a Formazin suspension. Another approved calibration standard is styrene divinylbenzene (SDVB). SDVB particles are spherical and dimensionally more uniform (0.28 ± 0.10 μm), thus less variability is expected for sensors calibrated with a SDVB standard.
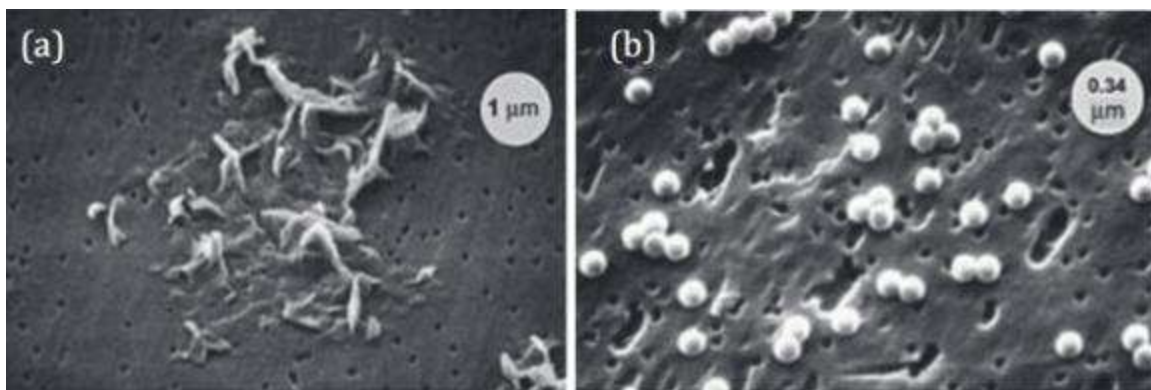
Figure 2.2: SEM images of (a) Formazin and (b) SDVB particles (images source: Campbell Scientific (Downing, 2005)).

The color of soil particles can absorb and scatter light differently. In particular, dark colored particles can cause less light scattering, which cause lower turbidity readings compared to samples with light colored particles in the same concentration. The color of water is usually due to dissolved organic matter which can absorb a significant amount of light, thus affect turbidity readings. This is a concern when measuring turbidity in lakes and streams, but may not

be an issue for stormwater runoff from the disturbed soil of a construction site, which typically has less organic matter.

Many modern turbidimeters use near infrared light as the illumination source, which has been approved to limit the color effect from both particles and water (Ankcorn, 2003), since long wave lights are less absorbed. Some turbidimeters use multiple light beams or photo-detectors that measure scattering from different angles. Readings from different angles can be combined through an algorithm to offset the color effect.

Variability caused by characteristics of soil in different regions and the different turbidity sensors has to be addressed and acknowledged by EPA or other environmental regulation agencies if future rules use turbidity as a measure to monitor or manage construction site runoff. At the minimum, any turbidimeter selected for these purposes has to be carefully calibrated by professionals and follow a unified standard procedure. The type of light source, photo-detector and the detection method also need to be specified, such that samples collected from different sites and under different environmental conditions are comparable.

2.3.3 Relation between Turbidity and the Concentration of Total Suspended Solids

Turbidity and the Total Suspended Solids (TSS) are both related to the particles in water, however, they are different measurements. TSS represents the total mass of small solid particles in water which will not settle out by gravity. It is usually measured by passing the water sample through a very fine filter (usually 0.45 micron). TSS measurements are represented in terms of solid mass in a certain water volume, such as milligrams per liter (mg/L). Turbidity is an optical property of water and it is determined by the amount of light scattered off the particles. Unlike TSS, turbidity values measured (e.g., NTU) are not physical units. For example, a measured water turbidity of 100 NTU may not be used to infer any physical quantities from the sample. Normally, turbidity measurements will be affected by colored dissolved organic matter which will absorb light instead of scattering it; however, this dissolved matter is not included in TSS measurement. Moreover, compared to TSS measurement in the lab, turbidity measurement is affected by many other factors. For the target sample, both particle size and particle shape will affect the measurement as has been described in section 2.3.2. Differences among instruments such as the angle of detection and light source wavelength can also affect the measurement.

Despite the differences between TSS and turbidity, many studies demonstrated strong correlation between them in practical applications. Due to the complexity of the TSS measurement, it is preferable to assess the negative impacts caused by storm water by measuring the turbidity of the runoff. Turbidity measurement is quick and cost effective. Portable turbidity sensor is easy to use and convenient for dynamic measurement. In addition, a submerged

turbidity sensor can be deployed for relative continuous in-situ monitoring which is more preferable than a sampling method.

It is advantageous to use turbidity as a surrogate for TSS, and this practice has been widely adopted to evaluate sediment concentration and load in rivers and streams (e.g., Susfalk et al 2008; Daphne et al., 2011); to assess the relation between TSS and turbidity in stormwater runoff (Memon et al., 2015); and even in combined sewer systems (Hannouche et al., 2011). Many of these studies showed a nearly linear relation between turbidity and TSS. The linear relation could be complicated in natural streams and lakes as other factors such as water color, dissolved organic matters, algae, and bacteria can affect their relations. Stormwater runoff from construction sites could be less affected these additional factors. For example, through their study of various land-use sites in South Korea, Memon et al. (2015) found that the correlation between TSS and turbidity is the strongest in construction site effluents, compared with those from other catchments without construction activities. It should also be noted that the proportionality of the linear relationship represented as the ratio of TSS to turbidity (in terms of mg/L over NTU) varied between 0.64~3.4 as determined through our literature search. Despite this variability, it still appears reasonable to adopt turbidity as a surrogate for TSS as long as the relationship is well calibrated for each specific site.

More detailed laboratory studies show that the TSS-turbidity relation is nonlinear. Holliday et al. (2003) proposed a power law relationship, i.e.,

$$\text{Turbidity} = \alpha\,\text{TSS}^{\beta} \tag{2.1}$$

Their measurement showed that the exponent β for two samples are very close to one, while the other sample differs significantly from 1.0, which indicates a nonlinear relation. Perkins et al. (2014) investigated turbidity-TSS relationships for conditions of Minnesota soil. Using synthetic runoff of 14 soil samples from 8 construction sites, their results indicated $\beta = 1.4$ represented all samples well, and the scaling parameter α was a function of percent silt, interrill erodibility and maximum abstraction. They proposed a model for the coefficient α, which can be used to universally describe all soil samples (cf. figure 2.3).
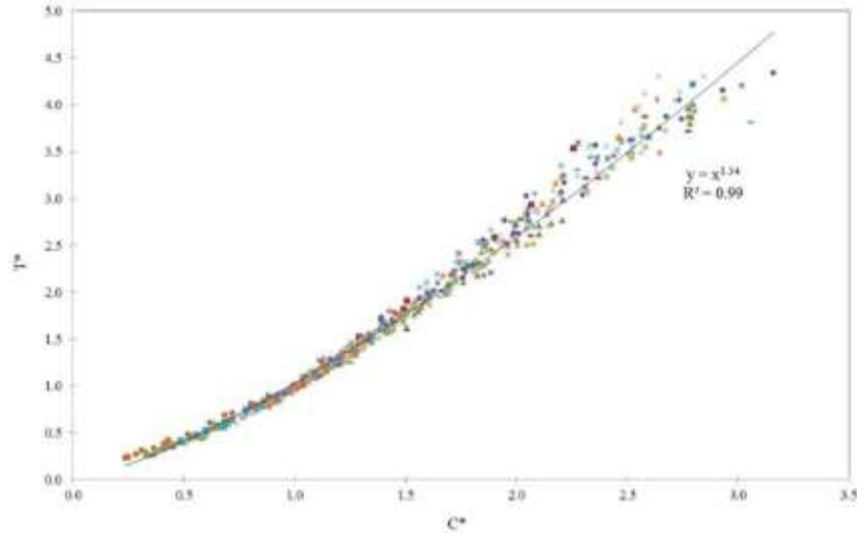
Figure 2.3: Normalized turbidity vs. TSS concentration for Minnesota soil samples. (adapted from Perkins et al. (2014))

TSS concentration can be measured following EPA's standard method #160.2. This method is also approved for NPDES. Detailed procedures of this method can be found in EPA's document (USEPA, 1999). The procedures are summarized as the following:

7. 0 Procedures

7.1 Preparation of glass fiber filter disc: Place the glass fiber filter on the membrane filter apparatus or insert into bottom of a suitable Gooch crucible with wrinkled surface up. While vacuum is applied, wash the disc with three successive 20 mL volumes of distilled water. Remove all traces of water by continuing to apply vacuum after water has passed through. Remove filter from membrane filter apparatus or both crucible and filter if Gooch crucible is used, and dry in an oven at 103-105°C for one hour. Remove to desiccator andstore until needed. Repeat the drying cycle until a constant weight is obtained (weight loss is less than 0.5 mg). Weigh immediately before use. After weighing, handle the filter or crucible/filter with forceps or tongs only.

7.2 Selection of Sample Volume For a 4.7 cm diameter filter, filter 100 mL of sample. If weight of captured residue is less than 1.0 mg, the sample volume must be increased to provide at least 1.0 mg of residue. If other filter diameters are used, start with a sample volume equal to 7 mL/cm2 of filter area and collect at least a weight of residue proportional to the 1.0 mg stated above. NOTE: If during filtration of this initial volume the filtration rate drops rapidly, or if filtration time exceeds 5 to 10 minutes, the following scheme is recommended: Use an unweighed glass fiber filter of choice affixed in the filter assembly. Add a known volume of sample to the filter funnel and record the time elapsed after selected volumes have passed through the filter. Twenty-five mL increments for timing are suggested. Continue to record the time and volume increments until filtration rate drops rapidly. Add additional sample if the filter funnel volume is inadequate to reach a reduced rate. Plot the observed time versus volume filtered. Select the proper filtration volume as that just short of the time a significant change in filtration rate occurred.

7.3 Assemble the filtering apparatus and begin suction. Wet the filter with a small volume of distilled water to seat it against the fritted support.

7.4 Shake the sample vigorously and quantitatively transfer the predetermined sample volume selected in 7.2 to the filter using a graduated cylinder. Remove all traces of water by continuing to apply vacuum after sample has passed through.

7.5 With suction on, wash the graduated cylinder, filter, non-filterable residue and filter funnel wall with three portions of distilled water allowing complete drainage between washing. Remove all traces of water by continuing to apply vacuum after water has passed through. NOTE: Total volume of wash water used should equal approximately 2 mL per cm2. For a 4.7 cm filter the total volume is 30 mL.

7.6 Carefully remove the filter from the filter support. Alternatively, remove crucible and filter from crucible adapter. Dry at least one hour at 103-105°C. Cool in a desiccator and weigh. Repeat the drying cycle until a constant weight is obtained (weight loss is less than 0.5 mg).

8.0 Calculations

8.1 Calculate non-filterable residue as follows:

$$\text{Non-filterable residue, mg/L} = \frac{(A - B) \times 1{,}000}{C}$$

where:
A = weight of filter (or filter and crucible) + residue in mg
B = weight of filter (or filter and crucible) in mg
C = mL of sample filtered

2.4   BMP Controls on Construction Sites

Best Management Practices (BMPs) according to EPA's definition, are a suite of structures or control devices and systems to treat polluted stormwater caused by the change of land use. BMPs are designed to reduce stormwater volume, peak flows, and non/point source pollution through evaporation, infiltration, detention and filtration or biological and chemical actions. BMP is the key component of EPA's C&D rules that applies for construction sites, as well as the NPDES permitting requirement.

BMPs are structural and non-structural practices that can be classified as erosion controls and sediment controls. Examples of these BMP controls widely used on construction sites are:

- *Erosion controls:* keeps sediment in place. Examples pertinent to construction projects include: Bonded Fiber Matrix, Erosion Control Blanket, Grading, Temporary Seeding, Soil Roughening, Straw Mulch, Vehicle Tracking Pads, etc.

- *Sediment control:* captures any sediment that is moved by stormwater before it leaves the site. Examples include: Fiber Wattle Roll Ditch Check, Inlet Protection (Perimeter Barrier), Rock Check Dams, Sediment Basin, Sediment Trap, Silt Fences, Straw Bale Ditch Check, and more recently, Flocculation, etc.

In an Indiana Department of Transportation (INDOT) project report, Corson (2006) reviewed and documented structural and non-structural BMPs suitable for use in construction, reconstruction, rehabilitation and retrofitting activities along INDOT roadways and facilities. Many of these identified BMPs are currently widely applied in Wisconsin DOT construction projects. Table 2.2presents a short description of a number of BMPs that are extensively applied in WisDOT construction sites, according to our field observations in this project. All descriptions are adapted from Corson's (2006) report (Appendix 3. Construction Phase BMP Fact Sheet), and sample pictures were taken during field surveys on several WisDOT construction sites.

Table 2.2: Common BMP measures applied on WisDOT construction sites.

BMP Controls	**Sample Pictures**
Grading: Applicable to sites with uneven or steep topography or easily erodible soils. Grading can be planned and used during and after construction to control surface runoff and minimize soil erosion and sedimentation. Grading activities should maintain existing drainage patterns where possible, and minimize slope lengths and steepness. Grading practices, such as selecting a milder side slope gradient (e.g. 6:1 vs. 3:1), can help reduce runoff velocity and help prevent rill erosion. Final grades selected should be based on considerations of the soil characteristics at the specific site (e.g. sands vs. clays).	
Soil Roughening: Soil roughening is a temporary erosion control practice useful with grading operations associated with sloped areas. Soil roughening involves increasing the relief of a bare soil surface with horizontal grooves, stair-stepping (running parallel to the contour of the land), or tracking using a cleated roller, crawler tractor, or similar construction equipment. Slopes that are not fine graded and that are left in a roughened condition can reduce erosion. Soil roughening reduces runoff velocity, increases infiltration, reduces erosion, traps sediment, and prepares the soil for seeding and planting by giving seed an opportunity to take hold and grow. It	

also reduces erosion and sedimentation resulting from wind.

Straw Mulch:

Straw mulching is a temporary erosion control practice which provides an immediate, effective, and inexpensive erosion control. It also improves the success of temporary and permanent seeding. Mulching is highly recommended as a stabilization method and is most effective when used in conjunction with vegetation establishment. Mulching can also reduce storm water runoff velocity. When used in combination with seeding or planting, mulching can aid plant growth by holding seeds, fertilizers, and topsoil in place, preventing birds from eating seeds, retaining moisture, and insulating plant roots against extreme temperatures.

Straw Bale Ditch Check and Fiber Wattle Roll Ditch Check:

Straw bale or fiber wattle roll ditch checks are small dams constructed across a swale or ditch. They are used to slow the velocity of concentrated flow thereby reducing erosion. As a lesser function, ditch checks can also be used to catch sediment from the swale itself or from the contributing drainage area as storm water runoff flows through the structure. However, the use of these ditch checks should not be a substitute for the use of other sediment-trapping and erosion control measures. Ditch checks are most effective when used in combination with other storm water and erosion and sediment control measures

Inlet Protection:

Storm drain inlet protection measures are controls that help prevent soil and debris from site erosion from entering storm drain drop or curb inlets. Typically, these measures are temporary controls that are implemented prior to large-scale disturbance of the surrounding site. These controls are advantageous because their implementation allows storm drains to be used during construction activities. Inlet protection is often the last opportunity to minimize sediment impact to a receiving water body. Inlet protection can cause inadvertent flooding of adjacent areas if not properly installed.

Silt Fence:

A silt fence is a fabric or wire mesh barrier used to retain sediment from small, sloping disturbed areas by reducing the velocity of sheet flow. Silt fence captures sediment by ponding water to allow deposition on the uphill side. Silt fences consist of a length of geotextile or wire mesh stretched between anchoring posts spaced at regular intervals along the site perimeter. The geotextile should be entrenched in the ground between the support posts. A silt fence is not recommended to divert water; nor is it to be used across a stream, channel, or anywhere that concentrated flow is anticipated. Silt fence should be used parallel to contour elevation lines only. Placing silt fence perpendicular to contour lines can actually increase erosion by concentrating flow along the disturbed embedment trench.

Riprap:

Riprap can be used to provide permanent and temporary erosion protection on small construction sites in several ways. Three such methods are inlet and outlet protection, temporary diversion structures, and permanent diversion structures. Pipe inlet and outlet protection is a protective armor for the immediate area around the inlet and outlet of a pipe or culvert to protect it and the receiving channel from scour and deterioration. This practice applies to culverts and principal spillways. Riprap should not be used in areas where native vegetation would be effective. However, riprap should be considered in areas of potential high velocity and areas below the ordinary high water level where vegetation will not easily establish.

Sediment Basin:

A temporary sedimentation basin is a controlled stormwater release structure formed by excavation, or by erecting an embankment of compacted soil or riprap, and installing an outlet structure and outlet pipe. The purpose of the basin is to detain the sediment-laden runoff from disturbed areas long enough for the majority of the sediment to settle out in the basin. This reduces sediment transport off-site. Generally, sediment basins are designed to be temporary. However, temporary sediment basins can be converted into permanent storm water runoff management ponds following site stabilization.

According to the description of these common BMP measures, it appears that most BMPs are designed to reduce erosion or to reduce the volume and speed of stormwater flow on surface. If well-constructed and managed, they can effectively reduce the total sediment load to receiving waters. However, fine silt and clay particles, which are the major contributors to turbidity, will not settle by gravity, hence BMP measures may not help to reduce the turbidity readings in the effluent. A more reasonable argument on the effects of BMPs on effluent turbidity is the fact that

since the total runoff volume can be reduced, the turbidity level will be lower when diluted with the receiving water, though it may not be reduced at the point of discharge.

More recently, the use of coagulants or flocculants, such as the polyacrylamide (PAM), on disturbed soil is considered as a more promising BMP measure to reduce the turbidity in stormwater runoff. When added to flows with sediments, the PAM can reduce the charges on colloidal suspensions to allow them clump together to form large particles that can settle out. PAM has already been widely used in irrigated agriculture for erosion control. Numerous studies have found that mixing PAM with irrigated water on furrows can significantly reduce sediment load in farmland runoff, and it can also enhance infiltration (Sojka and Lentz, 1997). PAM is applied as a solution in water using typical erosion control equipment such as hydroseeders or hydromulchers (cf. Figure 2.4). Usually, it is applied in combination with mulch and seeding, and application alone on soil should be avoided. As a long polymer, PAM helps to prevent erosion by forming bridges to soil particles through cations and anions of soil particles, thus coating the soil surface with a glue-like porous layer (cf. figure 2.5).

Figure 2.4: Application of PAM on sloped soil surface.
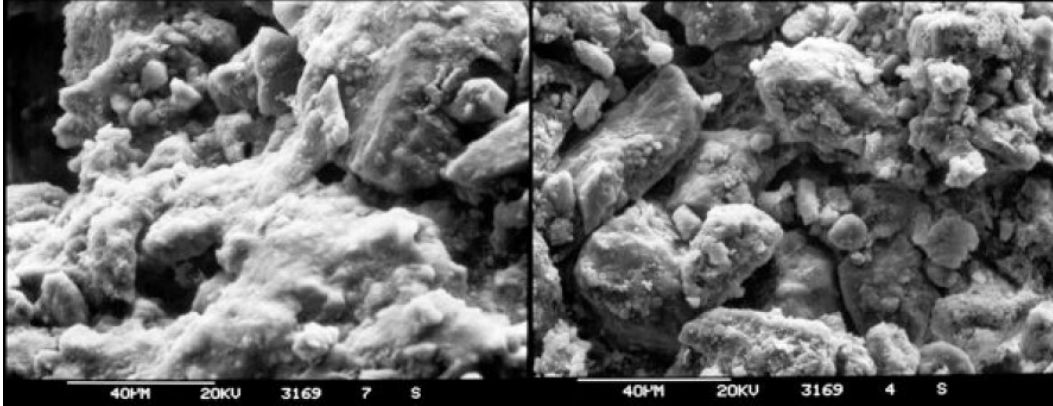
Figure 2.5: Scanning electron micrograph that shows the comparison of PAM-treated (left) and untreated (right) surface soil from irrigation furrows (Ross et al., 2003).

A number of laboratory studies showed that flocculation with PAM can reduced the turbidity of synthetic runoff from sample soils (Mclaughlin and Bartholomew, 2007; Rounce et al., 2012). Field studies also showed that treating exposed soil on construction sites with PAM and mulch can effectively reduce the turbidity in the effluent, particularly on milder slopes (McLaughlin, 2002; Hayes et al., 2005).

2.5   Related Research Work and Projects

A number of studies have reported that turbidity in construction sites runoff is generally much higher than the 280 NTU limit, which has been removed from EPA's new C&D rules. For example, a final report of the NCHRP project 25-25(74) reviewed existing data on runoff turbidity with various levels of BMP protections (see Table 2.3). It is estimated that turbidity level after conventional BMPs controls can still be as high as 500~2,000 NTU. In the final report of a Texas DOT project, McFalls et al. (2014) summarized the range of turbidity levels based on their literature review to be from 10~30,000 NTUs. The data they cited are based from (1) California DOT's monitoring results on 15 highway construction sites between 1998 and 2000; (2) McLaughlin (2002)'s field monitoring results from three construction sites in North Carolina; and (3) McLaughlin and Jenning's (2007) measurements that evaluate the effects of erosion control measures on turbidity reduction. Results adapted from their reports are presented in Table 2.4.

Table 2.3: Summary comparison of major classes of turbidity reduction technologies (adapted from NCHRP project report (2012))

Sediment control methods	Expected achievable turbidity range	Reliability	Monitoring and maintenance required	Relative cost
Conventional BMPs	500~2,000 NTU	Low	Low	Low
Enhanced Conventional BMPs	100~500 NTU	Low	Low	Moderate
Passive Coagulation	20~500 NTU	Moderate	Moderate	Moderate
Active Treatment	1~20 NTU	High	High	High

Table 2.4: Typical runoff turbidity from road construction projects. (Adapted from McFalls et al. (2014), Appendix B).

Source	Construction Type	Location State	Sampling Year	Runoff Turbidity Min	Max	Mean	Remark
Kayhanian et al. (7)	Roadway / Highway	CA	1998-2000	15	16000	702	15 sites
McLaughlin (8)	1:2 fill slope	NC	2001	50	5600	1638	PAM
	1:2 fill slope	NC	2001	25	4000	634	PAM+mulch+seed
	1:4 cut slope	NC	2001	200	5900	2272	PAM
	1:4 cut slope	NC	2001	50	400	182	PAM+mulch+seed
	1:4 fill slope	NC	2001	11	2000	360	PAM
	1:4 fill slope	NC	2001	18	500	116	PAM+mulch+seed
McLaughlin and Jennings (9)	Highway	NC	2004-2005	77	28160	2950	Final outlet
	Highway	NC	2004-2006	6	18223	1647	Final outlet
	Highway	NC	2004-2007	6	2272	159	Final outlet
	Highway	NC	2004-2008	3	9409	1178	Final outlet

Since the EPA established the numeric effluent limit, and is looking for data and research support, several state DOTs have requested to do research on this matter. For example, the following 3 research projects have been funded in response to EPA's new regulation on turbidity.

1. **Performance Testing of Coagulants to Reduce Stormwater Runoff Turbidity** (*Texas DOT* project number: 0-6638). This project aimed to conduct laboratory experiments to test PAM as a coagulant for soil erosion control and sedimentation control, and to conduct construction site field monitoring. The project final report has been published

(McFalls et al., 2014) and the major findings are: (1) PAM application on tested clay soils with 1:3 slopes was not effective in reducing runoff turbidity or soil loss; (2) PAM added in sedimentation devices increased sediment removal rate by 8 to 18 percent, compared with sedimentation without PAM treatment;

2. **Development and Evaluation of Effective Turbidity Monitoring Methods for Construction Projects** (*Minnesota DOT* project report number: MN/RC 2014-24). The objective of this project was to investigate turbidity relationships for conditions of Minnesota and to develop protocols for the design and installation of cost-effective monitoring systems. The project final report has been published (Perkins et al., 2014) and major findings include: (1) Relation between turbidity and TSS can be described by a power law with an exponent of 7/5 (a non-linear relation) based on fourteen different soil samples in Minnesota. (2) Field monitoring of runoff from construction sites found that turbidity often exceeded 1,000 NTU and sometimes surpassed 3,000 NTU.

3. **Using Flocculation to Reduce Turbidity of Construction Site Runoff (***USDOT-Mountain Plains Consortium and the South Dakota State University***, project number: MPC-436**). The objectives of this research were to (1) Determine the effects of PAM types and flocculation conditions on the turbidity reduction of runoff from highway construction sites; (2) Determine the impact of low temperatures on the effectiveness of PAM flocculation; (3) Provide recommendations on the application of PAM flocculation to reduce runoff turbidity levels for highway construction sites. The final report of this project has not yet been released.

Chapter 3
Research Methodology

This chapter describes the methods used to measure the stormwater turbidity, conductivity, pH value and the mass concentration of total suspended solids (TSS) both in the field and in the laboratory. Procedures for field sample collection including the selection of sampling locations are described in detail. Both laboratory and *in situ* turbidity meters are used in this study. All meters are calibrated with the same standard, and a number of samples are measured with both of these meters for cross-validation. Laboratory experiments are conducted to investigate the relation between turbidity and the concentration of TSS. An automated monitoring device is developed to collect time series of turbidity at the outfall locations of sampling site. The design, calibration and assembling of the device is also presented in this chapter.

3.1   Field Grab Sample Collection

Grab samples were collected during or after storm events. The main purpose was to quantify typical turbidity NTUs and other water quality parameters (specifically the conductivity and pH value) at various discharging points. Most of these parameters of grab samples were measured onsite while some samples were taken back to the laboratory for the purposes of validation.

Grab samples were collected with generic plastic bottles. Sample bottles used in this study are 500 ml capacity, white (nontransparent), chemically inert, cylindrical bodied with double caps. The inner cap ensures better sealing and secures the contents from evaporation and spill. Collecting a grab sample with the bottle is generally simple and straightforward, for example: holding the bottle under the stormwater falling from a draining pipe until filled. For the locations where it is difficult to collect samples with the large bottle, e.g., surface flow water was too shallow or water drained into a stormwater inlet, smaller plastic cups are used to collect water sample and then dumped into the large bottle for analysis.

A publication by the Washington State of Ecology (2006) has provided a thorough review and instructions for stormwater sampling. In this study, we have followed these instructions and paid great care to ensure that the samples are taken correctly by following these general principles:

- Bottles are thoroughly cleaned and rinsed with distilled water in the laboratory before taking to the field. Do not reuse bottles in the field without lab cleaning.

- Keep hands away from the bottle opening to avoid contaminating the sample with dirt or other particulates
- Always hold the bottle with its opening facing upstream to avoid collecting resuspended sediment due to the stirring flow.
- Stand downstream of the bottle if it is needed to step in the flow to collect sample.
- Do not set container lids on the ground.
- Label samples immediately after collection.

Figure 3.1 shows some examples of sampling work conducted for this project using sampling bottles or cups.

Figure 3.1: Sample photos of field grab sampling using plastic bottles and cups.

For each field task during or after a storm event, we attempted to identify the final discharging points as the ideal locations for sampling. For general erosion control BMPs, it would not be feasible to comparatively quantify the effectiveness, such as: with and without an

erosion control blanket/mat on a disturbed land. Therefore, we will only report the typical turbidity levels at identified discharging point. Common sample locations include:

- Ditches or storm drains carrying stormwater offsite;
- Pipe or stormwater pond outfalls;
- Runoff from disturbed or exposed soil areas into adjacent ditches or streams;
- Retention ponds when the water started to drain, etc.

For sediment control structures, the effectiveness in terms of NTU and TSS reduction can be directly measured. Samples were taken at locations before and after the treatment. For example:

- At the inflow and outlet of a sediment basin;
- Both sides of a silt fence;
- Behind every check dam along a swale or ditch;
- Before and after the filtration of an inlet protection, etc.

Some of these sampling locations identified during the fieldwork are presented in figure 3.2.

(a) Stormwater ditch

(b) Stormwater drain pipe

Figure 3.2: Typical locations for field grab sampling during or after storm events.

Most grab samples collected in this study were directly measured on site for the turbidity NTU, pH value and conductivity using handheld field meters (see section 3.3 for details).

3.2 Laboratory Procedures

3.2.1 Turbidity Measurement with Bench-top Nephelometer

Turbidity of grab samples are measured in the laboratory using a benchtop nephelometer following the EPA's standard method #180.1, which has been documented in detail in section 2.3.1. The nephelometer is a HS Scientific DRT-100B turbidimeter (cf Figure 3.3(a)), which has four adjustable ranges: 1, 10, 100, and 1,000 NTU, and a sensitivity of 0.01 NTU which exceeds the EPA's standard (0.02 NTU). The turbidimeter is calibrated and samples are measured following the manufacturer's user manual, which complies with EPA's standard.

The procedures adopted in this project is summarized below:

1. **Sample storage and transport:** Grab water samples collected during the field experiments were immediately stored in an iced container to keep the sample temperature less than 4°C to minimize microbiological decomposition of solids.
2. **Sample preparation:** Samples were analyzed in the Water Quality Laboratory at University of Wisconsin-Milwaukee after brought back from the construction site, usually less than 24 hours after they were collected. Samples were taken out from the iced container at least one hour before measurements, allowing them to come to the room temperature. Non-representative particulates such as leaves, grass clippings and lumps of organic matter were removed.
3. **Nephelometer calibration:** The turbidimeter was calibrated once every year before field experiments start with the primary calibration standard: 40 NTU Formazin polymer suspension purchased from Sigma-Aldrich. It was then calibrated for every laboratory experiment with the secondary calibration standard, 400 NTU Formazin polymer suspension purchased from Sigma-Aldrich for sensor validation. If the meter reading error was larger than 5 NTU, it was then recalibrated with the primary calibration standard.
4. **Sample measurement:**
   a. Grab samples were mixed in a 500 mL beaker, and the beaker was placed on magnetic stirrer to mix the sample.
   b. If the turbidity of the grab sample was greater than 40 NTU, it was first diluted to less than 40 NTU before measurement.
   c. Filled the mixed sample into the turbidimeter's sample cuvette (cf Figure 3.3(b)). The cuvette was cleaned and visually checked for blemish and scratches.
   d. The sample cuvette was inserted into the optical well of the turbidity meter and the appropriate scale (10, 100, or 1000 NTU) was selected. Turbidity value in NTU was then read and recorded.

e. Three turbidity measurements were made for the same grab sample by repeating the above procedures to examine the repeatability of the measurement.
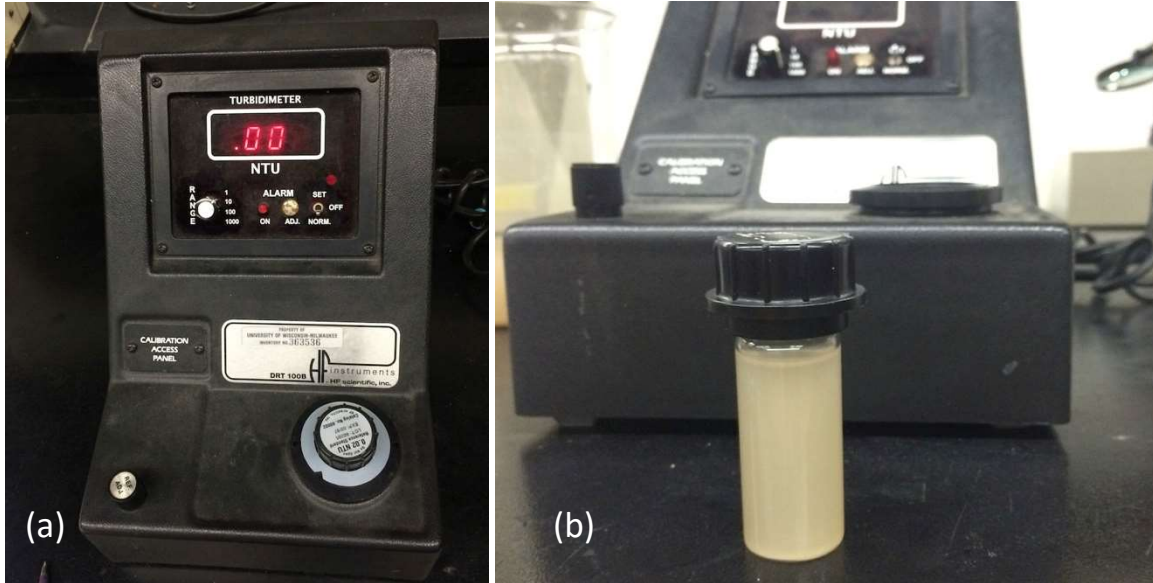
Figure 3.3: (a) HS Scientific DRT-100B turbidimeter used in this study (b) cuvette that contains sample for turbidity measurement.

3.2.2   Procedures for Total Suspended Solids (TSS) Measurement

We followed the EPA's standard method #160.2 to measure the concentration of TSS in field grab samples. The method has been well documented in Section 2.3.3, and the procedures adopted in this project are summarized as follows:

1. **Sample storage and transport:** Same as that in turbidity measurement.
2. **Sample preparation:** Same as that in turbidity measurement.
3. **Filter and filter support preparation:** No. 3 Gooch crucibles are used as the filter support. They were prepared before TSS measurement with the following steps:
    a. Gooch crucibles were put into the filtering apparatus and 2.1 cm glass fiber filters are then put in each of the crucibles.
    b. By applying suction, the filter was washed with 100 ml of distilled water to seal well.
    c. The crucibles and filters were dried in the oven at 105°C for one hour.
    d. Then the crucibles and filters were dried in a desiccator.

e. Weight of the crucibles and filters were measured with a Mettler Toledo ML54 Analytical Balance and recorded after drying.

4. **TSS measurement:** the following steps were taken to measure the concentration of TSS:

   a. A 100 mL portion of each of the samples was well mixed and measured out into a graduated cylinder.

   b. Prepared Gooch crucibles were dampened with distilled water.

   c. The sample was filtered through the Gooch crucible and suction was applied to facilitate filtration (cf. Figure 3.4(a)).

   d. Dissolved solids in the filter were washed out with 20 mL of distilled water, using 10 mL portions.

   e. The crucible was dried in the oven at 105°C for one hour (cf. Figure 3.4(b)).

   f. The crucible was cooled and dried in a desiccator for about 20 minutes (cf. Figure 3.4(c)).

   g. The total weight of the crucible, filter and remained solids were measured in the Mettler Toledo ML54 Analytical Balance with a resolution of 0.1 mg (cf. Figure 3.4(d)).

   h. The solid concentration was then calculated using equation specified in the EPA's standard method #160.2.
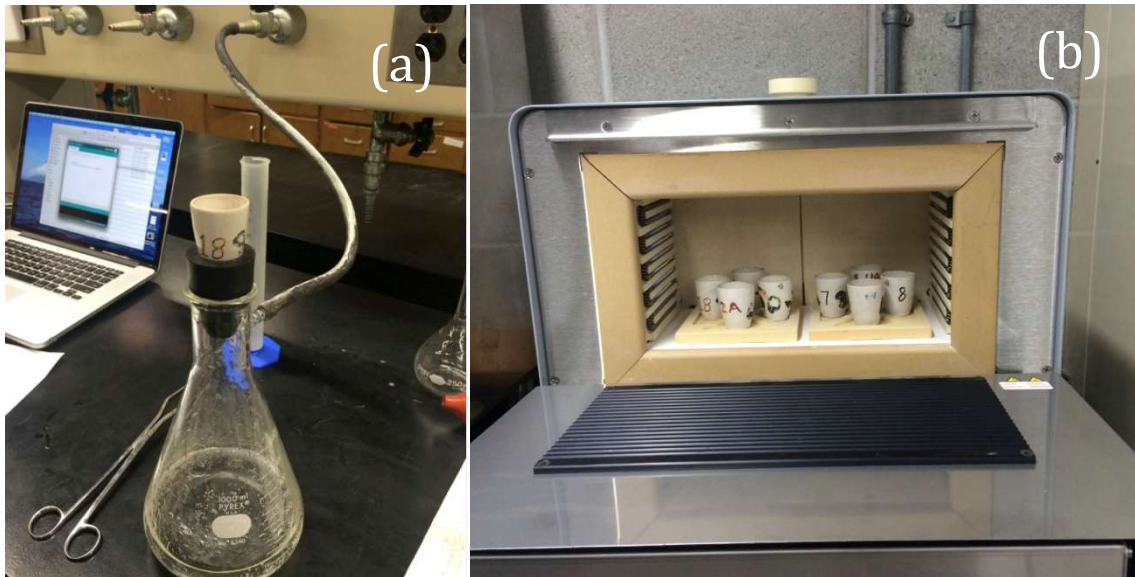
Figure 3.4: Procedures to measure the concentration of Total Suspended Solids (TSS) in samples. (a) sample filtration with a Gooch crucible (b) samples dried in an oven (c) samples cooled and dried in a desiccator (d) residue, crucible and filter weighed in a balance.

3.2.3 Other Water Quality Parameters

In addition to turbidity, the pH value and conductivity were also measured for some grab samples. Most of these measurements were conducted with a handheld meter on site (see section 3.3 for description). Some of these samples were also measured in the laboratory for validation and cross-check.

The pH value was measured electrometrically with a Fisher Scientific Accumet AB15 pH meter. Before every measurement, the pH meter was calibrated using the buffer solution of pH 4, 7 and 10. One value was recorded for every sample. The electrode of the meter was cleaned with distilled water before and after each reading.

The conductivity was measured with a Fisher Scientific Accumet Basic AB30 conductivity meter and the result was reported in (μS/cm). The conductivity meter was calibrated with buffer solutions before each measurement. One value for each sample was recorded. The electrode was cleaned with distilled water before and after each reading.

3.3 Handheld Instruments for Field Measurements

To minimize the potential error due to possible change of sample water quality and chemistry during handling, storage and transport, most samples collected in the field were directly measured using portable handheld meters. Turbidity was measured with a Turner Designs Cyclops-7 submersible turbidity sensor equipped with a compact controller/datalogger (cf Figure 3.5). The sensor method is a Nephelometer which, after careful calibration, complies with EPA's turbidity measurement standard. The Cyclops sensor uses an 850 nm light source and detects scattered light at a 90-degree angle, which is similar to many modern day bench-top Nephelometers. The sensor has a measurement range of 0~3,000 NTU and can be automatically adjusted by the controller depending on the overall NTU level of the sample. The datalogger can save data, time of measurement and the GPS location simultaneously for easy data management.

Measuring turbidity with the Cyclops sensor is straightforward. The sensor probe is directly submerged into the water sample and the result can be read from the screen of the datalogger. The reading result can also be saved into the logger by pressing a button. In order to avoid signal contamination due to reflection of the emitting light source from substrate surface, it is required that the sensor probe be more than 3 inches above the bottom, and clearance around the circumference of the sensor probe must be more than 2 inches. During our field measurements, if the measured water body was sufficiently deep, the sensor probe was directly inserted into the water (cf Figure 3.5(b)). Otherwise, the sample was first collected with the 500 mL plastic bottle, with the turbidity then measured by inserting the probe into the bottle.

Figure 3.5: (a) Turner Designs Cyclops turbidity meter and the handheld controller/datalogger (b) Measuring turbidity by inserting the sensor probe directly into water

Following the instruction manual provided by the manufacturer, the sensor was calibrated with the standard: a series of dilutions from a 400 NTU Formazin polymer suspension manufactured by Sigma-Aldrich. A linear relation is expected between the sensor's analog output voltage (V) and the sample turbidity (NTU):

$$NTU_{std} = R_S(V_{std} - V_{blank}) \qquad (3.1)$$

where NTU_{std} is the known turbidity level of the calibration standard, V_{std} is the voltage reading of the sensor when measuring the standard, and V_{blank} is the voltage reading when measuring clear water.

For calibration, the standard was diluted in series: 400, 200, 100, 40, 30, 20, and 10 NTU. Deionized water was used as the blank. Measured results in voltage were then plotted against the NTU value of the dilutions. Linear regression analysis is applied to evaluate the response slope R_S in equation (3.1). The linear regression process can be performed by connecting the controller/datalogger with a computer (via USB interface) and using the software provided by the manufacturer. The calibrated result was then saved into the controller/datalogger for the subsequent sample measurement, and the measurement result can be processed by the datalogger using

$$NTU_{sample} = R_S(V_{sample} - V_{blank}) \qquad (3.2)$$

On site measurements of the pH value and the conductivity was measured by a handheld ExTech ExStik EC500 pH/Conductivity Meter, which combines a flat surface pH electrode with an auto-ranging high accuracy conductivity cell (cf Figure 3.6). This device can measure 5 parameters using one electrode: pH, conductivity, total dissolved solids (TDS), salinity and temperature. In this study, only the pH value and conductivity is reported. Measurement was conducted by directly inserting the probe in to the sample bottle, and values of different parameters are read successively by pressing the "Mode" switch on the meter. Calibration of the sensor was conducted once every month using the conductivity standard and pH buffer purchased from the manufacturer.

Figure 3.6: ExTech ExStik EC500 pH/Conductivity handheld sensor, and the sensor probe.

3.4 Development and Deployment of Automated Turbidity Sampling Devices

Grab sampling during a storm event can only provide the runoff turbidity at a limited number of time points, while the runoff discharge into the receiving water (streams, ponds, storm drains, etc.) is expected to have a varying turbidity level. "Catching" a storm is a challenging strategy for field grab sampling, especially for sites that are remotely located. In this project, we have experienced with a number of situations that resulted in unsuccessful field trips, such as (1) precipitation events ended before we arrived at the construction site; (2) missed storm events that occurred during the night time; (3) heavy rains made some parts of the site inaccessible; (4) and trips with no samples due to an inaccurate weather forecast. In addition, sample results may not represent the peak value of the runoff turbidity. It is difficult to extrapolate data acquired as a limited number of "snapshots" to reveal the variability of the runoff process. A great number of uncertainties exist when we attempted to investigate the statistical relation between the runoff turbidity and the precipitation.

In order to acquire continuous time series of runoff turbidity, to obtain a good number of datasets for better statistical analysis, and to solve the problems mentioned above, we have developed a low-cost automated turbidity sampling device which can be deployed on site unattended. As it is prohibitively expensive to deploy multiple sensors at various locations of one construction site, only one device was deployed for a given site. Five devices were built for this project. For all devices deployed on four selected sites, four of them were retrieved and one was lost (possibly stolen or vandalized). A runoff pattern on a construction site is usually complicated and there can be several locations where runoff is discharged into the environment. For each sampling site we have identified the most significant outfall location for the sensor deployment. Usually they are at the locations where a storm drain pipe discharges the runoff into a natural stream or stormwater conveyance channel.

The automated sampler was developed with the Turner Designs submersible Cyclops turbidity probe, the same sensor used with the handheld turbidity meter for field grab samples (see section 3.3 for details). The turbidity signal was measured and saved through an Arduino Uno microcontroller. Analog output pins of the Cyclops sensor were wired to the Analog input of the Arduino board through a compatible underwater data cable (Impulse MCIL-6-FS-5). The microcontroller was programmed to read and digitized the voltage input at an interval of 5 seconds. Recorded data were saved to an SD memory card through a compatible Arduino shield. A 12 Volt Lithium- ion rechargeable battery was used as a power supply for both the turbidity sensor and the Arduino microcontroller. A DC power switch module was wired to the battery, and it was programmed to switch on and off the entire system with desired intervals. The module is limited to 17 on/off cycles every 24 hours. Therefore, it was programmed to turn on the device every 85 minutes(17 times per day). The Arduino starts to run the stored program when turned on. First it turns on the sensor and allows 30 seconds to elapse to stabilize the sensor, then it loops to acquire and save measured signal at 0.2 Hz. The DC switch will turn off

after 6 samples are acquired which is about 60 seconds after switch on, i.e., 30 seconds for warm up and 30 seconds for acquisition. As data were retrieved from the memory card, the turbidity value was reported as the average of every 6 readings. For every reported data point, the data consistency was checked by the criterion that the fluctuation of the 6 readings is less than 1% of their average.

All electronic components were contained in a waterproof box with the data cable penetrating the box, sealed and secured with a cord grip cable gland. A Turner Designs sensor shade cap was used to cover the sensor probe, which helps to ensure adequate clearance space around the sensor, minimizes ambient light interference, and prevents damage during deployment and recovery. Figure 3.7 shows all components of the automatic sampling device placed in the waterproof box. An example of deployment of the sensor probe (with the shade cap cover) is shown in Figure 3.8.

Figure 3.7: Electronic components of the developed automatic turbidity sampling device in the waterproof box.

Figure 3.8: Deployment of the automatic turbidity sensor in a stream near the outfall of a stormwater drain from a construction site near I-94 at Racine, WI.

The sensor calibration procedure is similar to that described for the handheld meter, except that voltage readings are reported by the Arduino microcontroller, which exports the result to a computer terminal via USB connection. Good linearity was found when applying linear regression using equation (3.1), with $R^2 > 99\%$ in the range of the calibration standard, i.e., a series of dilution of 10, 20, 30, 40, 100, 200, and 400 NTU.

Figure 3.9 shows the turbidity NTU calculated with the calibrated equation (3.2) against the known standard for all five sensors. During the calibration process, the standard suspension was also measured by the handheld and bench-top turbidimeters, and the readings are also presented in figure 3.8 for comparison. It appears that the five sensors reported almost identical values, which suggests excellent consistency.
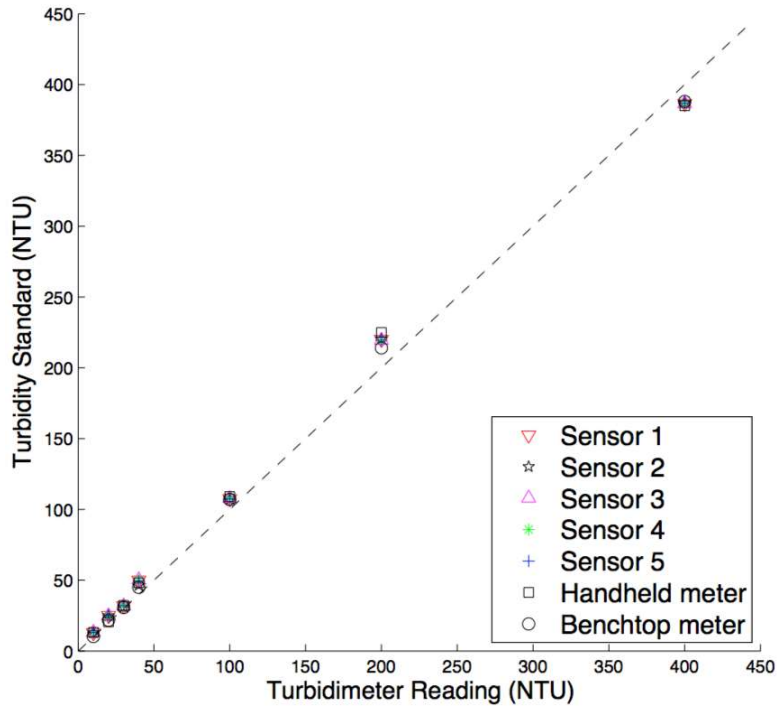
Figure 3.9: Turbidity measured by the calibrated sensors vs. the known turbidity standard.

Figure 3.10 shows the average errors of the 5 sensor units, and the errors of the handheld and bench-top turbidimeters at different standard concentrations. It appears that errors for all sensors increase substantially (up to 10 %) as the standard sample turbidity increases. Also the errors change from positive to negative as the sample NTU increases. The trend of these errors seems to be systematic, and they are nearly the same for all sensors. Therefore, errors are likely due to the non-linearity between the optical scattering and the particle concentration, rather than the instrument errors. EPA's standard method requires that samples with turbidity > 40 NTU be diluted to offset this nonlinearity. However, for field sensors designed for measuring high turbidities, the nonlinearity effect may not be accounted for. We expect different turbidity readings between a field sensor and a lab bench-top sensor that follows the EPA's standard method.
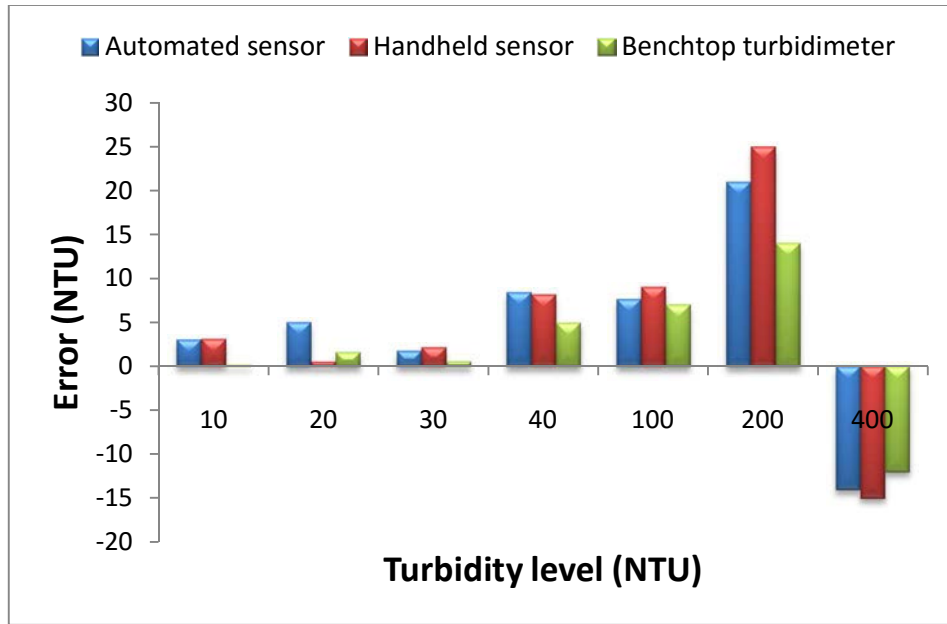
Figure 3.10: Average errors of the five automated turbidity sensors, and errors of the handheld and bench-top turbidimeters when measuring different standard concentrations diluted from a 400 NTU standard.

3.5 Relation between Turbidity and TSS concentration

The relation between turbidity and TSS concentration was examined in this project by measuring field grab samples. We hypothesized that the relation is largely determined by the property of the disturbed soil, while less dependent on other environmental conditions, such as the temperature, pH value, and the characteristics of the precipitation event. Therefore the turbidity-TSS relation was also examined by measuring a simulated turbidity runoff.

Soil samples were collected from the tested construction sites for runoff simulation. First the collected soil was broken down and sieved with a coarse mesh to remove large rocks, sticks and organic particulates. Then the soil was filled into a rectangular wood planter (purchased from a local garden store) as the test bed. A 1.5 inch perforated PVC pipe was inserted into the box to collect the runoff from the sample soil (cf. figure 3.11). Another PVC pipe was inserted at a higher position that was right above the soil surface to collect the simulated "surface runoff". The soil was gently packed and wetted before the rainfall-runoff simulation.

Simulated runoff was generated by sprinkling water evenly on the test bed. Turbid water from the surface runoff PVC pipe and that seeped out from the subsurface PVC pipe was collected separately with two sampling cups. Water samples were taken from each cup at different stages of the rainfall-runoff simulation with the expectation to obtain samples with different TSS concentration and turbidity level. Water samples of the two cups were then mixed and the turbidity of the mixtures was also measured. These samples were then analyzed and the measured TSS concentrations were plotted against the turbidity readings. Linear and nonlinear regression was applied to explore their relations. In cases where the variability of data was low, samples are diluted to expand the range.

In addition, turbidity and TSS concentration of grab water samples acquired from the same site at different times were plotted on the same graph. The purpose of this was to test the hypothesis that the turbidity-TSS relation is determined largely by the soil property, and the turbidity can be used as a surrogate for suspended solids concentration if well calibrated.

Figure 3.11: Simulated rainfall-turbidity runoff process experiment.

Chapter 4
Site Description and Field Grab Sample Results

Five WisDOT construction sites were identified during the project period. Locations of the five sampling sites are shown in figure 4.1. These sited were labeled according to the name of the nearest cities and the road intersection where construction activities were conducted:

(A) Kenosha site: STH-50 & I-94;
(B) Wauwatosa: STH-181 & I-94;
(C) Racine: STH-20 & I-94;
(D) Lake Geneva: STH-50 & US-12;
(E) Wrightstown: STH-96 & Fox River
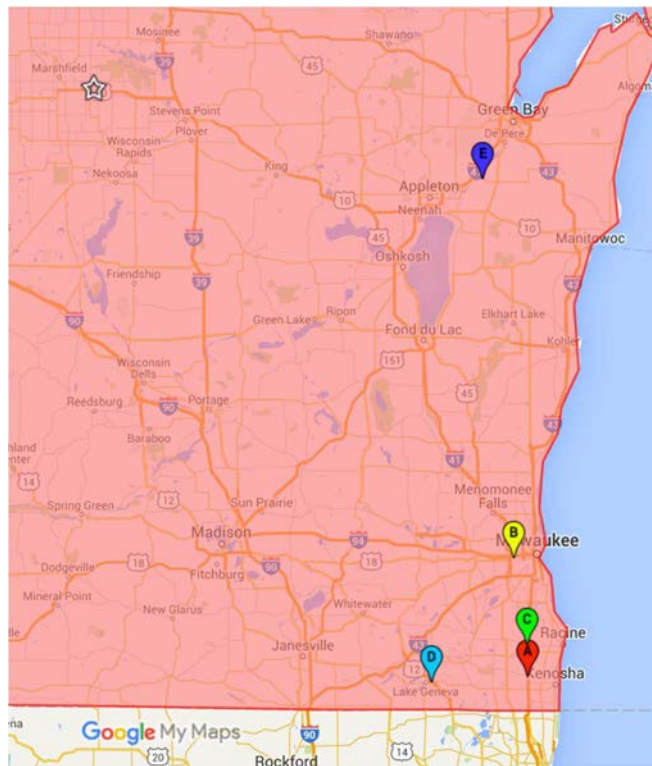
Figure 4.1: Locations of the five identified construction sites for turbidity runoff sampling

Field grab sampling work were conducted on four sites which are all within one hour of driving distance from the campus of University of Wisconsin-Milwaukee. However, we were not able to "catch" any storm event for the other site (the Wrightstown site), which is about 120 miles away. Only automated sampling data are available for this site.

This chapter describes all the five sampling sites, including construction activities, BMP protection methods, and identified sampling locations. Field sampling results from both on-site measurements and laboratory analyses are presented and discussed for the four nearby sites. Site description and results are presented in the chronological order according to the time when field samplings were conducted.

4.1 Site One: STH-50 and I-94 near Kenosha, WI

Construction activities were conducted at the intersection of Wisconsin State Trunk Highway (STH) 50 and Interstate 94 during 2013 and 2014. Two field-sampling trips were made in September and October of 2013. The area of soil disturbance was evaluated through site walk-through surveying. Three subareas of disturbed land surface were identified during that period; these are sketched out on Google Earth (cf. Figure 4.2).

Figure 4.2: Areas of disturbed land surfaces during September and October of 2013 at the Kenosha construction site: Area A at the southwest corner of the STH-50&I-94 intersection is about 4.56 acres; Areas B and C at the southeast corner of the intersection are 1.06 and 1.08 acres, respectively.

As shown in Figure 4.2, area of the three subareas were estimated through the area tool of Google Earth, which are 4.56, 1.06 and 1.08 acres in area, respectively. Visual observations during one storm event indicated that there were multiple stormwater drain locations on the construction sites. As shown in Figure 4.3, most runoff from subarea A was collected and drained at its south east corner via a stormwater inlet pipe (point 2 on the figure), which may

eventually drain into an underground stormwater sewer pipe. Runoff from subarea B and C primarily flows off the I-94 road following the west-east topographic slope, and drains into a "U" shaped retention pond. Water in the retention pond then drains into a storm inlet pipe at the northwest corner of the pond (point 1 on the figure).

Figure 4.3: Major stormwater drain locations, BMP structures and grab sampling locations at the Kenosha construction site.

The most noticeable BMP controls were straw mulch on the disturbed soil, particularly on slopes and around the retention pond. Fiber wattle roll ditch checks were laid in the "U"-shaped retention pond to reduce the flow speed and facilitate sedimentation. Other erosion controls included riprap structures around the inlet and outlets of pipes and culverts.

Two field trips were made to acquire grab samples on October 5, 2013 and October 31, 2013. Several sampling locations were identified and they are marked on figure 4.3:

- **Point A:** Turbidity was measured in the retention pond at 5 locations along the mean direction of flow in the pond, in each section that was separated by 6 fiber wattle roll ditch check
- **Point B:** In a stormwater ditch that drains into the retention pond
- **Point C:** The inlet point of the retention pond
- **Point D:** In a grass-lined ditch which drains runoff from undisturbed land surface (primarily a parking lot)
- **Point E:** On a paved surface
- **Point F:** in a stormwater swale that drains runoff from the subarea A (see figure 4.1)

Some pictures taken during the October 5 event on the construction site are shown in figure 4.4. Summaries of the sampling results are presented in table 4.1.

Figure 4.4: Pictures taken on the Kenosha construction site on October 5, 2013.

Table 4.1: Grab sampling results on the Kenosha sampling site (***Note:*** at locations A and F, i.e., the retention pond and the stormwater swale, multiple samples are collected along the path of flow. Their values are reported in the order that follows the flow direction)

	Event #1: October 5, 2013					
Precipitation	**Start time**	10/5 5PM	**End time**	10/5 7PM	**Duration (hr)**	2
	Total precipitation depth (in)	1.16	**Peak rainfall intensity (in/hr)**	1.09	**Average rainfall intensity (in/hr)**	0.58
Water sample results	**Sampling start time**		10/5 5:45 PM		**Sampling end time**	10/5 7:30 PM
	Sampling point	*Turbidity on-site (NTU)*	*Turbidity Lab (NTU)*	*pH*	*Conductivity (μS/cm)*	*TSS (mg/L)*
	A	860	NA	NA	NA	NA
		855	NA	NA	NA	NA
		870	NA	NA	NA	NA
		850	820	7.8	2,559	1,202
		840	NA	NA	NA	NA
		835	NA	NA	NA	NA
	B	648	702	7.2	1,420	690

C	857	850	7.5	1,703	1,175
D	12.1	20	8.0	445	12.2
E	55.0	56	7.9	933	43.7

Event #2: October 30, 2013						
Precipitation	**Start time**	10/30 5PM	**End time**	10/31 7PM	**Duration (hr)**	27
	Total precipitation depth (in)	0.84	**Peak rainfall intensity (in/hr)**	0.17	**Average rainfall intensity (in/hr)**	0.05
Water sample results	**Sampling start time**		10/31 2:00 PM		**Sampling end time**	10/31 4:30 PM
	Sampling point	*Turbidity on-site (NTU)*	*Turbidity Lab (NTU)*	*pH*	*Conductivity (µS/cm)*	*TSS (mg/L)*
	A	628	NA	NA	NA	NA
		650	NA	NA	NA	NA
		649	NA	NA	NA	NA
		603	600	8.1	1,903	536
		609	NA	NA	NA	NA
		609	NA	NA	NA	NA
	F	648	NA	NA	NA	NA
		625	621	7.7	1,722	505
		627	NA	NA	NA	NA

The two precipitation events were distinctively different: the Oct 5 event was short and intensive with 1.16 inch of total depth in just 2 hours, while the Oct 31 event lasted sporadically for 27 hours and the total depth is 0.84 inches. Both events were smaller in magnitude than the local 2-year 24-hour event (2.0~2.8 inches). Average turbidity levels in the retention pond were 852 and 625 NTU on Oct 5th and 31st, respectively. Samples in the storwmater swale were taken only on Oct 30 with an average value of 633 NTU, similar to the mean values in the retention pond on that day. Both these values exceeded the EPA's numeric limits of 280 NTU, despite various erosion control BMP measures. As a comparison, turbidity level in the grass-line ditch (point D) which drains the parking lot of the nearby Walgreens store was 12.1 NTU, and the turbidity level of water collected on the highway ramp (point E) with mixed runoff from both the paved surface and disturbed soil was 55 NTU.

Turbidity measured at multiple locations in both the retention pond and the swale did show a decreasing trend along the direction of the flow. It appeared that, with the fiber wattle roll ditch check intercepting and reducing the flow speed, it favored sedimentation. However the sedimentation was not able to significantly reduce the fine suspended sediment concentration, as represented by the turbidity. The NTU level was reduced from 860 to 835 on Oct 5 (a 3%

reduction) and from 628 to 609 (a 3% reduction) on Oct 30 in the retention pond, and it was reduced from 648 to 637 (a 1.7% reduction) on Oct 30 in the swale.

The overall distribution of turbidity and the direction of runoff in the retention pond and the surrounding areas measured in the two field experiments are shown in figure 4.5.

Figure 4.5: Turbidity in (NTU) measured at multiple locations in the retention pond and the nearby areas of the Kenosha construction site.

4.2   Site Two: STH-181 and I-94 near Wauwatosa, WI

Construction activities were conducted at the intersection of Wisconsin State Trunk Highway (STH) 50 and Interstate 94 in 2014. Seven field-sampling trips were made from June to September of 2014. The area of soil disturbance was evaluated through site walk-through surveying. Three subareas of disturbed land surface were identified during this period; these they are sketched out on Google Earth (cf. Figure 4.6).
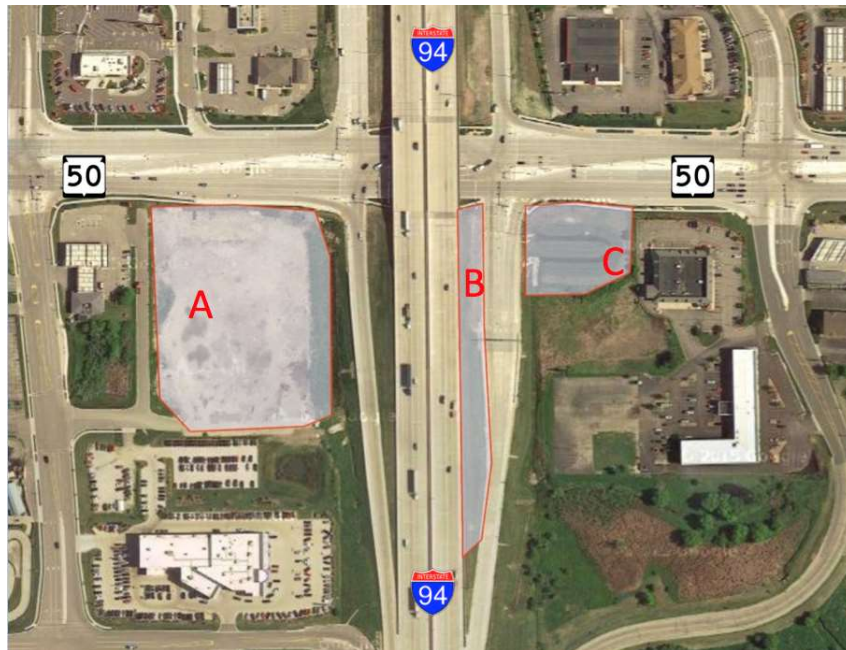
Figure 4.6: Areas of disturbed land surfaces during June~October of 2014 at the Wauwatosa construction site: subarea A at the northwest corner of the STH-181&I-94 intersection is about 2.3 acres; subarea B at the southwest corner of the intersection is about 1.3 acres; and subarea C at the southeast corner of the intersection is about 7.3 acres.

As shown in Figure 4.6, areas of the three subareas were estimated with the area tool of Google Earth, which are 2.3, 13 and 7.3 acres, respectively. Visual observations during storm events indicated that there were multiple stormwater drain locations on the construction sites. As shown in Figure 4.7, most runoff from subarea A was collected and drained into a nearby stream (point 1 in figure 4.7), either directly through broken silt fences or indirectly through stormwater pipes. Two stormwater sewer inlets were found in the subareas B and C, respectively (point 2 and 3 in the figure). It was likely that runoff collected by the two inlets eventually flowed into the stream as well, but that was not confirmed. The stream nearby was part of the Honey Creek, which is essentially a storm sewer channel rather than a natural stream (green dash-dotted line in the figure). Honey Creek flows through the cities of West Allies, Milwaukee, and Wauwatosa. Part of the stream flows through the Wisconsin State Fair Park as an underground concrete conduit. Honey Creek has a history of high bacteria levels. Routine water quality monitoring by the Milwaukee Metropolitan Sewerage District (MMSD) has shown chronically high levels of fecal coliform bacteria in the creek. Some of these bacteria are from human sewage, possibly due to the leak of sanitary sewers (Magruder et al., 2006).

The most noticeable BMP controls were fabric fibers and rock berms as the storm inlet protection; riprap structures on the side slopes and around the storm drain pipes along both sides of Honey Creek; and silt fences near the stream around disturbed soil. Bonded fiber matrix much and soil roughening were also occasionally applied on exposed soil for the purpose of erosion control. Filter bags that connected to water hoses were found near excavation and ponding water

areas, possibly used for dewatering. Filtered water was then discharged in to the storm drains or into Honey Creek directly. Figure 4.8 shows some of these BMP measures and structures.
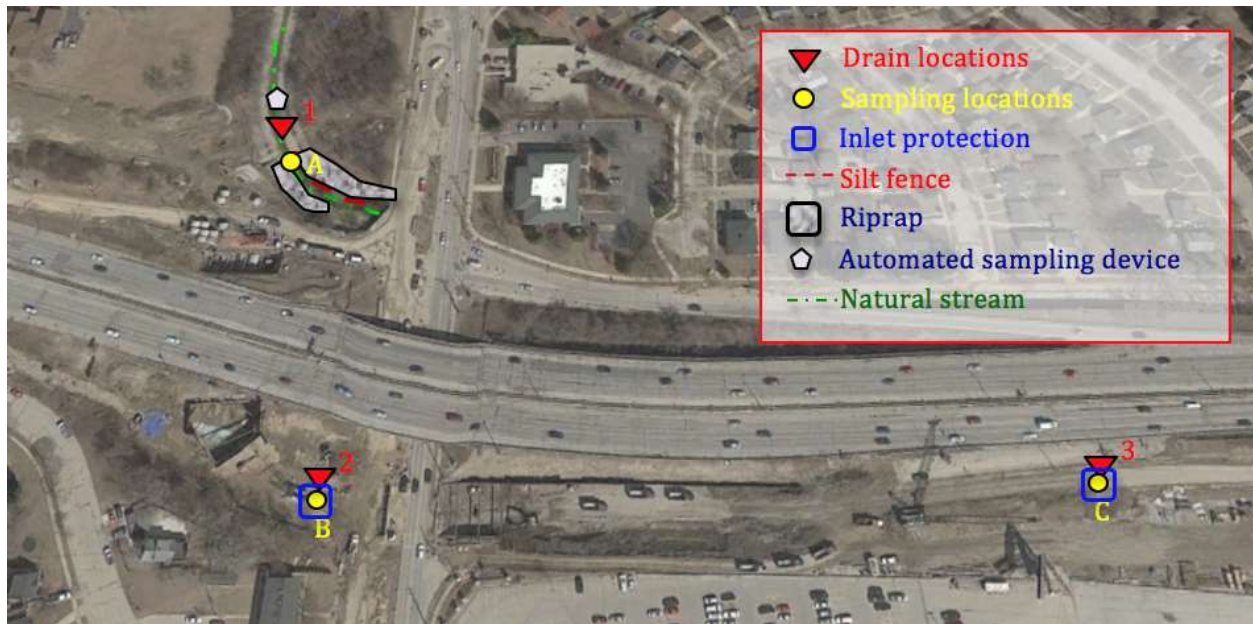
Figure 4.7: Major stormwater drain locations, BMP structures and sampling locations at the Wauwatosa construction site.

Seven field trips were made to acquire grab samples between June and September in 2014. Three sampling locations were identified and they are marked on figure 4.3:

- **Point A:** Turbidity was measured around areas where runoff drains into Honey Creek.
- **Point B:** Runoff water sampled immediately before it drains into the storm inlet.
- **Point C:** Runoff water sampled immediately before it drains into the storm inlet.

The automated turbidity sampling device was also deployed in Honey Creek for long term monitoring. The device was located at about 50 feet downstream of the disturbed land (see figure 4.7), where the stormwater had been well mixed, and the turbidity level can be considered as the average of runoff of a larger area which include the entire construction site. However, it may also include runoff from the nearby land without construction activities. As it will be shown in Chapter 6, turbidity readings from this site are much smaller compared with those from other sites. This is likely due to a dilution effect by runoff from undisturbed surfaces. The deployment method of the automatic sampling device is shown in figure 4.9.

Figure 4.8: Examples of BMP measures and structures on the Wauwatosa construction site.

Figure 4.9: Deployment of the automated turbidity sampling device in Honey Creek near the Wauwatosa construction site.

Seven field experiments were conducted between June and September of 2014, and the sampling results are presented in Table 4.2. The first four field experiments included all the three sampling locations, while for the three remaining events, we were only able to sample in the Honey Creek (point A in figure 4.7) as the other two locations were not accessible due to construction activities.

Significant excavation and construction activities were undergoing during the period from June to mid-August near sampling location A. Concrete walls were placed around the disturbed soil along the bank of Honey Creek to create a temporary sedimentation pond, in addition to other existent soil erosion controls (riprap, silt fence and bonded fiber matrix mulch). We were able to take two grab samples at this location, with one in the sedimentation pond and the other in the creek. These samples are denoted as "A (pond)" and "A (stream)", respectively in Table 4.2. These concrete walls were removed after August 21 (estimated date), allowing turbid runoff directly discharge into the creek from the banks. Turbidity was well mixed according to our visual inspection. Therefore, only one sample was taken from the polluted stream for the last two field trips. Figure 4.10 illustrates the turbidity values in the pond and the stream measured during these sampling trips.

Table 4.2: Grab sampling results on the Wauwatosa sampling site

Event #1: June 11, 2014					
Precipitation	**Start time**	6/11 0AM	**End time**	6/12 0AM	**Duration (hr)**	24
	Total precipitation depth (in)	0.76	**Peak rainfall intensity (in/hr)**	0.09	**Average rainfall intensity (in/hr)**	0.03

	Sampling start time		6/11 9AM		**Sampling end time**		6/11 10AM
Water sample results	***Sampling point***	***Turbidity on-site (NTU)***	***Turbidity Lab (NTU)***	***pH***	***Conductivity (µS/cm)***	***TSS (mg/L)***
	A (Pond)	410	388	9.1	NA	389
	A (Stream)	208	205	7.6	503	198
	B	405	410	8.9	2,680	400
	C	833	789	7.8	1,301	1,054

Event #2: June 20, 2014					
Precipitation	**Start time**	6/20 1AM	**End time**	6/20 3PM	**Duration (hr)**	14
	Total precipitation depth (in)	0.42	**Peak rainfall intensity (in/hr)**	0.13	**Average rainfall intensity (in/hr)**	0.03

	Sampling start time		6/20 1PM		**Sampling end time**		6/20 2PM
Water sample results	***Sampling point***	***Turbidity on-site (NTU)***	***Turbidity Lab (NTU)***	***pH***	***Conductivity (µS/cm)***	***TSS (mg/L)***

A (Pond)	281	NA	9.1	462	277	
A (Stream)	125	NA	8.2	385	118	
B	745	NA	7.7	1,322	971	
C	576	NA	8.1	1,400	628	

	Event #3: June 23, 2014					
Precipitation	**Start time**	6/23 4AM	**End time**	6/23 8AM	**Duration (hr)**	4
	Total precipitation depth (in)	0.55	**Peak rainfall intensity (in/hr)**	0.4	**Average rainfall intensity (in/hr)**	0.14
Water sample results	**Sampling start time**		6/23 10AM		**Sampling end time**	6/23 11AM
	Sampling point	***Turbidity on-site (NTU)***	***Turbidity Lab (NTU)***	***pH***	***Conductivity (µS/cm)***	***TSS (mg/L)***
	A (Pond)	145	NA	8.1	520	NA
	A (Stream)	155	NA	8.1	429	NA
	B	902	NA	7.9	1,723	NA
	C	872	NA	7.9	1,290	NA

	Event #4: July 1, 2014					
Precipitation	**Start time**	6/30 5PM	**End time**	7/1 3AM	**Duration (hr)**	10
	Total precipitation depth (in)	0.81	**Peak rainfall intensity (in/hr)**	0.25	**Average rainfall intensity (in/hr)**	0.08
Water sample results	**Sampling start time**		7/1 10AM		**Sampling end time**	7/1 11AM
	Sampling point	***Turbidity on-site (NTU)***	***Turbidity Lab (NTU)***	***pH***	***Conductivity (µS/cm)***	***TSS (mg/L)***
	A (Pond)	158	NA	8.2	NA	NA
	A (Stream)	25	NA	8.7	1,173	NA
	B	366	NA	7.8	1,173	NA
	C	611	NA	7.2	3,216	NA

	Event #5: August 19, 2014					
Precipitation	**Start time**	8/19 4AM	**End time**	8/19 6AM	**Duration (hr)**	3
	Total precipitation depth (in)	0.55	**Peak rainfall intensity (in/hr)**	0.50	**Average rainfall intensity (in/hr)**	0.18
Wat	**Sampling start time**		8/19 10AM		**Sampling end time**	8/19 11AM

	Sampling point	Turbidity on-site (NTU)	Turbidity Lab (NTU)	pH	Conductivity (μS/cm)	TSS (mg/L)
	A (Pond)	679	677	NA	NA	758
	A (Stream)	55	69	NA	NA	37

	Event #6: August 27, 2014						
Precipitation	**Start time**	8/27 5AM	**End time**	8/27 11 AM	**Duration (hr)**		6
	Total precipitation depth (in)	0.27	**Peak rainfall intensity (in/hr)**	0.12	**Average rainfall intensity (in/hr)**		0.05
Water sample results	**Sampling start time**		8/27 10AM		**Sampling end time**		8/27 11AM
	Sampling point	**Turbidity on-site (NTU)**	**Turbidity Lab (NTU)**	**pH**	**Conductivity (μS/cm)**		**TSS (mg/L)**
	A (Stream)	319	338	8.8	729		284

	Event #7: September 10, 2014						
Precipitation	**Start time**	9/10 7AM	**End time**	9/10 9PM	**Duration (hr)**		14
	Total precipitation depth (in)	0.45	**Peak rainfall intensity (in/hr)**	0.32	**Average rainfall intensity (in/hr)**		0.03
Water sample results	**Sampling start time**		9/10 3PM		**Sampling end time**		9/10 4PM
	Sampling point	**Turbidity on-site (NTU)**	**Turbidity Lab (NTU)**	**pH**	**Conductivity (μS/cm)**		**TSS (mg/L)**
	A (Stream)	403	NA	NA	NA		NA

Figure 4.10: Turbidity values in the stormwater pond and Honey Creek.

4.3 Site Three: STH-20 and I-94 near Racine, WI

Construction activities were conducted at the intersection of Wisconsin State Trunk Highway (STH) 20 and Interstate 94 during 2015. Four field-sampling trips were made from March to September of 2015. The area of soil disturbance was evaluated through site walk-through surveying. Three subareas of disturbed land surface were identified during that period; these areas are sketched out on Google Earth.
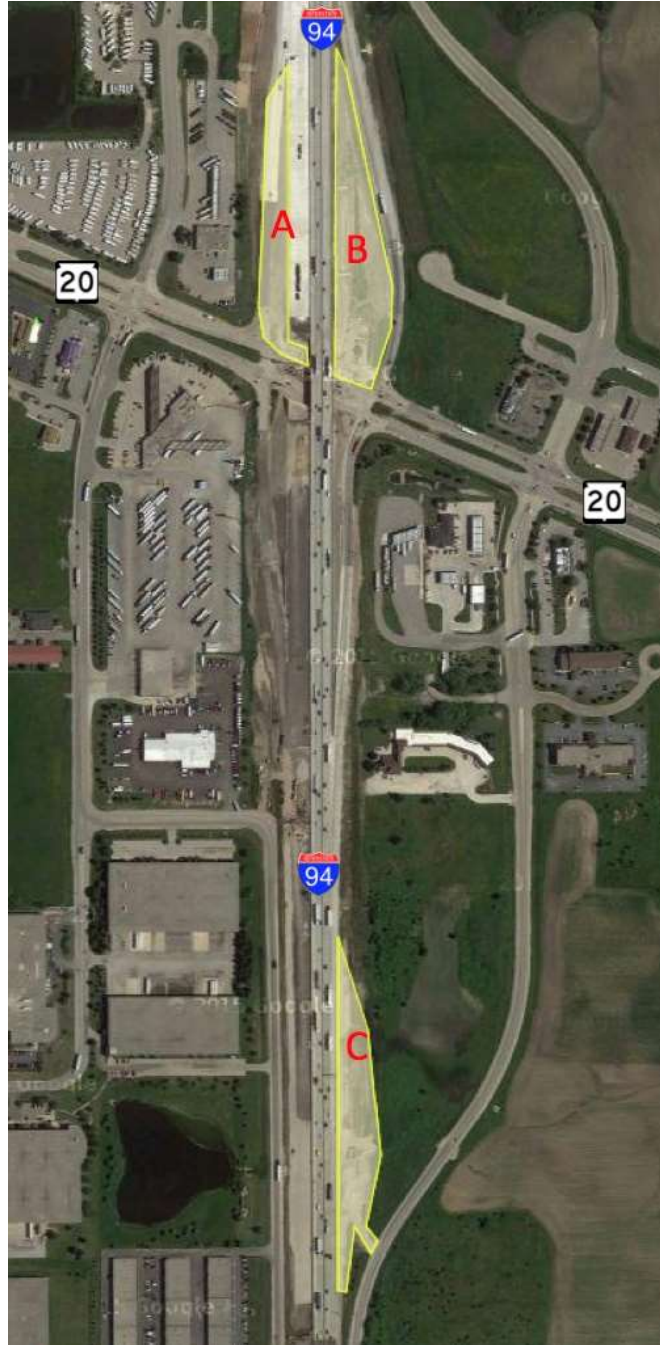
Figure 4.11: Areas of disturbed land surfaces during June~September of 2015 at the Racine construction site: Area A and B at the northwest and northeast corner of the STH-20 & I-94 intersection are about 2.28 and 3.05 acres, respectively; Area C at the southern end of the intersection is about 2.59 acres.

As shown in Figure 4.11, the three subareas were estimated through the area tool of Google Earth, which were 2.28, 3.05 and 2.59 acres, respectively. Visual observations during storm events indicated that there were multiple stormwater drain locations on the construction

sites. As shown in Figure 4.12, most runoff from subarea A was collected and drained through a storm pipe inlet (point 1 in the figure), which carries stormwater eastwards across the I-94 road and drains into a natural ditch. This water then combined with the runoff from subarea B and flowed into another storm pipe inlet (at point A in the figure). The runoff from both subareas then discharged into a natural stream at point 2 in figure 4.12. Subarea C was about 2,500 feet south of the intersection, on the east side of I-94. Runoff primarily flowed eastwards off the slope and convened into a stormwater swale which eventually drained into a natural stream (at point 3 in the figure).

Straw mulch was extensively applied on the steep slope at the east side of I-94. Other noticeable BMP measures included fiber wattle roll ditch checks in the swale near subarea C, and silt fences along two natural streams on the east side of I-94. Figure 4.13 shows some of these BMP measures and structures.
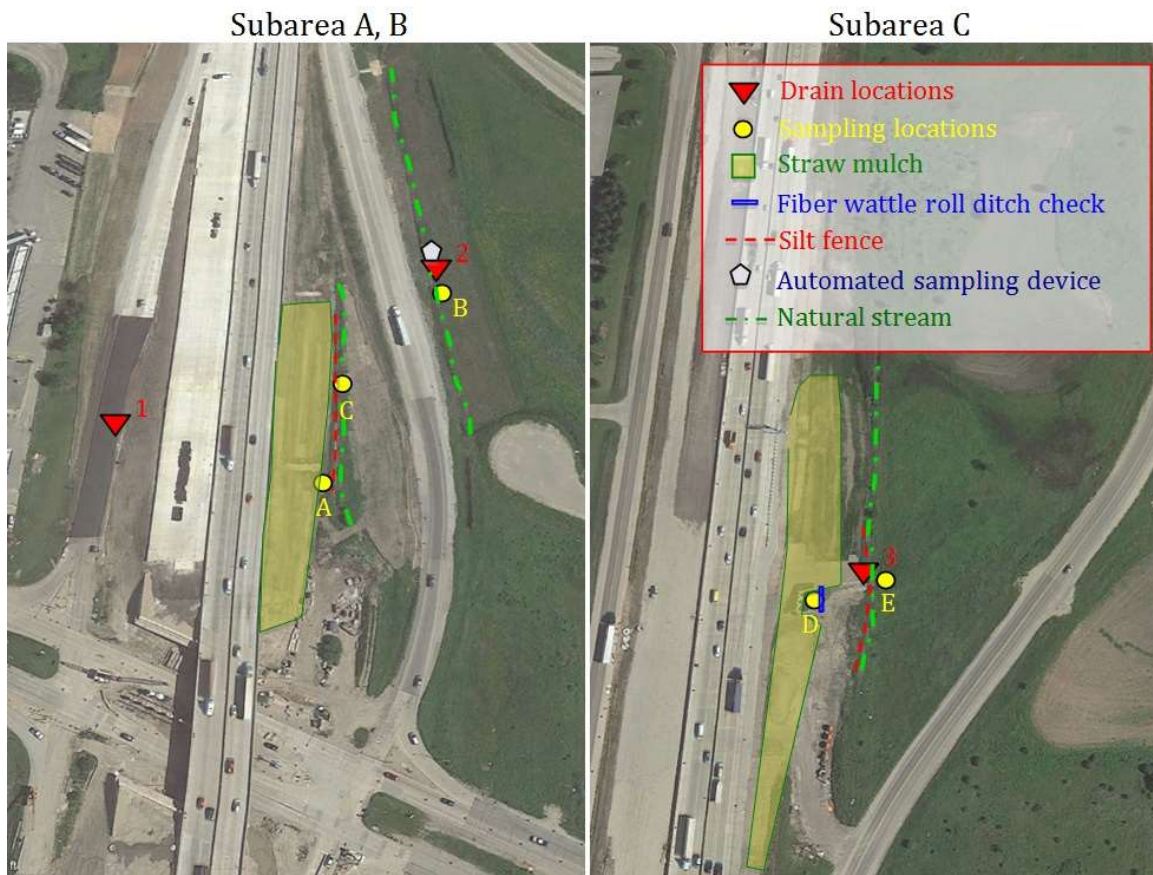
Figure 4.12: Major stormwater drain locations, BMP structures and sampling locations at the Racine construction site.

Figure 4.13: BMP controls on the Racine construction site. (a) Straw mulch covers disturbed soil and fiber wattle roll ditch check in the nature stream near sampling point C in figure 4.12; (b) silt fence and fiber wattle roll ditch check in the stormwater swale near sampling point D and E in figure 4.12.

Three field trips were made to acquire grab samples between March and July in 2015. Five sampling locations were identified and they are marked on figure 4.12:

- **Point A:** A natural stream (stormwater ditch) along disturbed soil, separated by a silt fence.
- **Point B:** A stormwater pipe outfall on the east side of the I-94 ramp which discharged into a natural stream.
- **Point C:** In the stream (stormwater ditch) before and after a fiber wattle roll ditch check.
- **Point D:** In a stormwater swale before and after a fiber wattle roll ditch check.
- **Point E:** East end of the stormwater swale near a natural stream, separated by silt fence.

The first field trip to this site was taken on March 6, 2015, when the air temperature was rising up quickly from freezing within 24 hours and significant runoff was generated from snow melting. The other two field sampling trips were conducted during the summer storm season. Measurement results of all filed experiments are listed in Table 4.3. At locations A, C, D and E, sample were collected on both sides of a BMP structure (silt fence or fiber roll ditch check), they are denoted as "upstream" and "downstream", respectively to indicate water sample before and after the BMP treatment. Figure 4.15 illustrates the turbidity values on both sides of these BMP controls measured during the field experiment on May 30, 2015.

The automated turbidity sampling device was deployed at the stormwater pipe outfall point (at the sampling point B in figure 4.12). This location is the outfall of runoff from subarea A and B on both side of I-94. The deployment method of the automatic sampling device is shown in figure 4.14.

Figure 4.14: Deployment of the automated turbidity sampling device near the outfall of a stormwater outfall at the Racine construction site.

Table 4.3: Grab sampling results on the Racine sampling site

Event #1: March 6, 2015 (Snow melting)					
Sampling start time		03/06 4PM		**Sampling end time**	03/06 5PM
Sampling point	*Turbidity on-site* (NTU)	*Turbidity Lab* (NTU)	*pH*	*Conductivity* (μS/cm)	*TSS* (mg/L)
A (upstream)	NA	463	7.8	2,760	326
A (downstream)	NA	468	7.9	2,780	339
D (upstream)	NA	266	8.2	1,366	263
D (downstream)	NA	357	7.9	2,680	311

Event #2: May 30, 2015					
Start time	5/30 4AM	**End time**	5/30 4PM	**Duration (hr)**	12
Total precipitation depth (in)	0.76	**Peak rainfall intensity (in/hr)**	0.09	**Average rainfall intensity (in/hr)**	0.06
Sampling start time		5/30 12PM		**Sampling end time**	5/30 1PM
Sampling point	*Turbidity on-site* (NTU)	*Turbidity Lab* (NTU)	*pH*	*Conductivity* (μS/cm)	*TSS* (mg/L)

A (upstream)	NA	190	8.1	986	99
A (downstream)	NA	179	7.9	1139	97
B	NA	292	7.5	1,463	198
C (upstream)	NA	273	7.5	1,493	199
C (downstream)	NA	286	7.5	1,415	187
D (upstream)	NA	110	7.7	1,762	NA
D (downstream)	NA	110	7.6	1,745	NA
E (upstream)	NA	354	7.7	1,766	210
E (downstream)	NA	389	7.7	1,764	267

Event #3: July 18, 2015					
Start time	07/18 1PM	**End time**	07/18 3PM	**Duration (hr)**	2
Total precipitation depth (in)	0.80	**Peak rainfall intensity (in/hr)**	0.77	**Average rainfall intensity (in/hr)**	0.40
Sampling start time		07/18 5 PM		**Sampling end time**	07/18 6 PM
Sampling point	*Turbidity on-site (NTU)*	*Turbidity Lab (NTU)*	*pH*	*Conductivity (µS/cm)*	*TSS (mg/L)*
B	1,224	1,429	7.3	2,004	767
C (upstream)	845	821	8.2	1,890	529
C (downstream)	829	834	8.1	1,917	571
D (upstream)	1,077	1,120	7.7	1,791	662
D (downstream)	1,135	982	7.9	1,781	679
E (upstream)	1,189	1,221	7.3	1,799	628
E (downstream)	1,175	1,245	8.1	1,787	677

Sampling point A — 190, 179

Sampling point C — 273, 286
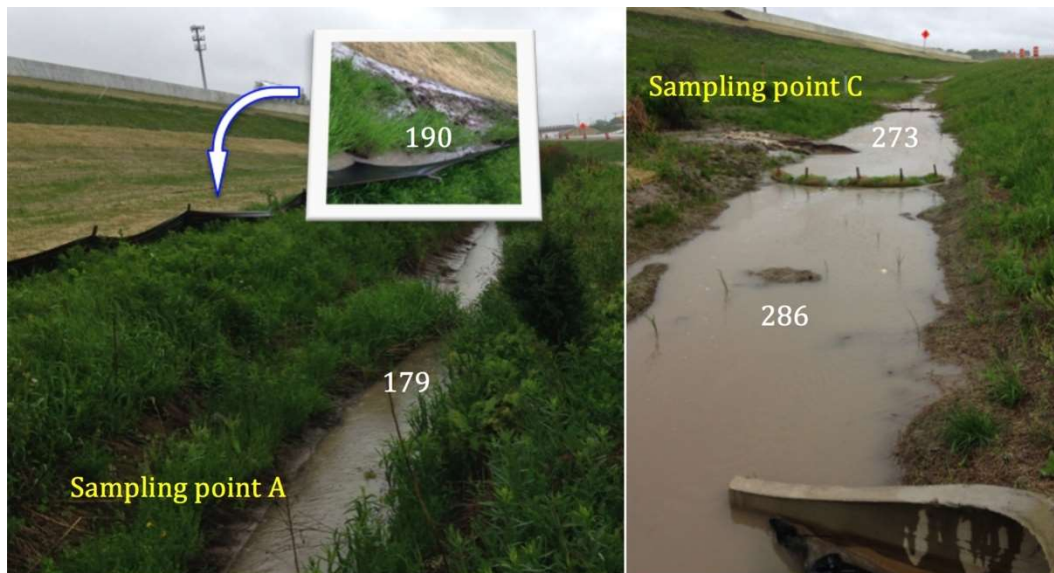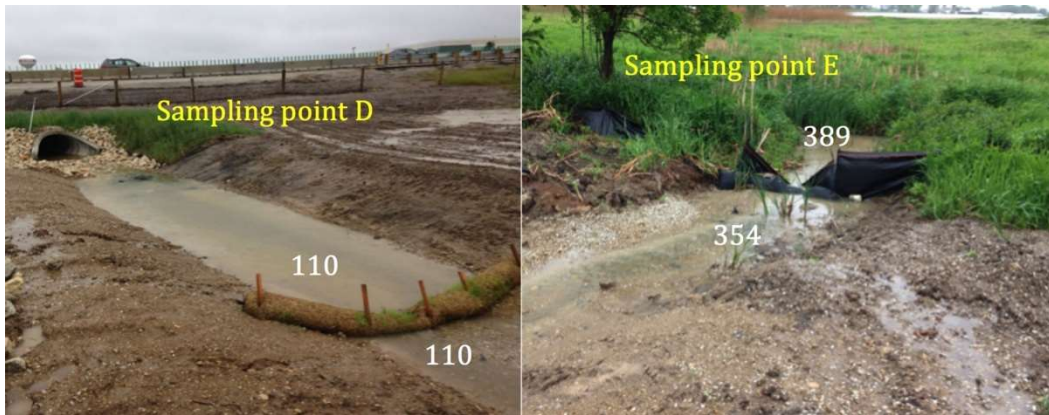
Figure 4.15: Turbidity values before and after BMP controls measured at the Racine site on May 30, 2015.

4.4   Site Four: STH-50 and US-12 near Lake Geneva, WI

Construction activities were conducted at the intersection of Wisconsin State Trunk Highway (STH) 50 and US Highway 12 during 2015. Three field-sampling trips were made from March to September of 2015. The area of soil disturbance was evaluated through site walk-through surveying. Two subareas of disturbed land surface were identified during that period; these are sketched out on Google Earth (cf. Figure 4.16).

Figure 4.16: Areas of disturbed land surfaces during June~September of 2015 at the Lake Geneva construction site: Area A at the northeast corner of the STH-50&US-12 intersection is about 6.25 acres. Area B at the southwest and southeast corners of the intersection is about 5.50 acres.

As shown in Figure 4.16, areas of the two subareas were estimated through the area tool of Google Earth, which were 6.25 and 5.50 acres, respectively. Visual observations during storm events indicated that there were two major stormwater discharge locations on the construction sites. As shown in Figure 4.16, runoff from subarea A flowed concentrically into the depressed area enclosed by the ramp. Since silt fences were installed around the perimeter of the circular area, most runoff from the southwest corner of this subarea convened at a natural stream. The runoff was then carried by the stream and flowed out of the area through a culvert inlet at point 1 shown in figure 4.17. In addition, a dewatering pipe was found at this site, which pumps water from northeast corner of the intersection to the culvert inlet area on the west side of US-12. Turbid water pumped out is then mixed with clean water and flows to the east through the stream, which also drained out of the area at point 1. Most runoff from the subarea B flowed into a stormwater pond through a stormwater pipe inlet at point 2 shown in figure 4.17.

Silt fences along the perimeter of disturbed land was the only major BMP measure that was identified during field experiments. This was possibly due to the relatively large vegetated areas around the construction site that may help to intercept stormwater runoff.
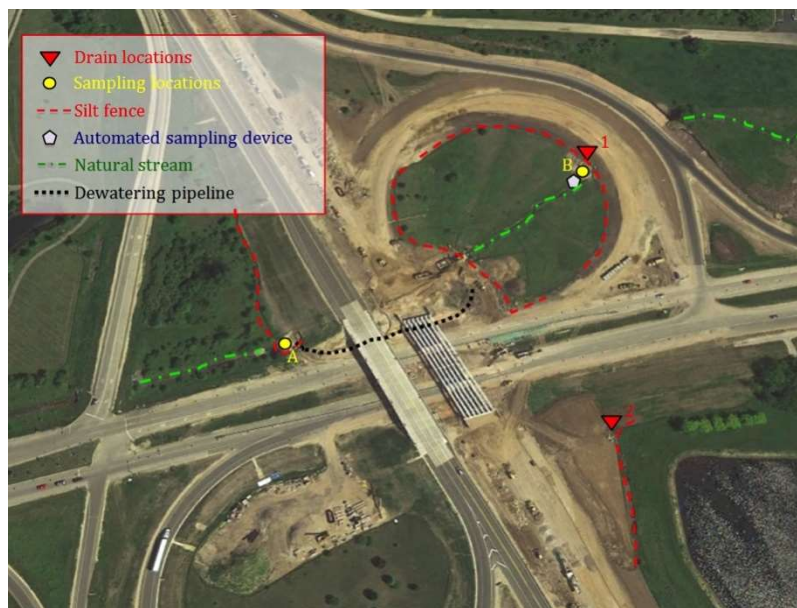
Figure 4.17: Major stormwater drain locations, BMP structures and sampling locations at the Lake Geneva construction site.

Three field trips were made to acquire grab samples between March and July in 2015. Two sampling locations were identified and they are marked on figure 4.17:

- **Point A:** A culvert inlet on the west side of US-12.
- **Point B:** A culvert inlet which drains the entire northeast corner of the intersection.

At point B, a silt fence was placed around the inlet to separate disturbed soil from the standing water. Samples were taken from both sides of the silt fence, denoted as "upstream" and "downstream", respectively. At point A, where the dewatering pipe discharged turbidity from the east side of the site, water samples were taken near the filter bag attached to the pipe and in the stream, and they are denoted as "filter bag" and "stream", respectively. Figure 4.18 shows the BMP structures and some sampling locations on the Lake Geneva construction site.

Figure 4.18: BMP measures and sampling locations on the Lake Geneva construction site. (a) silt fence around the depressed area on the northeast corner of the intersection, and the culvert inlet at sampling point B; (b) dewatering pipe running below the US-12 bridge; (c) dewatering pipe draining into the culvert inlet at the west side of US-12, and the sampling location A.

The first field trip to this site was taken on March 6, 2015, when the air temperature was rising up quickly from freezing within 24 hours, and significant runoff was generated from snow melting. The other two field experiments were conducted during the summer storm season. Measurement results of all filed experiments are listed in Table 4.4. Figure 4.20 illustrates the turbidity values measured on both sides of BMP controls of the two sampling locations.

The automated turbidity sampling device was deployed in the stream within the subarea A, just before the culvert inlet. The configuration of the deployed automatic sampling device is shown in figure 4.19.

Figure 4.19: Deployment of the automatic sampling device at the Lake Geneva construction site.

Table 4.4: Grab sampling results on the Lake Geneva sampling site

Event #1: March 6, 2015 (Snow melting)					
Water sample results	**Sampling start time**	03/06 2PM		**Sampling end time**	03/06 3PM
	Sampling point	*Turbidity on-site* (NTU)	*Turbidity Lab* (NTU)	*pH*	*Conductivity* (μS/cm)	*TSS* (mg/L)
	B (upstream)	NA	290	8.2	2,550	253
	B (downstream)	NA	196	7.7	1,638	129

Event #2: May 30, 2015					
Precipitation	**Start time**	5/29 9AM	**End time**	5/30 4PM	**Duration (hr)**	30
	Total precipitation depth (in)	0.76	**Peak rainfall intensity (in/hr)**	0.16	**Average rainfall intensity (in/hr)**	0.03
Water sample results	**Sampling start time**	5/30 3PM		**Sampling end time**	5/30 4PM
	Sampling point	*Turbidity on-site* (NTU)	*Turbidity Lab* (NTU)	*pH*	*Conductivity* (μS/cm)	*TSS* (mg/L)
	A (upstream)	NA	283	8.8	501	198

A (downstream)	NA	857	7.2	388	804
B (upstream)	NA	856	8.6	1,102	778
B (downstream)	NA	53	7.2	405	44

Event #3: July 18, 2015					
Precipitation	**Start time**	07/18 12PM	**End time**	07/18 2PM	**Duration (hr)**	2
	Total precipitation depth (in)	1.30	**Peak rainfall intensity (in/hr)**	1.17	**Average rainfall intensity (in/hr)**	0.65

Water sample results	**Sampling start time**		07/18 3:00 PM	**Sampling end time**		07/18 4:00 PM
	Sampling point	**Turbidity on-site (NTU)**	**Turbidity Lab (NTU)**	**pH**	**Conductivity (μS/cm)**	**TSS (mg/L)**
	A (upstream)	2,292	NA	7.9	1,501	1,864
	A (downstream)	1,970	NA	7.8	1,723	1,930

Figure 4.20: Turbidity values measured on both sides of BMP controls at the two sampling locations on May 30, 2015.

4.5 Site Five: STH-96 and Fox River near Wrightstown, WI

Construction activities were conducted near the bridge of Wisconsin State Trunk Highway (STH) 96 crossing over the Fox River at Wrightstown, WI. No field sampling trips were successful due to the distance from the UWM lab. The automated turbidity sampling device was deployed, however, to monitor the stormwater runoff from August to October, 2015. The area of soil disturbance was evaluated through site walk-through surveying. The area of disturbed land surface was identified during that period; this is sketched out on Google Earth (cf. Figure 4.21).

Figure 4.21: Areas of disturbed land surfaces during August~October of 2015 at the Wrightstown construction site: on the east bank of the Fox River along both sides of STH96, which is about 2.77 acres.

Figure 4.22: Major stormwater drain locations, BMP structures and sampling locations at the Wrightstown construction site.

As shown in Figure 4.21, the disturbed land area was estimated through the area tool of Google Earth, which was about 2.77 acres. Visual observations during storm events indicated that there were two major stormwater discharge locations on the construction sites. As shown in Figure 4.22, runoff from the area north of the bridge is collected and drained to a stormwater

inlet (point 1) and carried away southward through an underground pipe. Then stormwater from the pipe and the southern part of the area discharged at point 2. The effluent at point 2 then flowed into a swamp which could potentially drain to a stream at the south end. The stream flowed into the Fox River.

The Wrightstown site had a relatively small disturbed land area during the sensor deployment period. Silt fences along the perimeter of disturbed land were the major BMP measures that we could identify during field experiments (cf. Figure 4.22). In addition, pebbles were placed on some parts of the exposed soil for vehicle traffic which also helped to reduce erosion. Inlet protection was implemented at the stormwater drain (point 1).

Figure 4.23: (a) Low lying area under the bridge protected by silt fence; (b) Silt fence at the south side of the bridge that separates disturbed soil and a swamp; (c) stormwater drain pipe at the south side of the bridge; (d) Automated turbidity sensor deployed near the stormwater drain.

The automated turbidity sampling device was deployed near the drainage point 2 as shown in figure 4.20. Figure 4.23 shows the sample images of the construction site, BMP measures and the configuration of the deployed automated sampling device.

4.6   Summary of Field Grab Sampling Results

Four parameters of the stormwater runoff were measured from 54 field grab samples: turbidity, pH value, conductivity and total suspended solids (TSS). For 24 out of the 54 samples, turbidity was measured both on site with a handheld turbidimeter and in laboratory with a benchtop turbidimeter. Figure 4.24 presents the comparison of results with the two different methods, where the dashed line represents a 1:1 relation. A very good correlation (R^2=98%) is found between the two sensors. This indicates that a field turbidimeter may be as reliable as a more accurate laboratory device for turbidity measurement. It was also noticed that the difference between the two methods seemed to increase significantly when the turbidity level was high. For example, we found the average difference was greater than 10% as the turbidity was higher than 1,000 NTU. It should also be noted that samples with high turbidity level (>40 NTU) are diluted to an appropriate range before measurement in the lab procedure. Some of the difference can be attributed to the dilution effect, i.e., non-linear relation between turbidity and concentration of suspended solids and optical scattering.
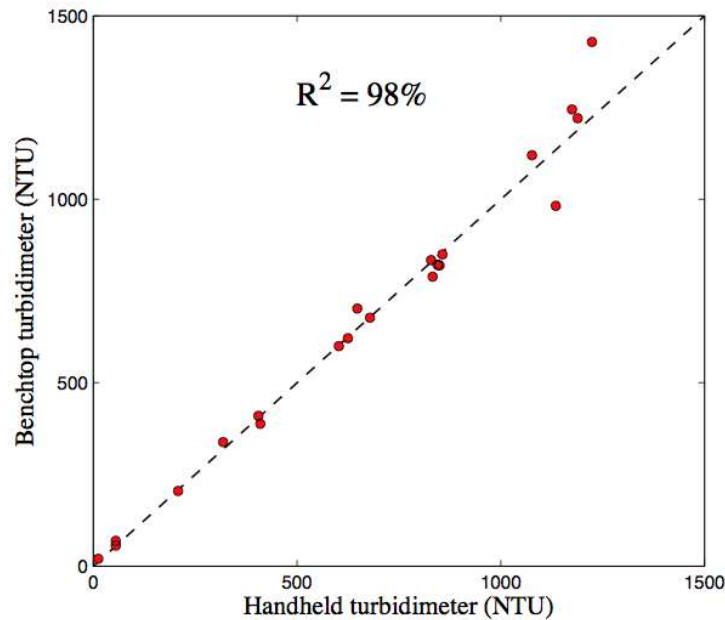
Figure 4.24: Comparison of turbidity levels measured by the handheld turbidimeter for on-site measurements and those by the laboratory bench-top turbidimeter. The dashed line represents a 1:1 relation.

Figure 4.25 shows the histogram of all measured turbidity levels for the 54 grab samples. On-site turbidity results were primarily used for this analysis, and lab measurement results were used when on-site results were not available.
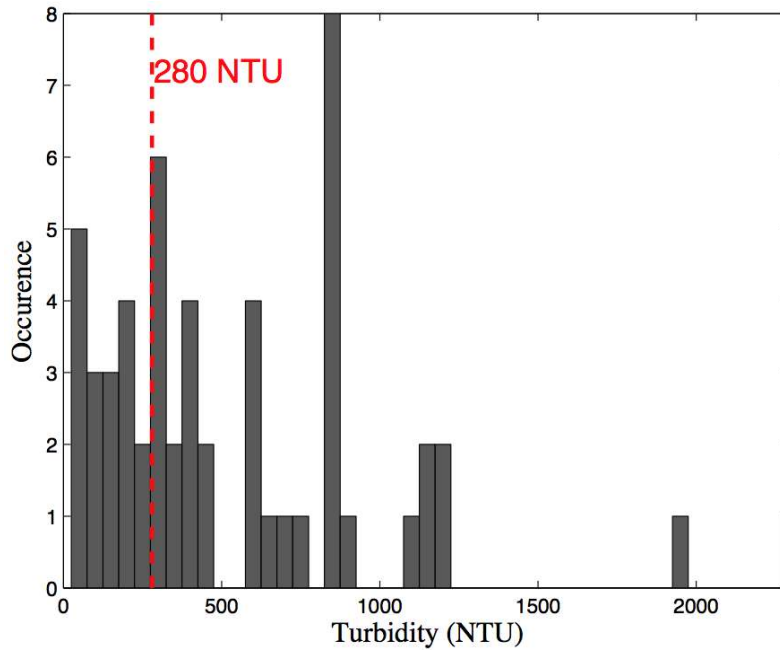
Figure 4.25: Histogram of turbidity of the 54 field grab samples.

Measured turbidity ranged from 20 to 2,300 NTU, and the average was about 570 NTU. 37 out of the 54 samples (69%) are higher than EPA's numeric limits of 280 NTU, even though all areas of disturbed land in this study were less than 20 acres, and all storm events were smaller in magnitude compared with that of the local 2-year 24-hour event.

pH values were measured from 51 out of the 54 samples. Figure 4.26 shows the histogram of the pH values. Measured pH values ranged from 7.2 to 9.2, with an average of 7.9. Most of these samples were within the required numeric limit of 6.0~9.0. Most high pH samples (pH>8.8) were found in the Wauwatosa site where concrete work was the most significant among all sampled sites.
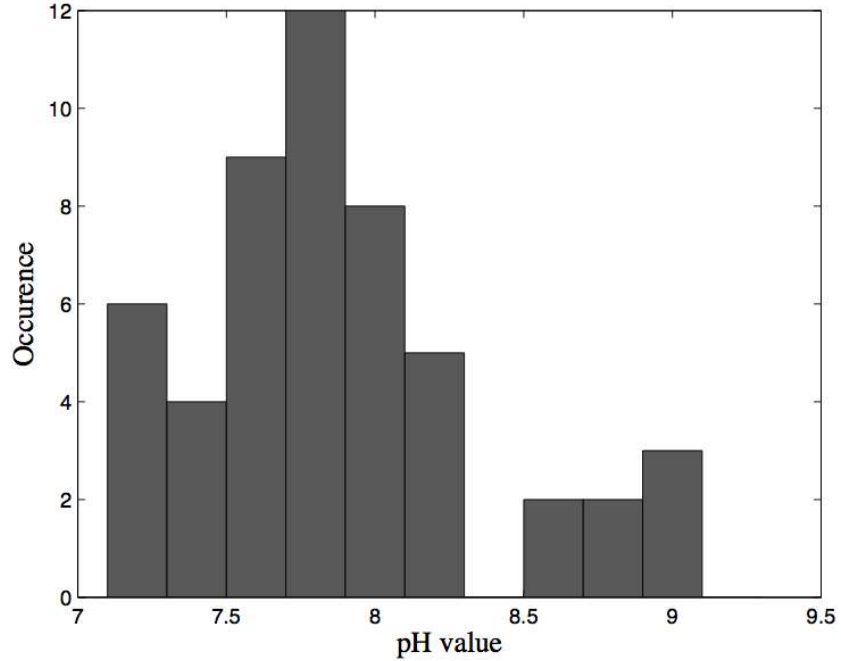
Figure 4.26: Histogram of pH value of field grab samples.

Conductivity was measured for 49 out of the 54 grab samples and figure 4.27 shows the histogram of these samples. Measured conductivity ranged from about 380 to 3,200 μS/cm, with an average of about 1,500 μS/cm.
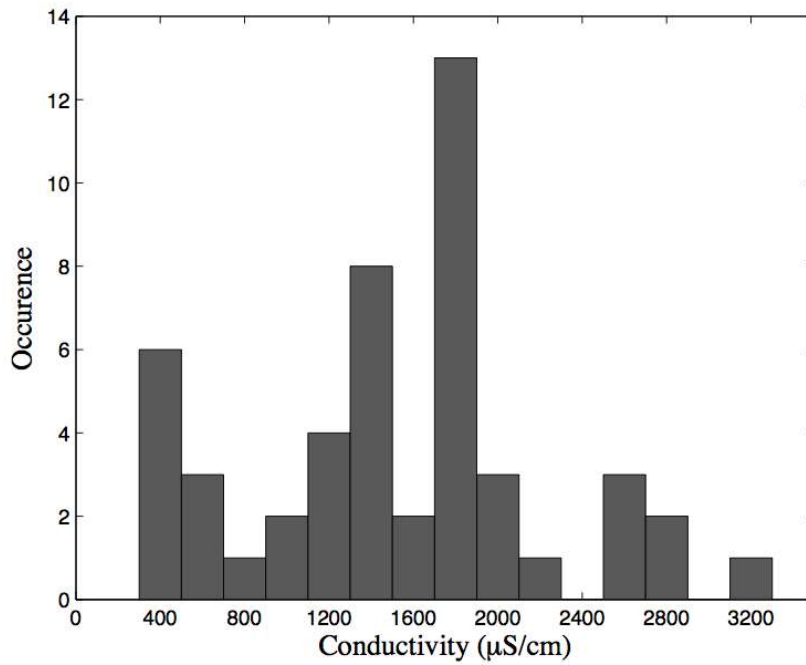
Figure 4.27: Histogram of conductivity of field grab samples.

TSS concentration was measured for 44 out of the 54 samples and figure 4.28 shows the histogram of these samples. Measured TSS ranged from about 12 to 1,930 mg/L, with an average of about 550 mg/L.
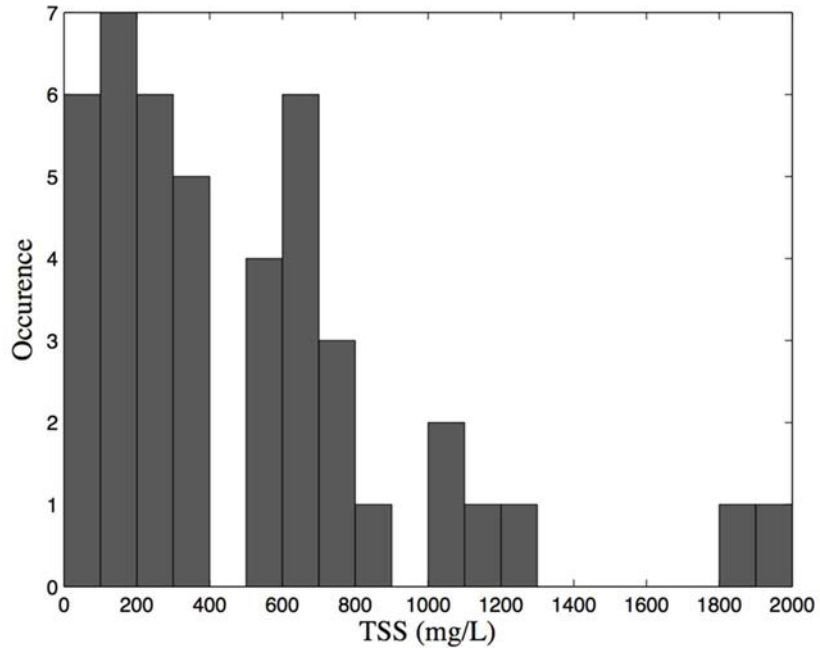
Figure 4.28: Histogram of TSS concentration of field grab samples.

No correlation could be found among the turbidity, conductivity and pH value, as shown in figure 4.29.
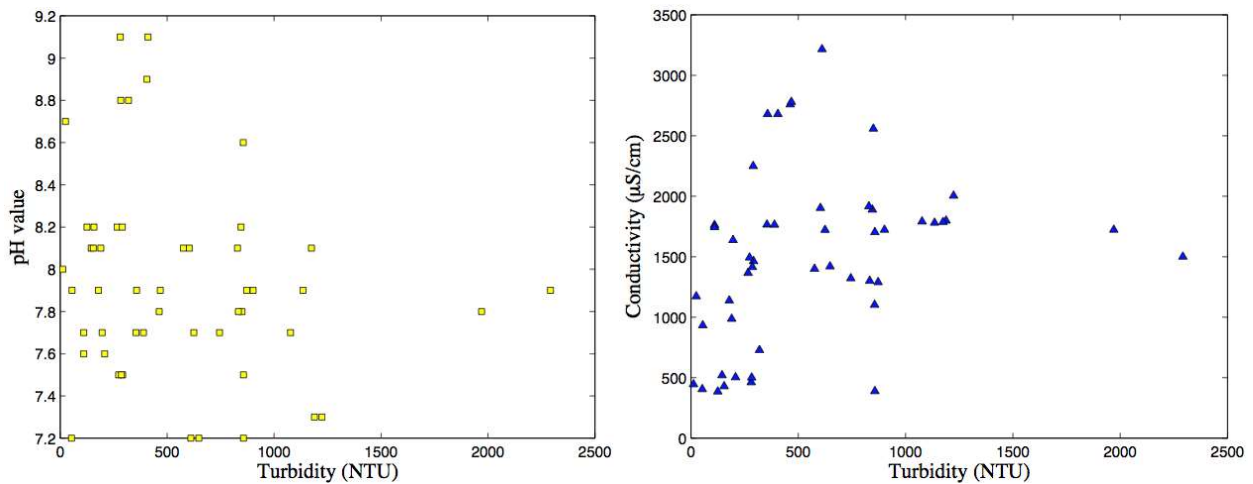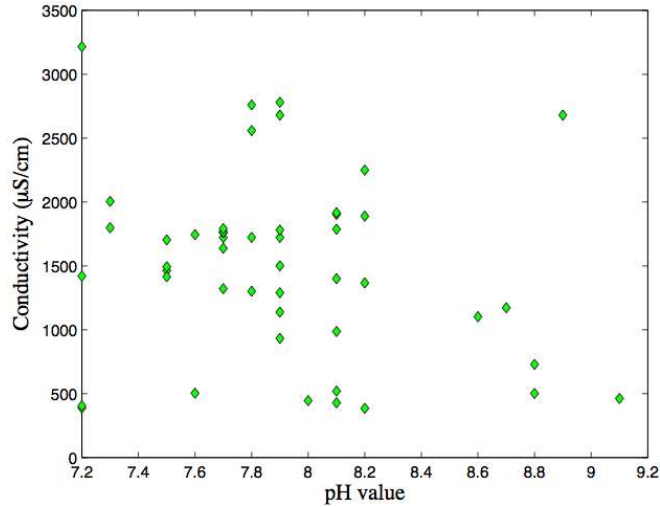
Figure 4.29: Relations among turbidity, pH value and conductivity of field grab samples.

Samples with measured values of both TSS concentration and turbidity were selected to evaluate their correlation. As shown in figure 4.30, an overall linear relation is found for most of these samples. Soil samples from these sites were also collected to generate synthetic turbidity runoff and to study the TSS-turbidity relation. Results from modeled samples and the field grab samples are discussed in detail in Chapter 5.
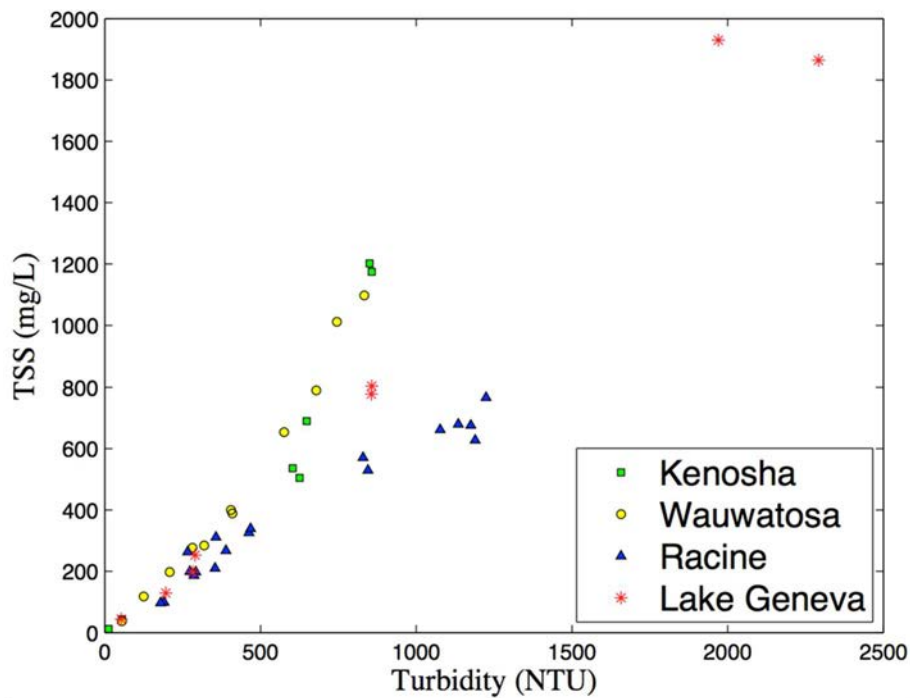
Figure 4.30: Correlation between TSS concentration and turbidity in NTU for field grab samples collected at four construction sites.

Field observations found that traditional BMP controls are not able to effectively reduce the turbidity. As shown in figure 4.5 and 4.15, straw bale checks or fiber wattle rolls in stormwater ditches can reduce the water flow speed, and hence may help to reduce the concentration of large particles through settling. They have, however, little effects on the turbidity level, which is largely due to suspended fine soil particles.

Field observations found that turbid water can leak out of a silt fence through subsurface flow, and the turbidity level does not seem to decrease as it flows through the soil media. However, silt fence should still be considered as an effective way to control turbidity runoff since it can intercept a significant amount of surface runoff, reduce flow speed, and facilitate infiltration, thereby reducing the total sediment discharge into a receiving water body. Silt fence failures were frequently found during our field surveys, particularly at locations where they were placed against a concentrated flow (cf Figure 4.15).

A slight decrease of turbidity was observed as runoff flows through a retention pond (cf Figure 4.5), possibly due to the settling of larger particles. Thus retention pond should not be considered as an effective method for turbidity control unless coagulants are applied to facilitate settling of fine particles.

Chapter 5
Turbidity and TSS Concentration Relation

This chapter presents results of laboratory experiments that examined the correlation between the turbidity (in NTU) and the concentration of total suspended solids (TSS), using samples collected from a lab simulated rainfall-runoff system and from the field experiments. The time series of runoff turbidity from the simulated system is also presented.

5.1   Time Series of Turbidity of Lab-Simulated Runoff

Soil samples from four selected sites (Kenosha, Racine, Wrightstown and Wauwatosa) were collected to generate laboratory simulated rainfall-runoff processes, following the procedures described in section 3.5. Water samples from both surface runoff and subsurface interflow runoff were collected to measure the turbidity and TSS. Time sequences of turbidity in effluents from the Racine soil sample were also recorded to examine the general variation of turbidity as a function of time. Two tests were conducted on the same soil sample. The second test started 16 hours after the end of the first. For both tests, the simulated rainfall (from a garden hose sprinkler) intensity was adjusted to avoid excessive ponding on the soil surface. Runoff water from both the near surface PVC pipe and the buried PVC pipe were then collected at designed intervals. Turbidity was measured for the both samples separately and for their mixture, which represents the combined runoff from both surface flow and the subsurface groundwater flow (interflow). The time series of turbidity from the two tests are shown in Figure 5.1.
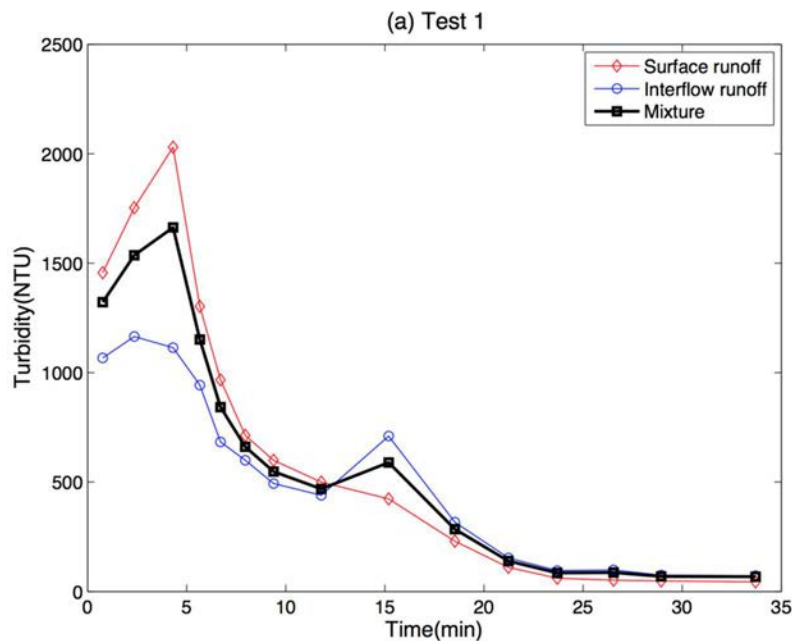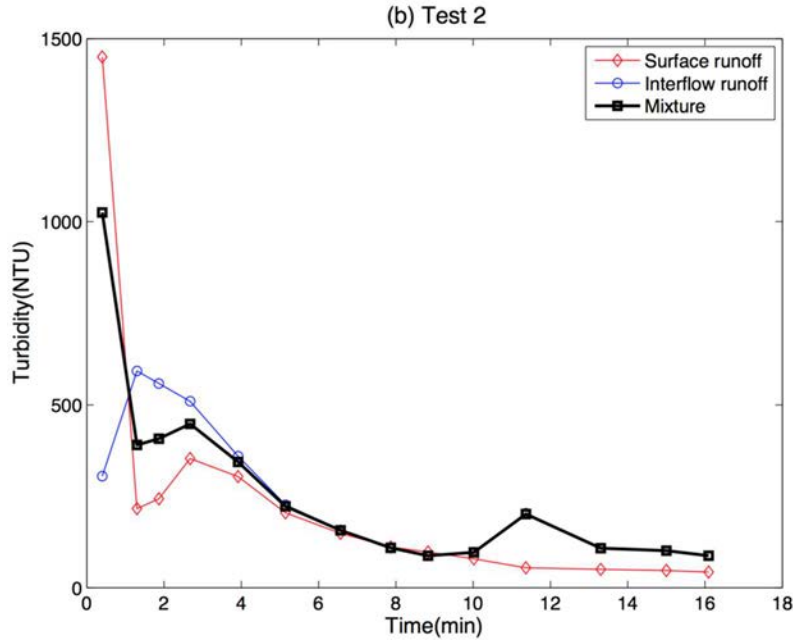
Figure 5.1: Time series of turbidity in the effluents of the laboratory simulated rainfall-runoff process.

For both tests, the turbidity level in the effluent increased rapidly to a peak value as rainfall started. It then decreased gradually as time progressed. The volumetric flow rate from the buried interflow pipe was much lower than that from the surface flow pipe at the beginning of the process, but it began to exceed the surface runoff after about 10 minutes. Consequently, the turbidity level reached a second peak soon after the interflow exceeded the surface runoff (at about 15 minutes in test 1 and 12 minutes in test 2). For the surface runoff, however, the turbidity decreased monotonically without a secondary peak. The second peak can also be observed for the combined runoff (mixture of two samples) as the interflow volume dominated at that time.

The maximum turbidity in the combined runoff of test 1 reached to 1,663 NTU at about 5 minutes after the "rainfall" started. As the second test started 16 hours after the first, when the soil was still nearly saturated, the surface runoff turbidity was high at the beginning (about 1,450 NTU). It decreased sharply to 216 NTU after 1 minute. If the initial high level of turbidity which lasted for a short period of time can be ignored, the peak turbidity (354 NTU) in the surface runoff started at about 3 minutes into the procedure. Overall, turbidity was much lower in test 2 compared with that in test 1. This suggests that significant amount of fine soil particles was washed out during the first test, which started with a dry condition. Runoff turbidity could be lower if the precedent soil moisture is high, as suggested by test 2.

5.2 Relation between Turbidity and TSS

Linear regression analyses were applied to examine the relation between turbidity and TSS using the equation:

$$\text{TSS} = b \, \text{Turbidity} \tag{5.1}$$

where the coefficient b is a parameter which may depend on geometric and optical characteristics of the particles, as well as the configuration of the light beam of the turbidimeter. Linear regression was applied to both lab samples from the rainfall-runoff simulation and from field grab samples, as shown in figure 5.2. For the Wrightstown site, only the simulated samples are used since no field grab samples were available.
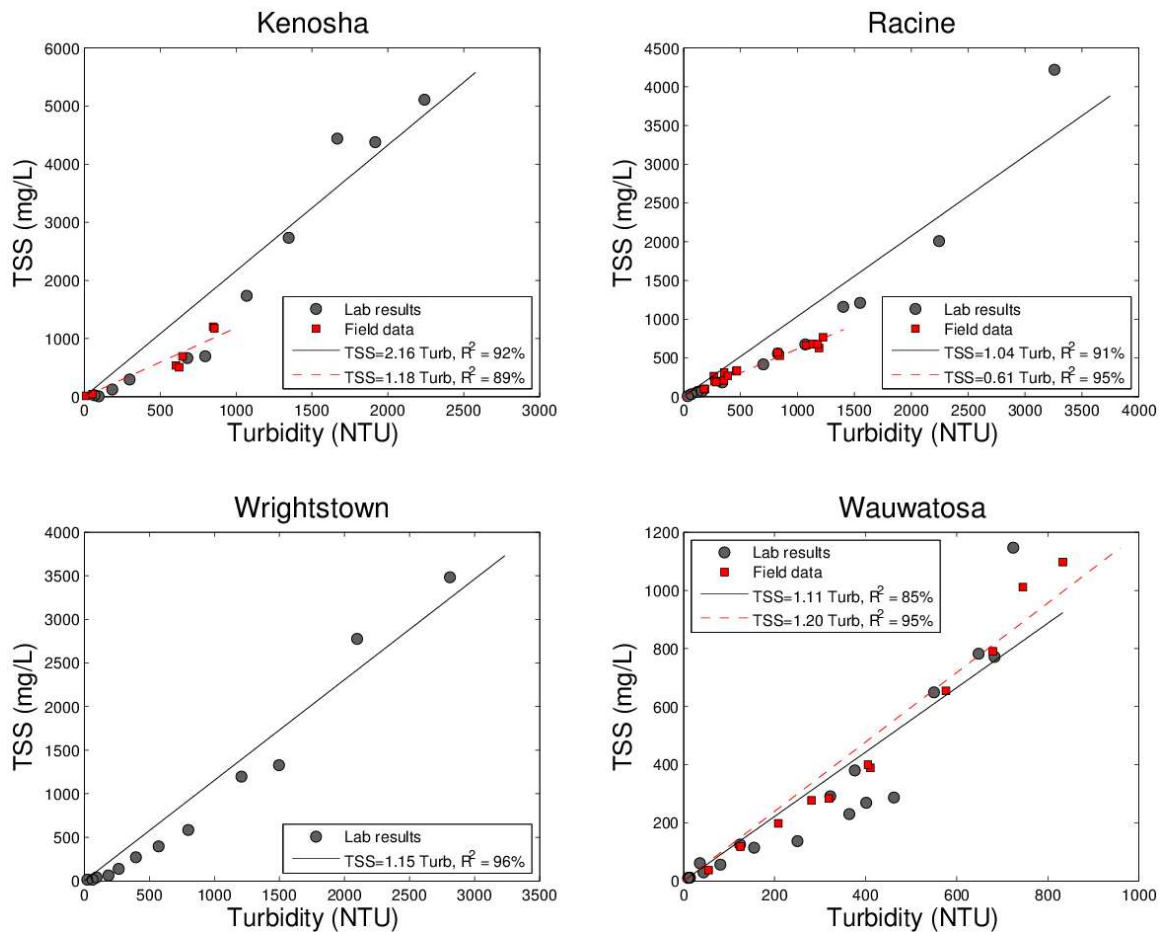
Figure 5.2: Linear regression between TSS and turbidity NTU for both lab simulated samples and field grab samples.

All samples show a good linear relation between TSS and NTU, however the coefficient *b* varied between 0.61 and 2.16. For Racine, Wrightstown and Wauwatosa sites, the coefficient *b* obtained from lab simulated runoff samples were very close, which are 1.04, 1.15 and 1.11, respectively. It was however, much higher for samples from the Kenosha site (*b*=2.16). Moreover, this coefficient differed significantly between the lab sample and field grab sample for the Kenosha and Racine sites. A close inspection indicated that the difference can be explained by the nonlinear relation for higher turbidity and TSS values presented in the lab simulated samples. In the lower range, the linear relation seemed to agree better between the lab and field samples. Figure 5.3 shows the same analysis applied for the turbidity range from 0 to 1,500 NTU for Kenosha and Racine site samples. It appeared that the linear relations were more consistent between the lab and field samples, and all data seemed to collapse well into a unified relation.
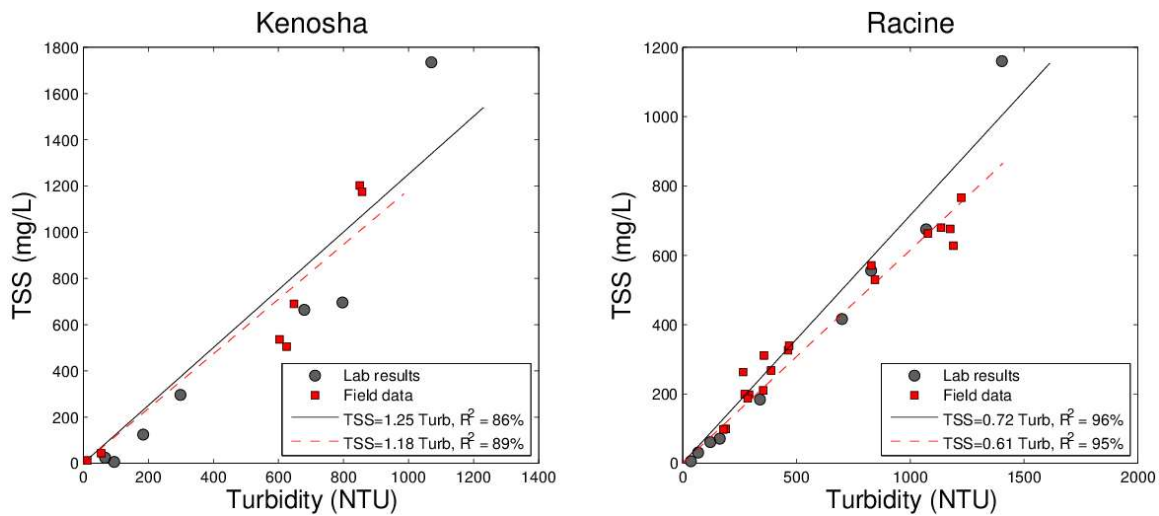
Figure 5.3: Linear regression between TSS and turbidity NTU for both lab simulated samples and field grab samples with the turbidity ranged from 0 to 1,500 NTU.

As pointed out by Perkins et al. (2014), the TSS-turbidity relation should be more generally considered as nonlinear, and a power-law function can be applied for a wider range of applications. In this study, an iterative nonlinear curve fitting was applied to lab-simulated samples with the following equation:

$$\text{TSS} = \alpha \, \text{Turbidity}^{\beta} \qquad\qquad (5.2)$$

the best fit parameters α and β are also applied to predict the relation for field grab samples. Results of this analysis are shown in figure 5.4.
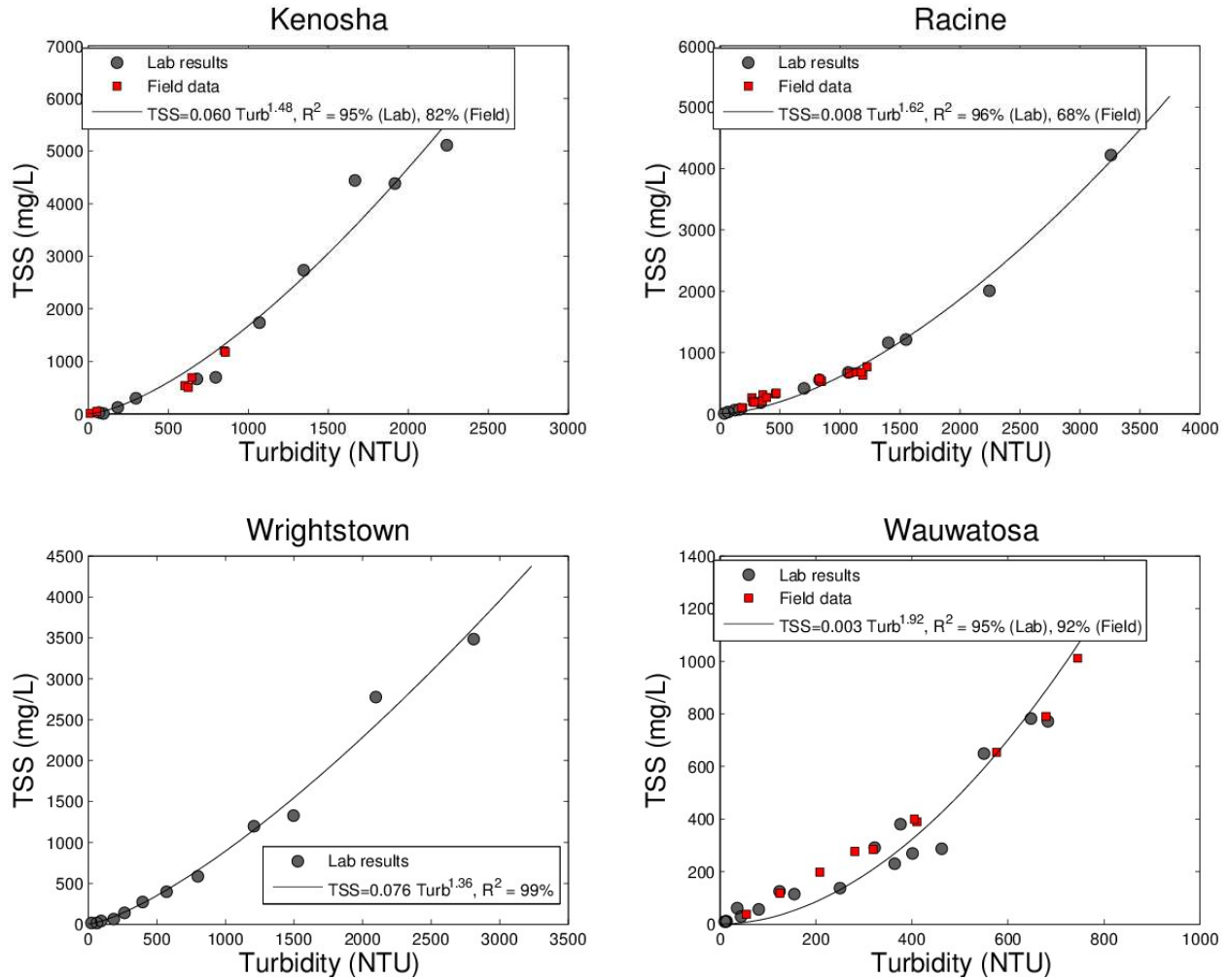
Figure 5.4: Power law based nonlinear regression between TSS and turbidity NTU for lab-simulated runoff samples, and the prediction result of the field grab samples with the best-fitted parameters.

The nonlinear fitting showed that the power law can describe the TSS-turbidity relation very well for lab-simulated runoff water, with the coefficient of determination $R^2 > 95\%$ for all four samples. The fitted model can also predict the TSS-turbidity relation for field grab samples fairly well ($R^2 = 82\%$, 68% and 92% for the Kenosha, Racine, and Wauwatosa sites, respectively). The exponent β for the four site samples varied between 1.36 and 1.92, which falls into a fairly narrow range. It should be noted that Perkins et al. (2014) found that Turbidity $\sim TSS^{1.4}$ is a good model for all soil samples from 14 construction sites in Minnesota. Transforming this relation into a format which is equivalent to equation (5.2) in this study, i.e., representing TSS as a function of Turbidity, it suggests

$$TSS \sim Turbidity^{\frac{1}{1.4}} = Turbidity^{0.714} \tag{5.3}$$

Their result ($\beta = 0.714$), however, differs significantly from what was determined for the four construction sites in Wisconsin, where $\beta = 1.36 \sim 1.92$.

Despite the good fit with the power law model, the coefficient α for the four sites varies from 0.003 to 0.06. It appears to be very sensitive to the variation of soil samples and measurement errors.

Results and analyses presented in this chapter show that for the three sites where both lab and field samples were available, the TSS-turbidity relation can be well characterized by generating simulated runoff from soil samples. The relation, once calibrated, can be used to estimate the concentration of suspended solids with a much simpler turbidity measurement. This allows continuous monitoring of TSS concentrations of effluent from construction sites.

Chapter 6
Correlation between Runoff Turbidity and Precipitation

6.1   Introduction

To date, there is no reported literature that documents the relation between the turbidity of stormwater runoff from construction sites and the hydrological properties of precipitation events. Questions remain whether statistical correlations exist, and his information is critical for future construction site stormwater management and for the possible change of policies from U.S. EPA and other environmental regulation agencies. For example, according to the initial effluent limitations guidelines published by EPA in 2009, the 280 NTU limitation does not apply on days when the total precipitation on that day is greater than the local 2-year, 24-hour storm event.

Parameters that may affect the relationship between turbidity and precipitation include, but are not limited to: precipitation depth, intensity and duration, land area disturbed, type of soil, topography, the runoff coefficient of the disturbed area, as well as geographic location. Rapid changes to the landscape of the site during each phase of the construction activities may also contribute to the variation of sediment concentration and turbidity during stormwater runoff events.

Large sets of data are needed and there are numerous challenges to explore these correlations, if they ever exist. Field grab sampling during a storm event is a relatively reliable method to obtain accurate turbidity result at desired locations. It is, however, expensive to obtain a large dataset from a site for a number of events, especially for remote sites. For a given construction site, the volume of runoff and the sediments carried vary in spatial location and time. Plans for field data acquisition should consider the location and time of sampling as important parameters for conducting statistical analysis on the measured results.

In this study, data for statistical analysis have been largely acquired from the developed automated turbidity sampling system described in Chapter 3.4. Hydrological data are obtained through a publicly available database from either NOAA or USGS. This chapter presents the time series of turbidity measured from major outfall locations at 4 of the 5 selected sampling sites during the summer and fall of 2014 and 2015. Parameters of turbidity include its peak and mean values, and the runoff duration for each storm event. Statistical analysis was applied to these parameters to explore their correlation with precipitation data, which included the total depth, peak and mean rainfall intensity as well as the duration.

6.2 Characteristics of Precipitation Events at the Sampling Construction Sites

Precipitation is considered as the primary hydrological driving term for the sediment runoff from construction sites. Precipitation data were obtained from NOAA's National Centers for Environmental Information (formerly the National Climate Data Center, NCDC) through the public link: http://www.ncdc.noaa.gov/orders/qclcd/. The source data are ASCII files, with one file per month for all NOAA land based stations. A Matlab program was developed to extract the hourly precipitation according to the specific weather station ID. The station ID is denoted as "WBAN" in the NOAA's published weather data file. The WBAN for the nearest stations to the 4 sampling sites and the description of these stations are listed in Table 6.1.

In addition, precipitation near the Wauwatosa sampling site was obtained from US Geological Survey (USGS)'s online real-time database through the public link: http://waterdata.usgs.gov/wi/nwis/rt. The nearest USGS station to the West Allis sampling site and its description are also listed in table 6.1.

The geographic locations of these weather stations and the sampling locations for the 5 selected construction sites are presented in figure 6.1. Most rain gage stations are less than 10 miles away from the construction sites (except for the Lake Geneva sampling site, which is about 10.6 miles away from the rain gage station). It was assumed the precipitation time series (i.e., the hyetograph) recorded with a one-hour interval represented the actual rainfall process that occurred on the construction site.

Magnitudes of storm events are usually categorized by their recurrence interval (or frequency, return period) and duration, e.g., a 10-year 24-hour storm. Events described by frequency and duration can be translated to a specific rainfall amount in terms of precipitation depth, depending on the local meteorological conditions. Such a translation is also known as the rainfall Intensity-Duration-Frequency (IDF) relation, where the intensity is defined as the precipitation depth divided by the duration. The 2-year precipitation depth-duration relations for the 5 sampling sites are shown in figure 6.2, with data obtained from the National Weather Service (NWS) Precipitation Frequency Data Server (PFDS, http://hdsc.nws.noaa.gov/hdsc/pfds/other/wi_pfds.html). Precipitation depth of the 2-year 24-hour event, hereafter denoted by $P_{2\text{-}24}$, has been considered as a reference magnitude for the analysis, according to EPA's 2009 ELG requirement. The corresponding $P_{2\text{-}24}$ values of the five sampling sites are presented in table 6.2. Due to the geographic proximity, rainfall depth-duration curves for the three sites in the southeast Wisconsin region (Kenosha, Racine and Wauwatosa) are almost indistinguishable, as shown in figure 6.2. Overall, the Lake Geneva site has the highest precipitation depth and the Wrightstown site is the lowest among all five sites. Averaged $P_{2\text{-}24}$ for the five sites is 2.32 inches, with a standard deviation of 0.14 inches.

Table 6.1: Description of NOAA and USGS weather stations near turbidity sampling sites

Turbidity Sampling sites	Local Weather Station ID	Data source	Station description	Latitude	Longitude	Distance from the sampling site (mile)	Data period
Kenosha	04845	NOAA	Kenosha regional airport, Kenosha, WI	42.595	-87.93806	1.6	No data
Racine	94818	NOAA	John H Batten airport at Racine, WI	42.7611	-87.81361	7.7	06/01/2015~09/01/2015
Lake Geneva	04866	NOAA	Burlington municipal airport, Burlington, WI	42.69	-88.30361	8.4	06/01/2015~09/01/2015
Wrightstown	14898	NOAA	Austin Straubel International airport, Green Bay, WI	44.4794	-88.1366	10.5	09/01/2015~10/20/2015
Wauwatosa	0487088	USGS	Underwood creek, Wauwatosa, WI	43.0547	-88.0461	2.3	08/01/2014~09/30/2014
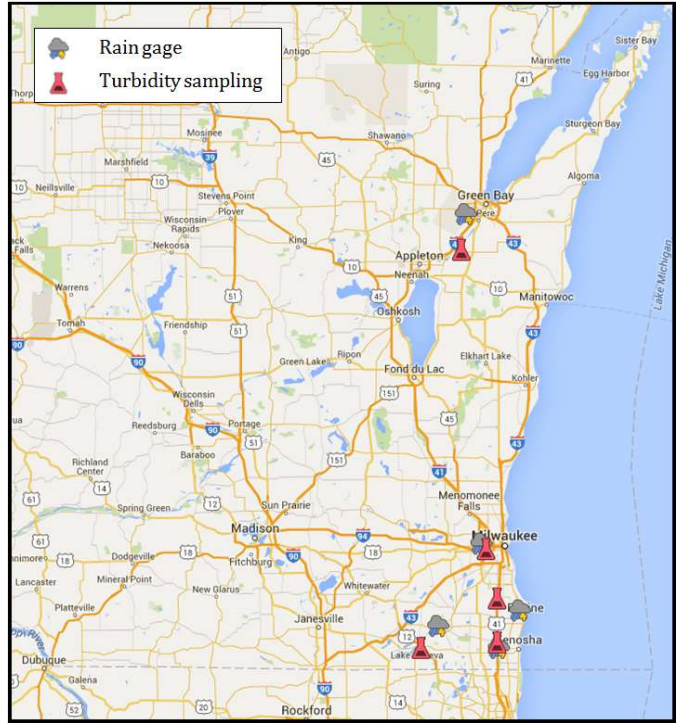
Figure 6.1: Locations of automatic turbidity sampling deployments and the nearby NOAA/USGS weather stations.

Figure 6.2: Precipitation depth-duration relation for 2-year events at the five sampling sites
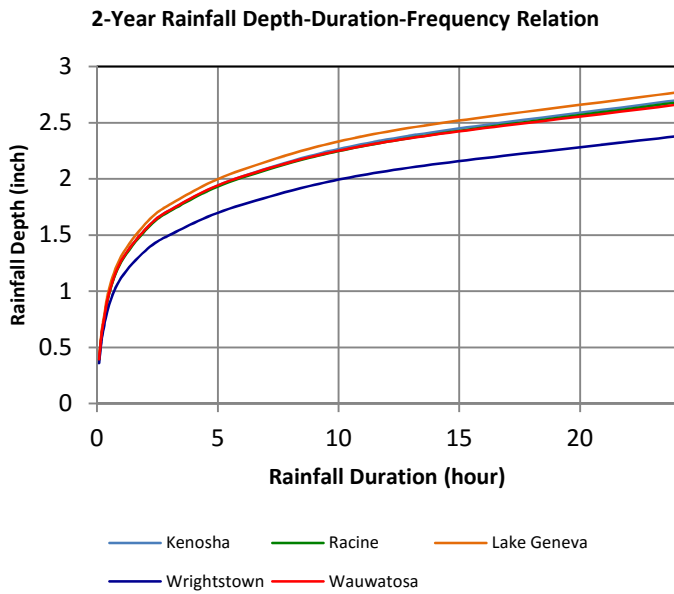
Table 6.2: Precipitation depth of 2-year 24-hour events ($P_{2\text{-}24}$)at the five sampling sites

Sampling sites	$P_{2\text{-}24}$ (inch)
Kenosha	2.70
Racine	2.68
Lake Geneva	2.77
Wrightstown	2.38
Wauwatosa	2.66

Summarized precipitation events, including the total depth, average intensity and duration during the deployment period of the automatic turbidity sampling systems at four sites are shown in figures 6.3~6.6. Here, each individual event was defined in such a way that the separation time between two consecutive events is longer than 12 hours. This threshold was selected based on our observation that turbidity runoff events observed in this study had an averaged time scale of about 12 hours. Most events presented here were continuous events. The pause period (i.e., the period when rainfall intensity = 0) in each event was usually less than 2 hours.

The rainfall-runoff volume relation can be estimated with the Curve Number (CN) method according to the USDA Natural Resources Conservation Service (formerly called the US Soil Conservation Service). The direct runoff, or the rainfall excess (P_e) after accounting for infiltration and other abstractions, is related to the precipitation depth (P) using the Curve Number equation:

$$P_e = \begin{cases} 0 & \text{if } P - \dfrac{200}{CN} + 2 < 0 \\[2ex] \dfrac{\left(P - \dfrac{200}{CN} + 2\right)^2}{P + \dfrac{800}{CN} - 8} & \text{if } P - \dfrac{200}{CN} + 2 > 0 \end{cases} \qquad (6.1)$$

where CN is the curve number that is related to the soil type, soil infiltration capacity, antecedent soil moisture and the land surface cover. Typical Wisconsin soil consists primarily of clay with a high swelling potential, thus the infiltration rate is low when thoroughly wetted. A category D can be assigned in the Curve Number method, and the typical CN value for disturbed land on these construction site can be selected as $CN = 85$. According to equation (6.1), no direct runoff will be generated if the cumulative rainfall depth is less than 0.35 inches.

Many rainfall events recorded in this study were less than 0.35 inches (see figures 6.3~6.6), however, significant turbidity increase was observed for these minor events even no direct runoff is expected. The increased turbidity could be due to the interflow runoff from the unsaturated subsurface zone. Therefore, these minor events are also included in our analysis. Events with total depth less than 0.1 inches are excluded as no significant turbidity increase was observed.

It should also be noted that no recorded events during the sampling period exceeded the local 2-year 24-hour magnitude ($P_{2\text{-}24}$).
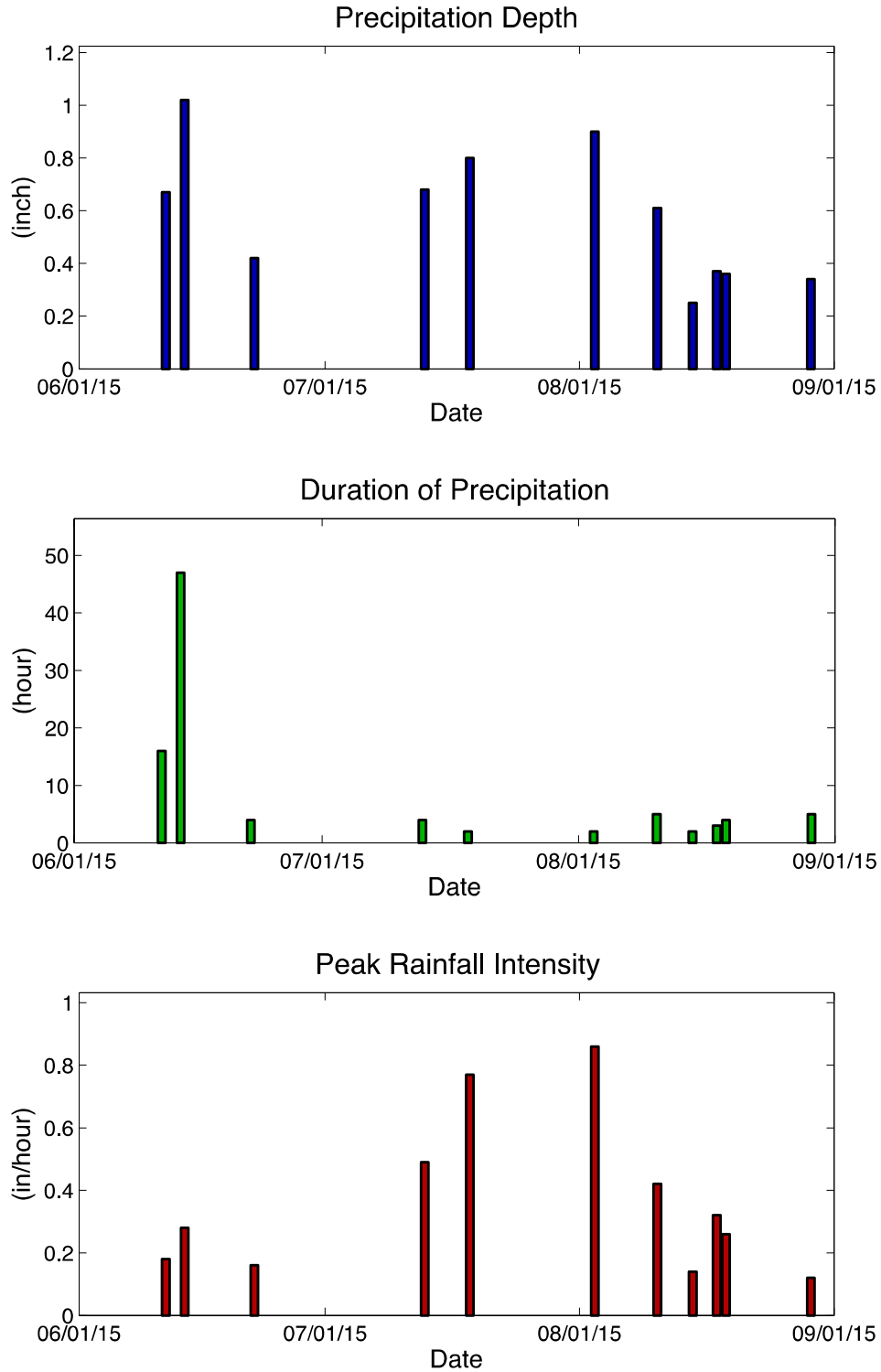
Figure 6.3: Major precipitation events (rainfall depth >0.1 inches) at the Racine construction site from June 1st to September 1st, 2015.
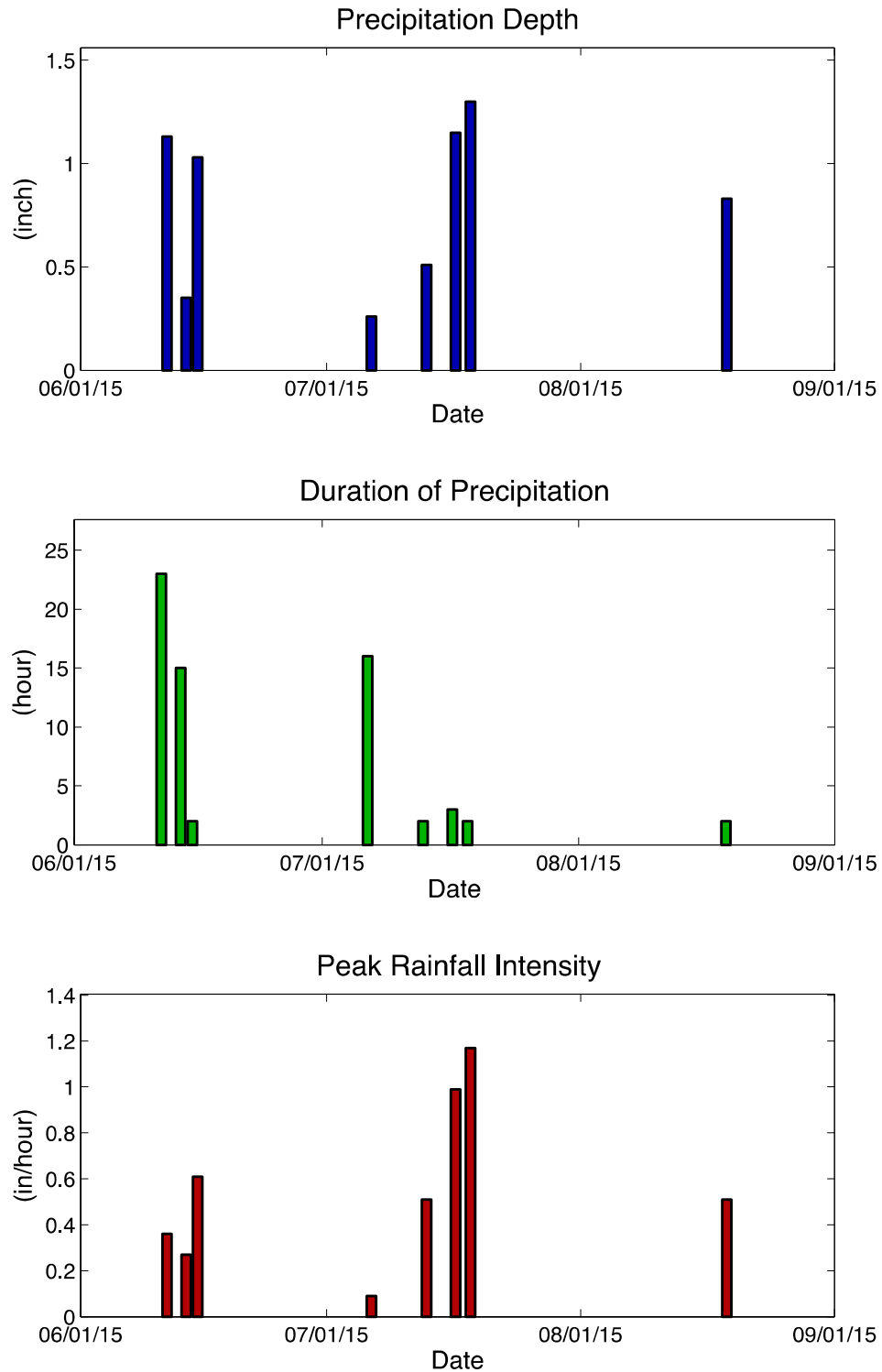
Figure 6.4: Major precipitation events (rainfall depth >0.1 inches) at the Lake Geneva construction site from June 1st to September 1st, 2015.
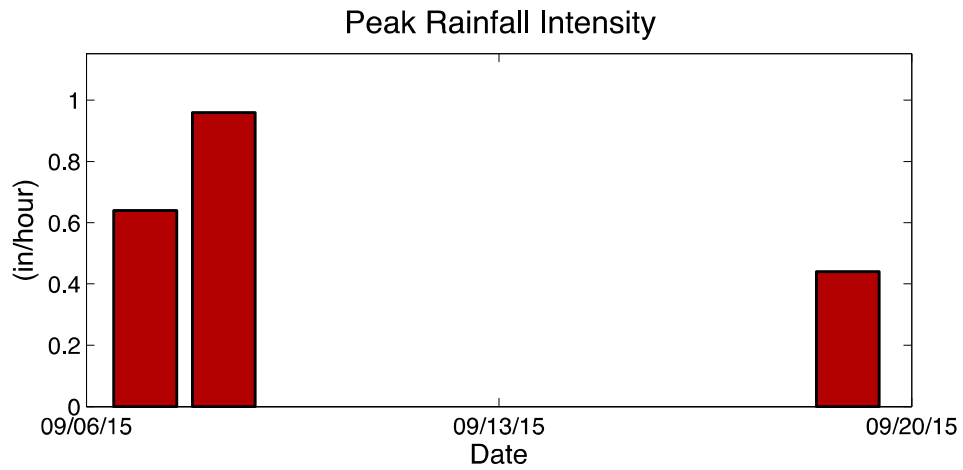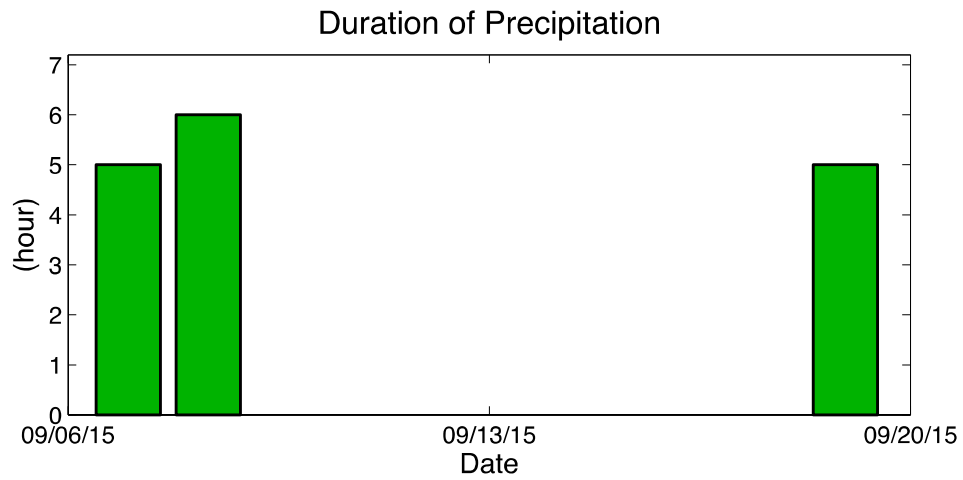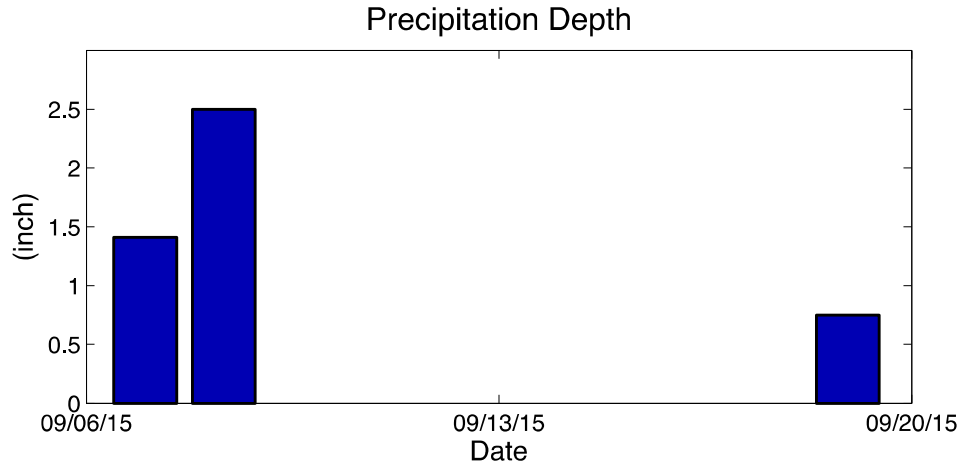
Figure 6.5: Major precipitation events (rainfall depth >0.1 inches) at the Wrightstown construction site from September 6th to September 20th, 2015.
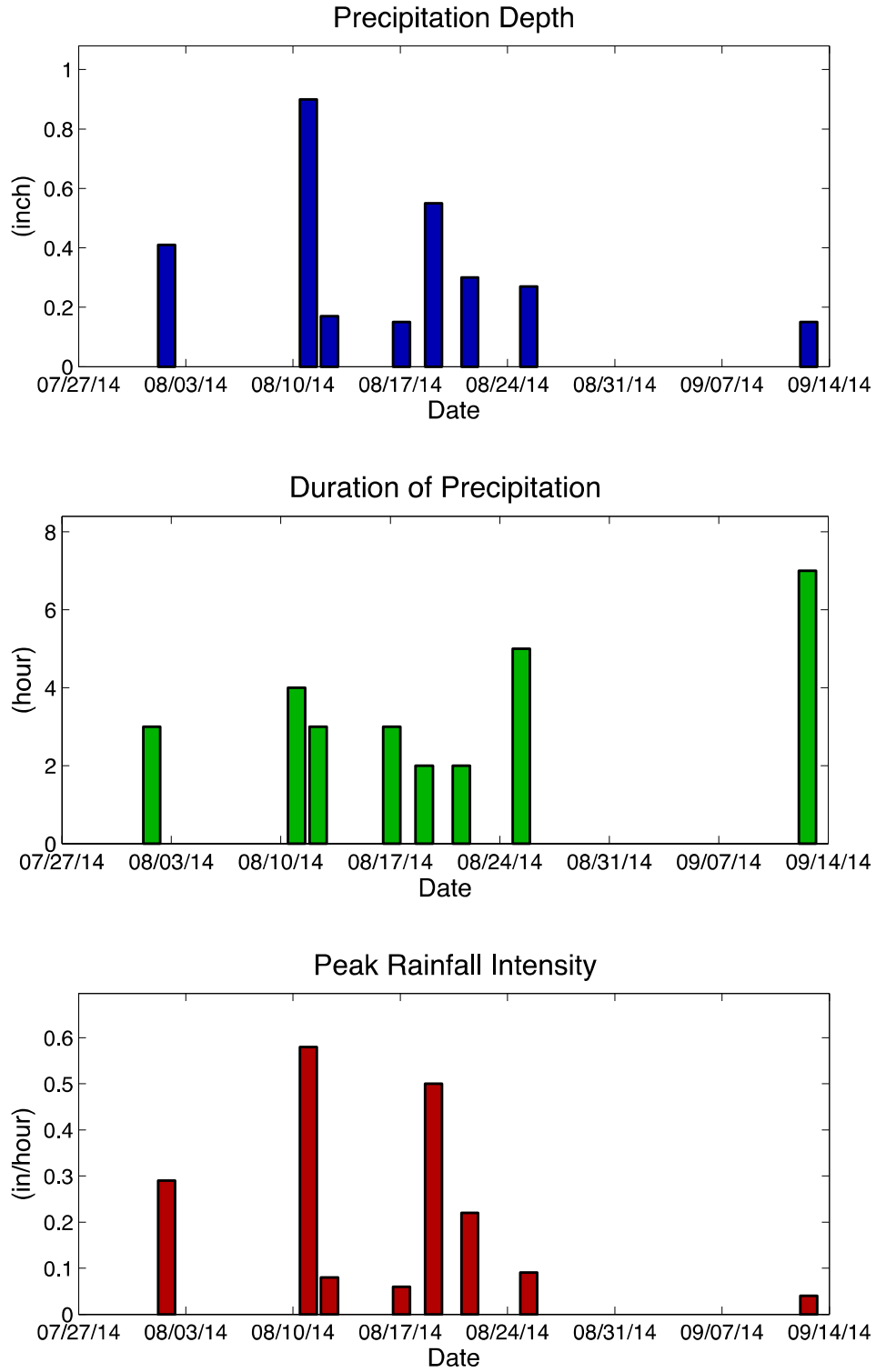
Figure 6.6: Major precipitation event (rainfall depth >0.1 inches) at the Wauwatosa construction site from July 27th to September 14th, 2014.

6.3   Rainfall-Turbidity Runoff Relation

As introduced in Chapter 3.4, turbidity levels of the stormwater runoff at major outfall locations of the four construction sites were continuously recorded by the automatic sampling system at a frequency of 17 samples per day. The time series of turbidity for every major precipitation event were extracted from the continuous records, and they are presented in figures 6.7~6.10 along with the time serious of rainfall intensity, i.e., the hyetograph.

Time series of most recorded turbidity runoff processes were similar to those of runoff discharge hydrography, i.e., turbidity increases rapidly shortly after the rainfall starts and it decreases more gradually after the peak. Turbidity value remains high for an extended period after the rain stops.

Racine Construction Site
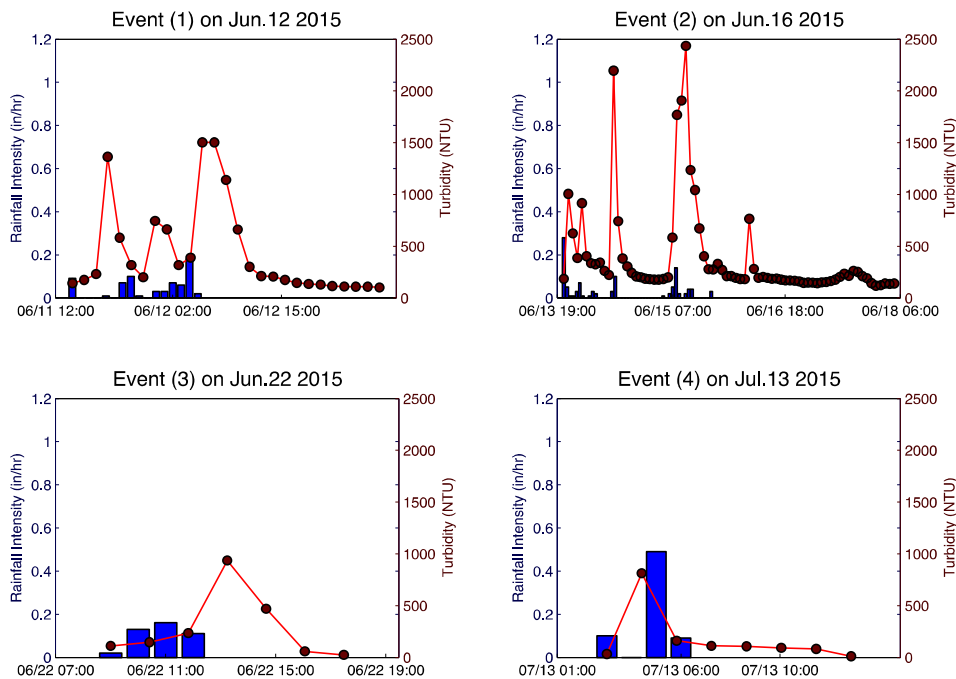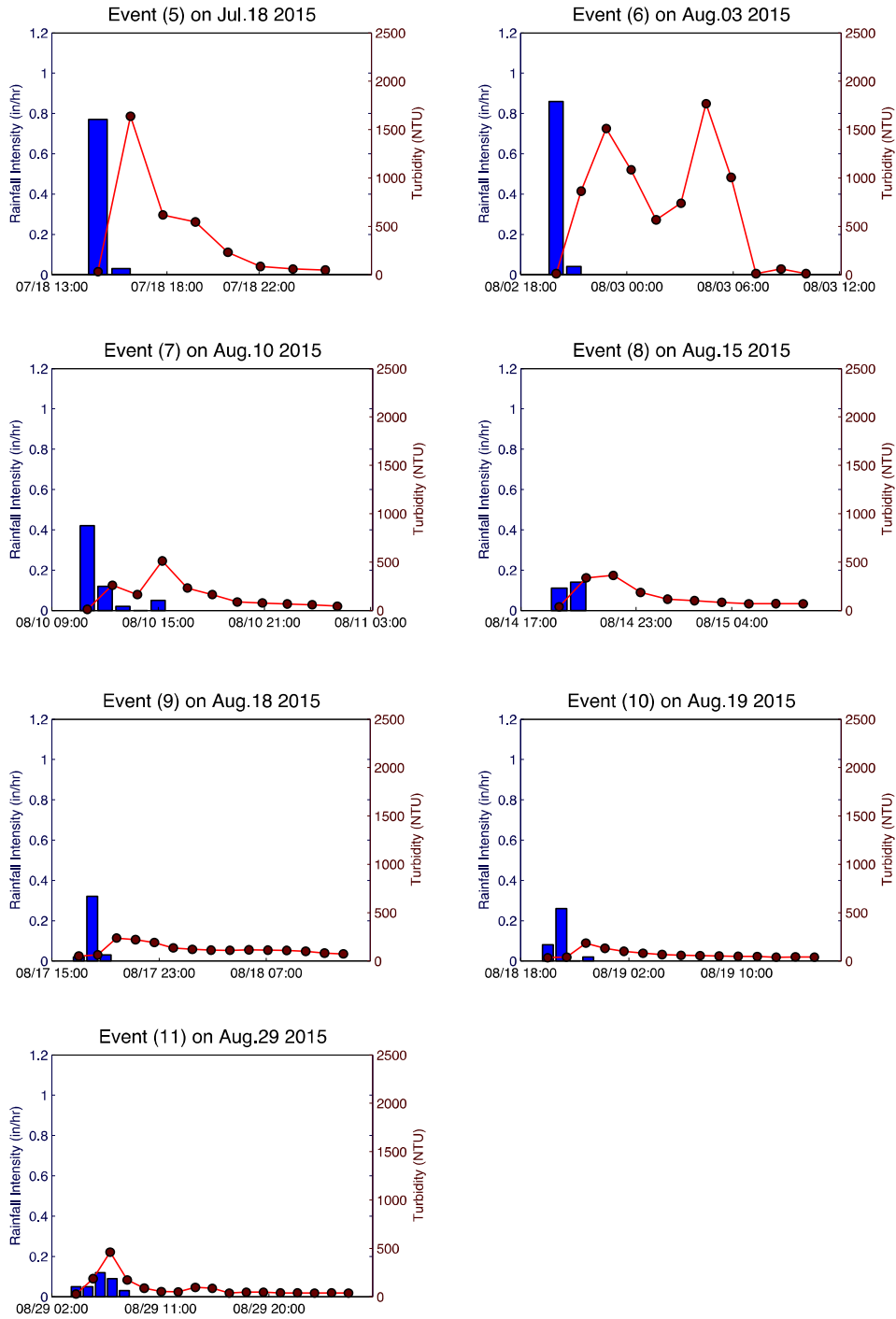
Figure 6.7: Time series of rainfall intensity and turbidity runoff from the Racine construction site.

Lake Geneva Construction Site
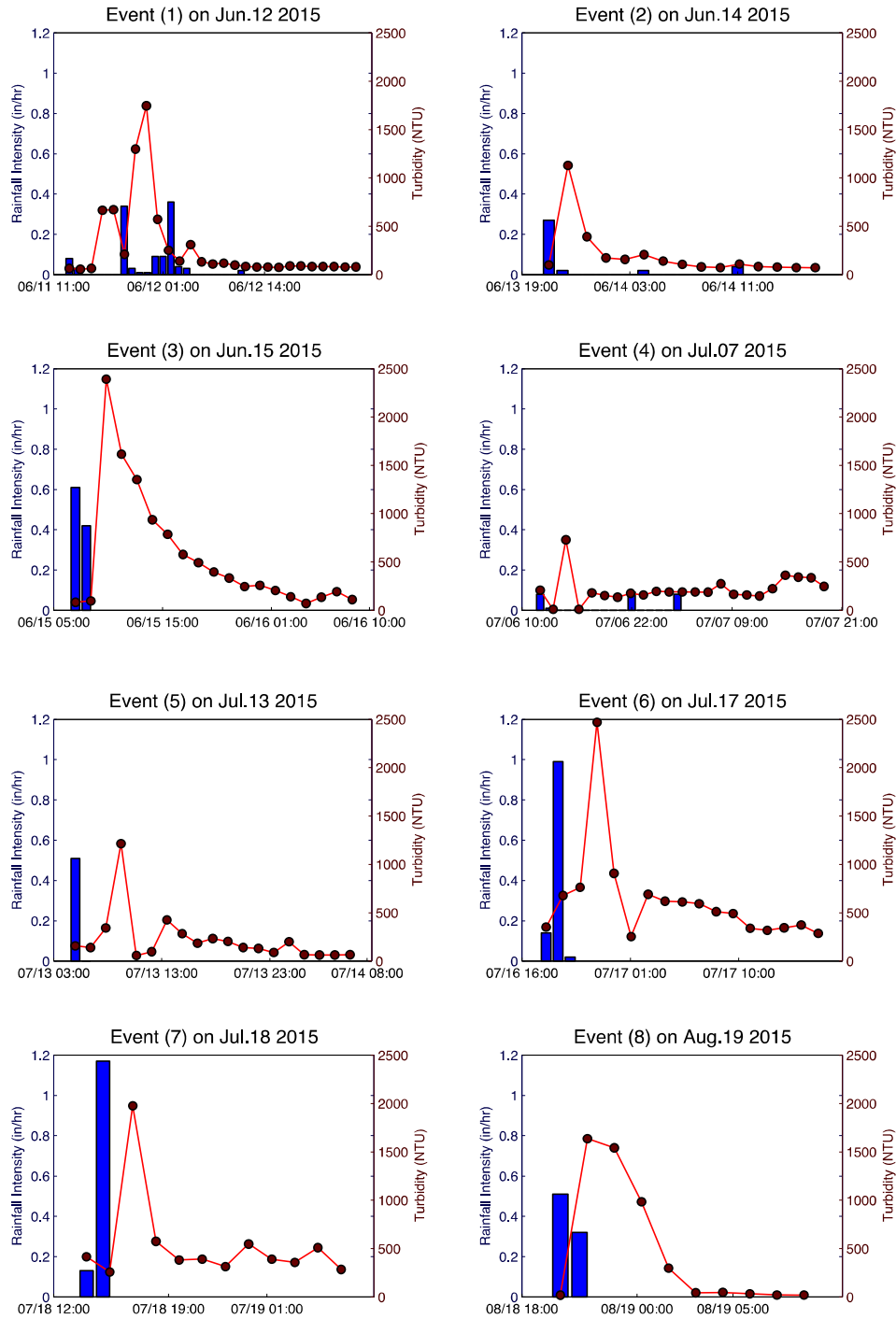
Figure 6.8: Time series of rainfall intensity and turbidity runoff from the Lake Geneva construction site.

Wrightstown Construction Site
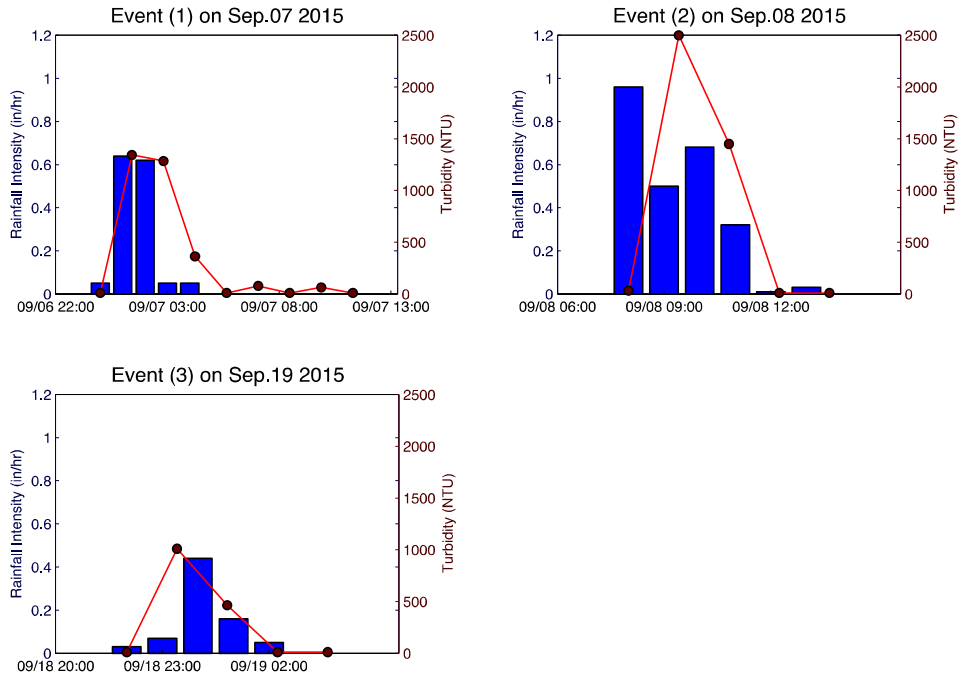
Figure 6.9: Time series of rainfall intensity and turbidity runoff from the Wrightstown construction site.

Wauwatosa Construction Site
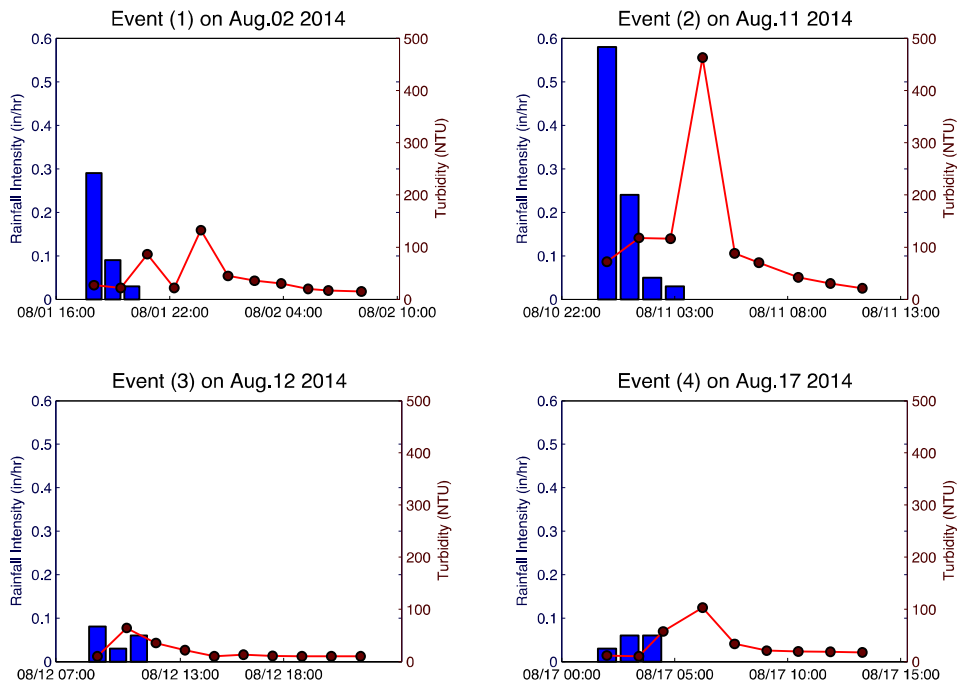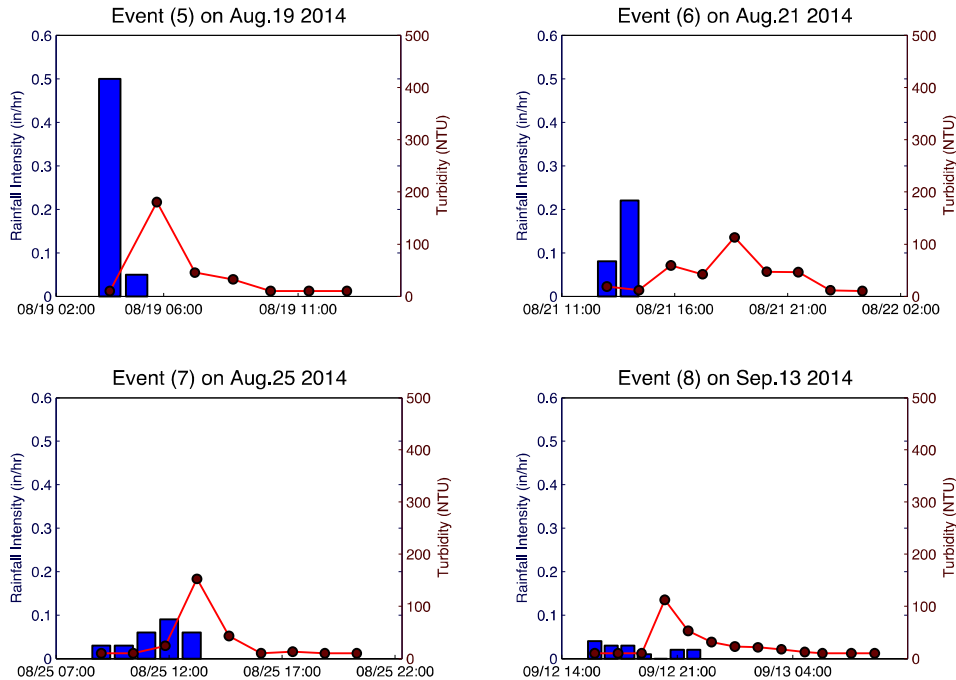
Figure 6.10: Time series of rainfall intensity and turbidity runoff from the Wauwatosa construction site.

From these rainfall-turbidity runoff time series, basic statistics of the process can be calculated, including:

- **Total rainfall depth** (in)
- **Average rainfall intensity** (in/hr): here the intensity is calculated as the mean of rainfall depth divide by the duration when the precipitation depth is greater than 0.01 in for a given time interval.
- **Peak rainfall intensity** (in/hr): the maximum intensity for a given event
- **Average turbidity** (NTU)
- **Peak turbidity** (NTU)
- **Maximum 24-hour turbidity** (NTU): this parameter was required to be monitored according to the EPA's 2009 C&D rule, where it was required to be less than 280 NTU. In this study, it was calculated as the maximum value of the running average of the turbidity series with a 24-hour averaging window.

In addition, the following statistics were also calculated:

- **Turbidity runoff duration** (hr): the start and end of a turbidity runoff is estimated as the time when the turbidity level reaches and falls below 1% of the peak turbidity level.

- **Rainfall centroid time** (hr): the centroid of the rainfall intensity distribution in time with respect to the start of the precipitation event
- **Turbidity runoff centroid time** (hr): the centroid of the turbidity time series with respect to the start of the precipitation event.

These statistics for all recorded events at the four automatic sampling sites are presented in Table 6.3. The difference between the turbidity runoff duration and the rainfall duration can be interpreted as the time characteristics of the response of the runoff with respect to the rainfall input. The mean and standard deviation of the time difference for the four sites are: 17.5 ± 14.2 (hr) for the Racine site; 16.9 ± 6.4 (hr) for the Lake Geneva site; 3.6 ± 3.5 (hr) for the Wrightstown site; and 10.0 ± 1.8 (hr) for the Wauwatosa site, respectively.

Table 6.3: Basic statistics of all recorded rainfall-turbidity runoff events at the four automatic sampling sites, where $P \sim$ total rainfall depth; $I_a \sim$ average rainfall intensity; $I_p \sim$ peak rainfall intensity, $T_a \sim$ average turbidity level, $T_p \sim$ peak turbidity level, $T_{24} \sim$ maximum 24-hr turbidity, $D_p \sim$ rainfall duration, $D_t \sim$ turbidity runoff duration, $C_p \sim$ rainfall centroid time and $C_t \sim$ turbidity runoff centroid time.

Racine construction site

Event ID	P (in)	I_a (in/hr)	I_p (in/hr)	T_a (NTU)	T_p (NTU)	T_{24} (NTU)	D_p (hr)	D_t (hr)	C_p (hr)	C_t (hr)
1	0.67	0.061	0.18	436	1,502	662	16	38	10.4	16.0
2	1.02	0.049	0.28	395	2,434	727	47	104	17.5	40.2
3	0.42	0.105	0.16	325	936	379	4	10	2.9	5.5
4	0.68	0.227	0.29	227	811	335	4	11	2.8	4.3
5	0.80	0.400	0.77	622	1,637	761	2	11	1.0	4.2
6	0.90	0.450	0.86	1,077	1,767	1,077	2	16	1.0	7.2
7	0.61	0/153	0.42	166	511	235	5	16	1.6	6.8
8	0.25	0.125	0.14	142	362	246	2	14	1.6	6.1
9	0.37	0.123	0.32	122	238	152	3	21	2.0	10.4
10	0.36	0.120	0.26	67	185	98	4	21	1.9	9.6
11	0.34	0.068	0.12	91	462	225	5	24	3.0	8.6

Lake Geneva construction site

Event ID	P (in)	I_a (in/hr)	I_p (in/hr)	T_a (NTU)	T_p (NTU)	T_{24} (NTU)	D_p (hr)	D_t (hr)	C_p (hr)	C_t (hr)
1	1.13	0.094	0.36	433	1.747	594	23	38	10.8	13.4
2	0.35	0.088	0.27	198	1,130	541	15	21	3.1	7.0
3	1.03	0.515	0.61	671	2,390	1,108	2	27	1.4	9.3

94

4	0.26	0.065	0.09	236	728	316	16	32	9.1	18.0
5	0.51	0.510	0.51	227	1,215	382	2	27	1.0	10.5
6	1.15	0.383	0.99	623	2,468	1,034	3	24	1.9	10.3
7	1.30	0.650	1.17	534	1,978	884	2	17	1.9	8.0
8	0.83	0.415	0.51	1,138	1,636	1,065	2	14	1.4	4.4

Wrightstown construction site

Event ID	P (in)	I_a (in/hr)	I_p (in/hr)	T_a (NTU)	T_p (NTU)	T_{24} (NTU)	D_p (hr)	D_t (hr)	C_p (hr)	C_t (hr)
1	1.41	0.282	0.64	767	1,343	880	5	12	2.6	4.1
2	2.50	0.417	0.96	1,975	2,500	1,975	6	7	2.2	3.3
3	0.75	0.150	0.44	736	1,009	736	5	7	3.2	3.3

Wauwatosa construction site

Event ID	P (in)	I_a (in/hr)	I_p (in/hr)	T_a (NTU)	T_p (NTU)	T_{24} (NTU)	D_p (hr)	D_t (hr)	C_p (hr)	C_t (hr)
1	0.41	0.137	0.29	41	133	58	3	16	1.4	7.4
2	0.90	0.225	0.58	125	463	171	4	13	1.5	5.7
3	0.17	0.057	0.08	21	64	36	3	14	1.9	5.8
4	0.15	0.050	0.06	32	103	43	3	13	2.2	6.5
5	0.55	0.275	0.50	86	180	79	2	10	1.1	3.9
6	0.30	0.150	0.22	44	113	49	2	13	1.7	6.8
7	0.27	0.054	0.09	42	153	48	5	13	3.4	6.2
8	0.15	0.025	0.04	35	112	39	7	18	3.3	8.3

Based on the observed time sequences, a characteristic response function of the turbidity can be developed. The base time of the function (T_B) is determined as the average difference of durations between the turbidity runoff and the rainfall series plus one hour, i.e., $T_B = \overline{D_t} - \overline{D_p} + 1$, where the overbar represents averaging. The concept of the turbidity response function is analogous to the unit hydrograph approach: it is the time sequence of runoff turbidity caused by a hypothetical unit rainfall event, e.g., a one-hour one-inch precipitation. The developed unit response function can then be combined with the unit hydrograph to predict the time sequence of turbidity runoff, as well as the total sediment discharge from a calibrated construction site.

Assuming the rainfall-turbidity process is linear; the time sequence of the precipitation of an event is given by $\{P_1, P_2, \ldots, P_M\}$; the time sequence of runoff turbidity produced by this event

is given by $\{T_1, T_2, \ldots, T_N\}$; and the unit response function is represented by a sequence $\{U_1, U_2, \ldots, U_L\}$, then the linear system can be described by the following system equation:

$$T_n = \sum_{m=1}^{n \leq m} P_m U_{n-m+1} \quad \text{for} \quad n = 1, 2, \ldots, N \tag{6.2}$$

and $N = M + L - 1$, where N, M and L are the number of hours of rainfall duration, turbidity runoff duration and the base time, respectively.

The rainfall series were given at one-hour intervals while the turbidity data were recorded 17 times per day. Since the unit runoff turbidity approach requires a unified time unit, a linear interpolation was applied to the turbidity series to obtain a series with one-hour intervals. Rainfall and the interpolated turbidity data for all recorded events were used to reconstruct the unit runoff turbidity response function U_n. An over-determined system was established by applying all data available into equation (6.2). Solving the system with a least-square fit, one can obtain the estimated response function.

Estimated unit runoff turbidity functions for the four sampling sites are shown in figure 6.11. For better visualization, spline interpolations are applied to produce smoother curves. The overall error of the approach is defined as the standard error of the difference between observed turbidity levels and the predicted ones by the unit response approach, i.e., equation (6.2), for all events. In figure 6.11, errors are represented as the percentage with respect to the peak value of the reconstructed response function. It can be observed that

1. The reconstructed unit runoff turbidity response functions reasonably describe all recorded turbidity runoff events, as relative errors were generally less than 15% of the peak turbidity level.
2. For 3 out of the 4 sites, peak turbidity levels after a one-hour one-inch precipitation event were nearly the same, i.e, in the range of 1,350 ~ 1,460 NTU. Peak turbidity at the Wauwatosa site was much lower (340 NTU). The sensor was deployed in the Honey Creek near the Wauwatosa site, which received runoff from both the construction site and the nearby catchments without soil disturbance. The recorded turbidity was likely diluted by the upstream flow in the creek.
3. Peak turbidity arrival time was 2, 3, 4 and 5 hours after the start of precipitation for the Wrightstown, Racine, Lake Geneva and Wauwatosa sites, respectively. The arrival time may relate to the disturbed area, landscape and the location of the sampling point, etc.
4. A minor second peak existed for the Racine and Lake Geneva site. A possible explanation is that the first peak was caused by the saturated surface runoff, while the second peak arose due to subsurface interflow. Two peaks were also observed at the Wauwatosa site, while the first peak was smaller than the second. Again, this could be explained by the dilution from the upstream flow for the reduced first peak. As the

surface runoff from the upstream flow decreased, the interflow runoff from the construction site contributed to the second and higher peak with less dilution effect.
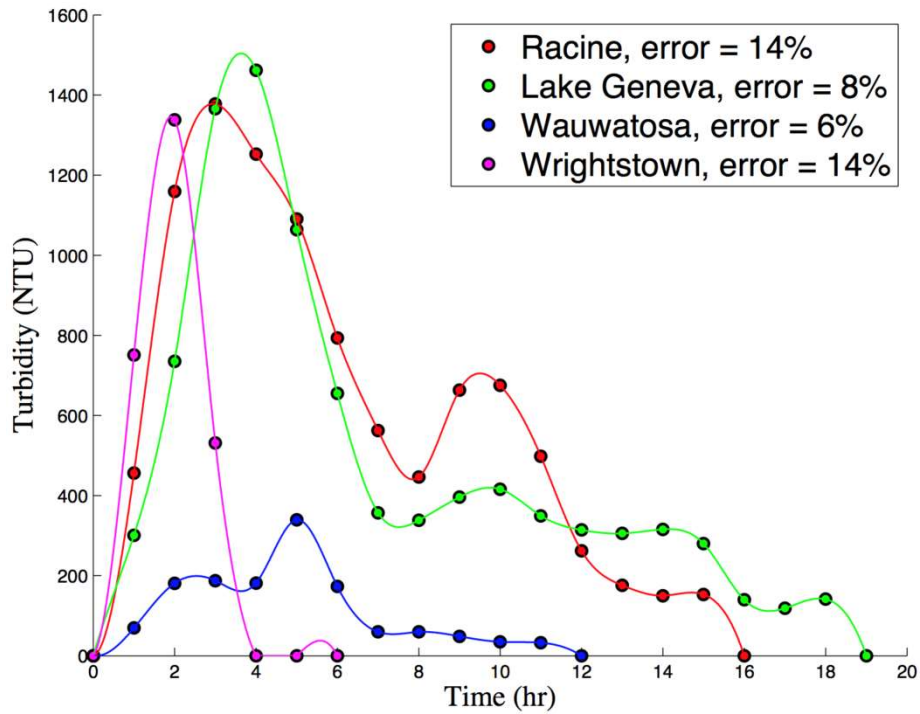

Figure 6.11: Reconstructed unit runoff turbidity response function from rainfall-turbidity events recorded at the four sampling sites. Time = 0 represents the start of rainfall.

6.4 Statistical Correlations between Runoff Turbidity and Precipitation

Simple linear regression analysis was applied to basic statistical measures reported in Table 6.3 to explore correlations between the runoff turbidity and the precipitation. Measured data were fitted with a linear model:

$$Y = aX + b \qquad (6.3)$$

where X are statistics of precipitation such as total depth, average or peak intensity; Y are statistics of the runoff turbidity such as mean and peak turbidity in NTU; and a and b are the slope and intercept. For each sampling site, 6 correlation tests were conducted when pairing the two turbidity statistics with the three rainfall statistics, as shown in figures 6.12~6.15. The degree of correlation can be evaluated through the coefficient of determination (the R^2 value), and the P-value of the hypothesis test with null and alternative hypotheses that

$$\begin{aligned} H_0\text{: } a &= 0 \\ H_1\text{: } a &\neq 0 \end{aligned} \qquad (6.4)$$

In this study, we declare that the given pair of data are significantly correlated when both the two conditions are satisfied:

1. Linear regression $R^2 > 75\%$
2. The hypothesis testing on the null hypothesis is rejected with $P < 0.05$.

With the two criteria, Table 6.4 summarizes the correlated and uncorrelated turbidity-rainfall statistics for the four sites with data obtained in this study.

Table 6.4: Correlations between rainfall and runoff turbidity statistics. Statistics are assumed to be correlated if the linear regression has $R^2 > 75\%$ and the P-value < 0.05 of the hypothesis testing on the slope of the linear fit $= 0$. ($\sqrt{}$ ~ correlated, $\times$ ~ uncorrelated)

	Racine	Lake Geneva	Wrightstown	Wauwatosa
Mean turbidity (T_a) vs. mean rain intensity (I_a)	×	×	×	×
Peak turbidity (T_p) vs. mean rain intensity (I_a)	×	×	×	×
Mean turbidity (T_a) vs. peak rain intensity (I_p)	×	×	×	√
Peak turbidity (T_p) vs. peak rain intensity (I_p)	×	×	√	×
Mean turbidity (T_a) vs. total rain depth (P)	×	×	×	√
Peak turbidity (T_p) vs. total rain depth (P)	√	√	√	√

Racine Construction Site

Figure 6.12: Linear regression tests between runoff turbidity and precipitation at the Racine construction site.

Lake Geneva Construction Site

Figure 6.13: Linear regression tests between runoff turbidity and precipitation at the Lake Geneva construction site.

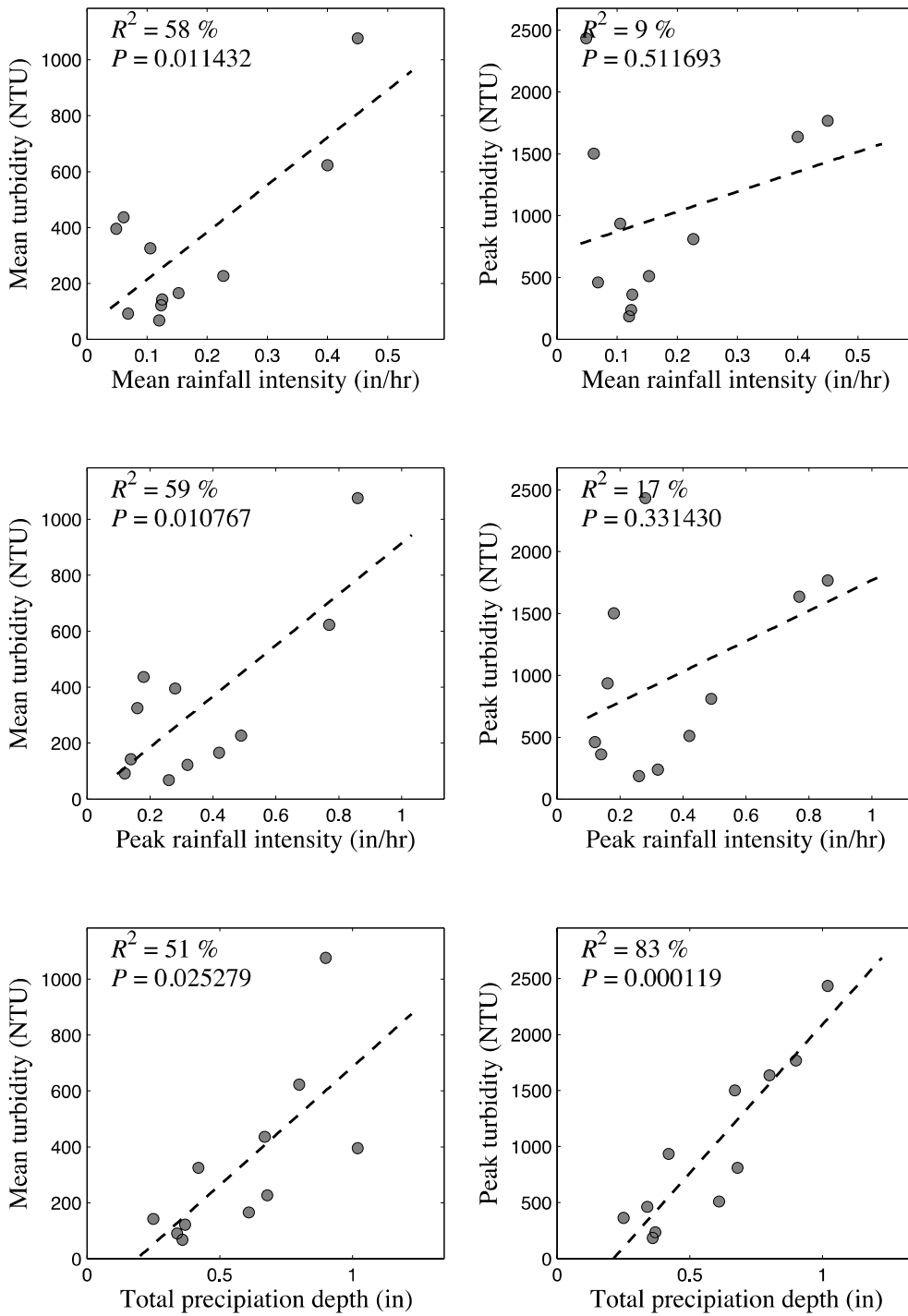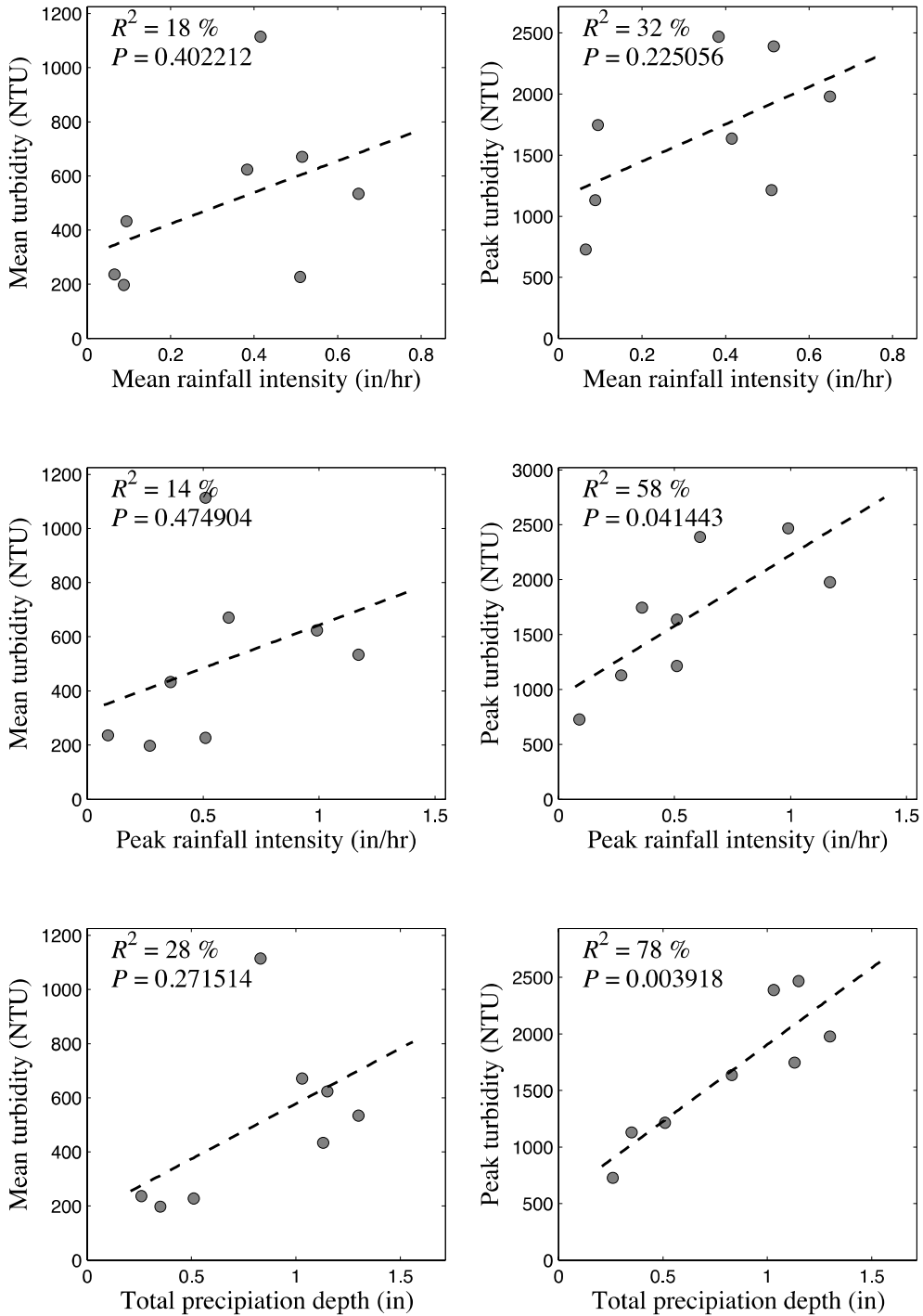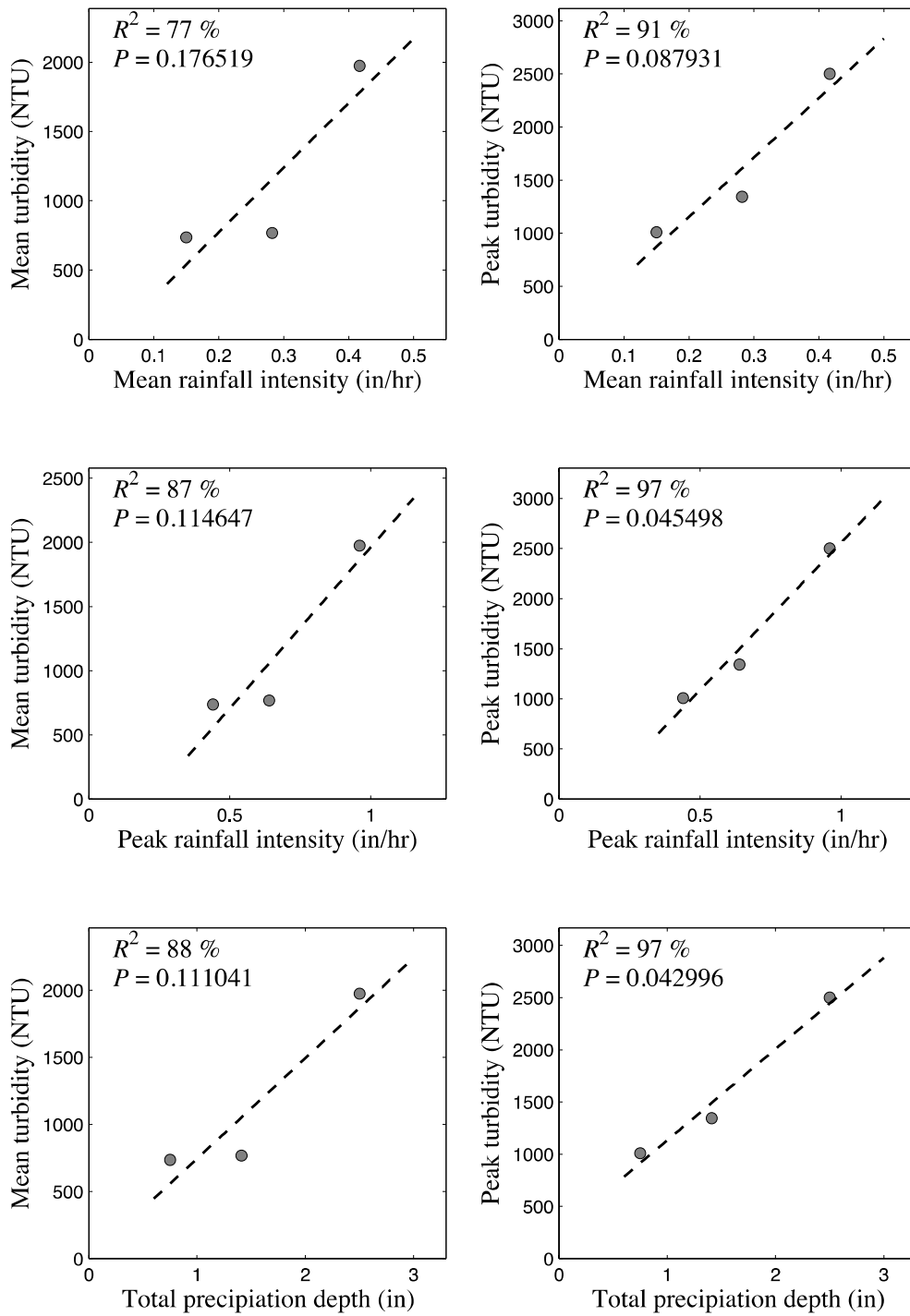**Wrightstown Construction Site**

Figure 6.14: Linear regression tests between runoff turbidity and precipitation at the Wrightstown construction site.
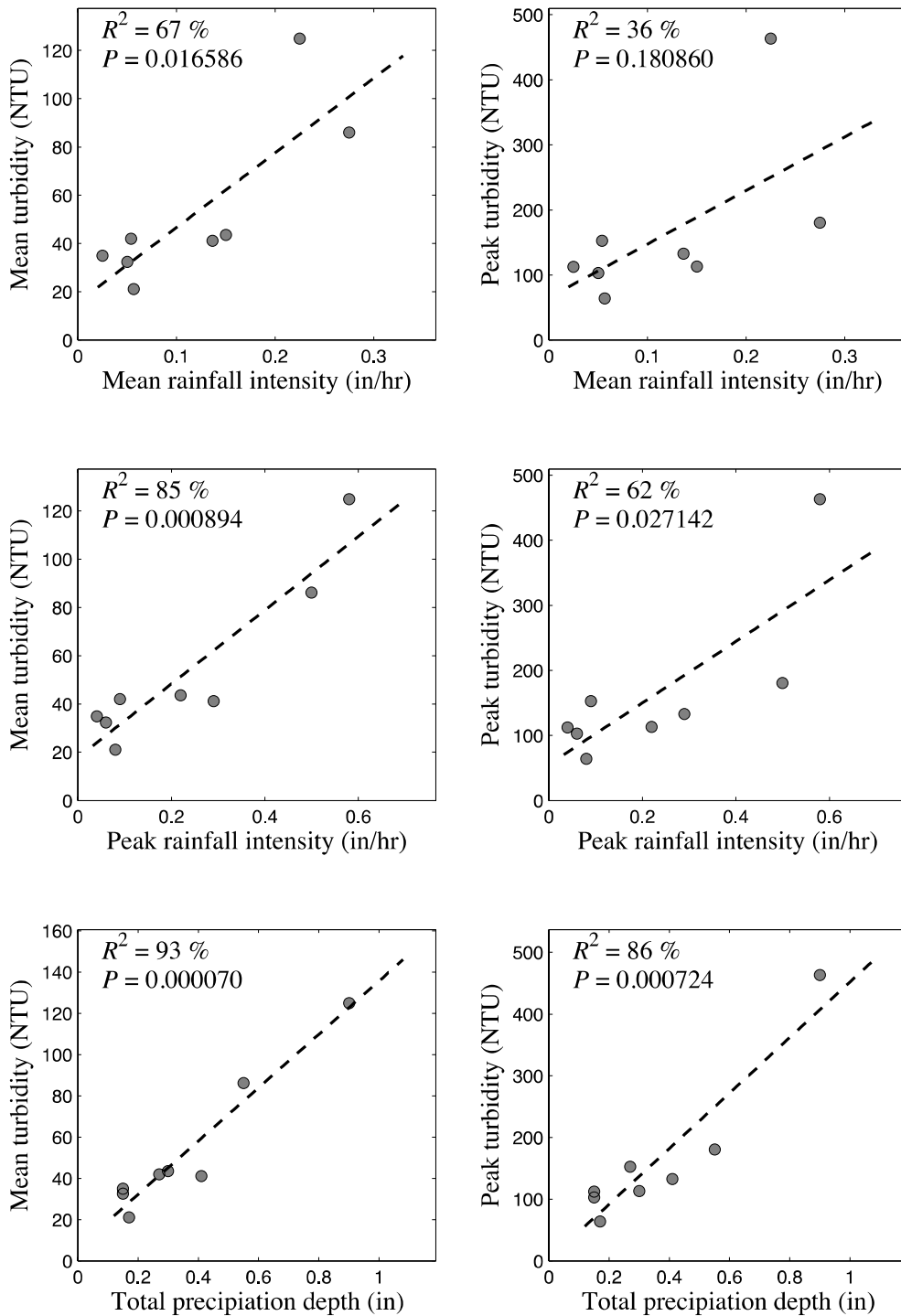
Wauwatosa Construction Site

Figure 6.15: Linear regression tests between runoff turbidity and precipitation at the Wauwatosa construction site.

As shown in figures 6.12 ~ 6.15 and table 6.4, both the mean and the peak turbidity generally increase with the total precipitation depth, and the mean or peak of rain intensity. However, significant correlation exists only between the peak turbidity and the total rain depth for all data from the four sites. It appears that good correlations are found for all linear correlation tests for the Wrightstown site. However, since only three data points were available for this site, most of these correlations may not be statistically significant.

A closer investigation was conducted to examine the correlation between the peak turbidity and the precipitation depth. First, it is more reasonable to fit the data with a zero-intercept linear equation, i.e.,

$$T_p = aP \tag{6.5}$$

instead of equation (6.3). Secondly, a power law equation is also possible to describe their relation, i.e.,

$$T_p = \alpha P^\beta \tag{6.6}$$

which can be tested with a log-linear regression analysis:

$$\log T_p = \beta \log P + \log \alpha \tag{6.7}$$

Following these arguments, linear regressions with (6.5) and (6.7) were applied using data from the four sites, and the results are shown in figure 6.16~6.19. In these figures, fitted parameters (a, α and β) are presented. Since a regression model is only valid when residuals are normally distributed random variables, the normality test was also conducted to address this assumption. Denoting the residual error, E, as the difference between the predicted peak turbidity values from equation (6.5) or (6.7) and the measured values, then it can be given as

$$E = z\sigma \tag{6.8}$$

where σ is the standard deviation of the normally distributed residual errors, and z is the inverse function of the standardized normal distribution CDF, $\Phi = P(Z < z) \equiv P$, the probability P for a given residual value can be estimated by Weibull's formula, i.e.,

$$P = \frac{rank(E)}{n+1} \tag{6.9}$$

where n is the number of samples. The z position can then be estimated as

$$z = \Phi^{-1}\left(\frac{rank(E)}{n+1}\right) \tag{6.10}$$

Plotting the residual error E vs. the calculated z position, a linear relation is expected for a normal distribution. Therefore the normality test with better linearity (e.g., in terms of the R^2 value) suggests a better agreement with the normal distribution assumption.

Racine Construction Site

Figure 6.16: Test of the linear and log-linear relations between the measured peak turbidity and the total precipitation depth at the Racine construction site.

Lake Geneva Construction Site

Figure 6.17: Test of the linear and log-linear relations between the measured peak turbidity and the total precipitation depth at the Lake Geneva construction site.

Wrightstown Construction Site

Figure 6.18: Test of the linear and log-linear relations between the measured peak turbidity and the total precipitation depth at the Wrightstown construction site.

Wauwatosa Construction Site

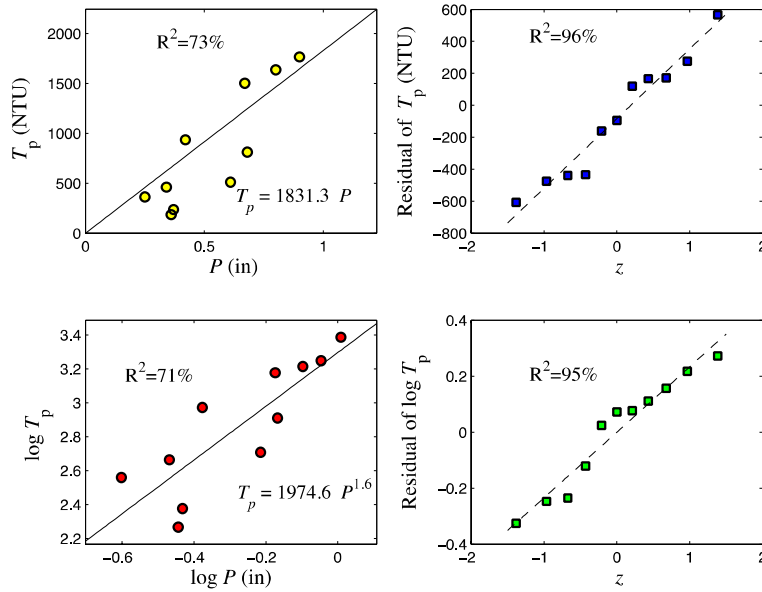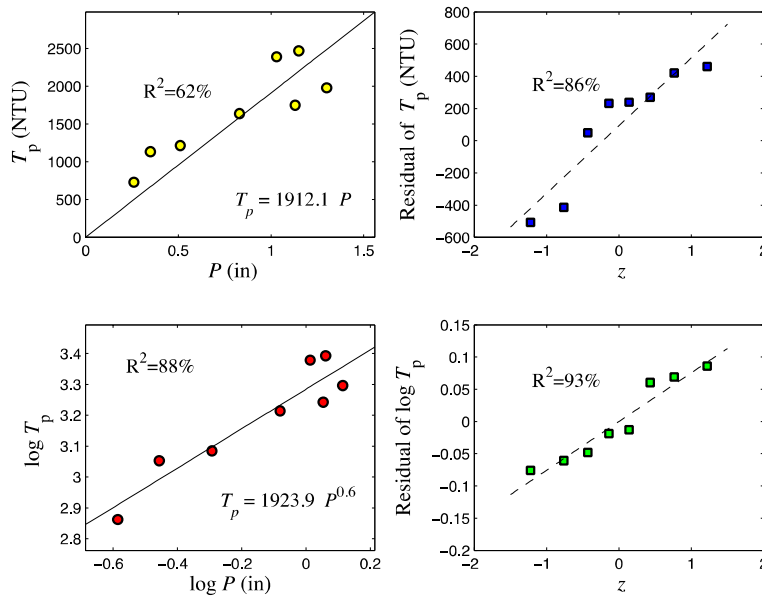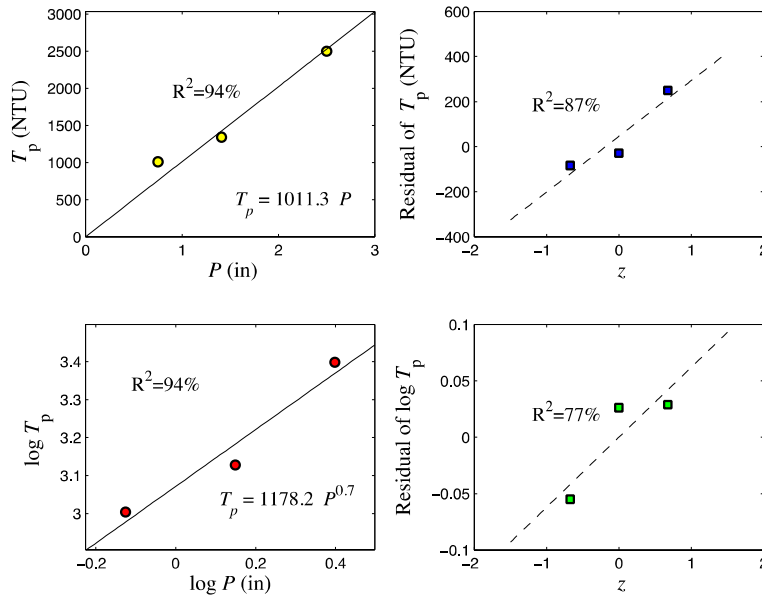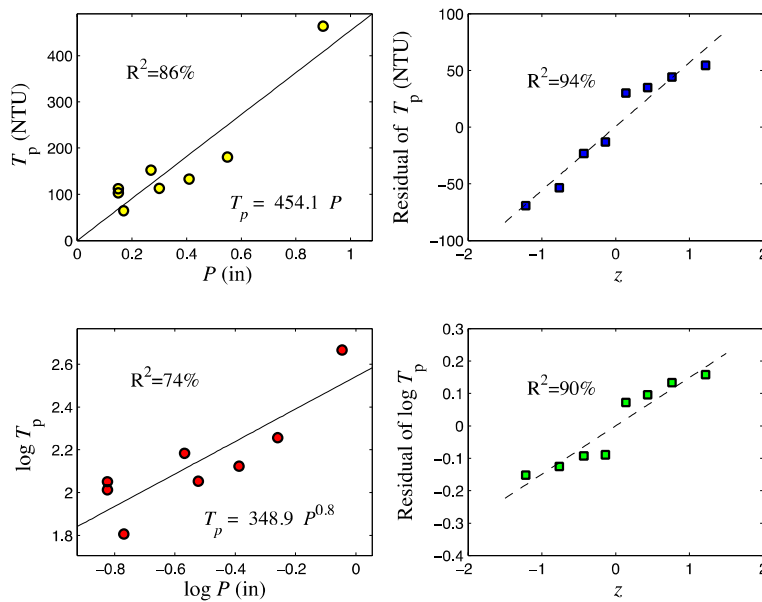**Figure 6.19:** Test of the linear and log-linear relations between the measured peak turbidity and the total precipitation depth at the Wauwatosa construction site.

The linear and log-linear tests indicated that both models can accurately describe the relation between the peak turbidity and total precipitation depth. By forcing the intercept to zero in the linear regression, the overall correlation decreased for all sites, R^2 = 73%, 64% 92%, and 86%, for the Racine, Lake Geneva, Wrightstown and Wauwatosa sites, respectively, compared with 83%, 78%, 97% and 86% for the case without limiting the intercept. The log-linear (power law) model, however, did not perform significantly better than the linear model in predicting the correlation, as shown by the R^2 value and the residual normality test, except for the case at the Lake Geneva site. Moreover, the exponent β according to the best fit scattered over a wide range, β = 1.6, 0.6, 0.7 and 0.8 for the four sites, respectively. Therefore, it does not appear to be a better option than the simple linear model.

Combining all available data from the four sites, the measured peak turbidity (T_p) values are plotted against aP in figure 6.20. A good correlation is found with R^2 = 87%. The coefficient a is 1831, 1912, 1178, and 349 for the Racine, Lake Geneva, Wrightstown and Wauwatosa sites, respectively. The lower value at the Wauwatosa site is expected as the turbidity has been diluted by the upstream flow in the Honey Creek.

From the statistical analysis, it is convincing that the peak value of turbidity in the construction site runoff has a strong linear correlation with the total precipitation depth for a storm event. The linear proportionality seems to correlate with the total area of soil disturbance. However, the number of sites in this study may not be large enough for us to draw a concrete conclusion. Other factors may also contribute to the coefficient, including the soil type, land topography, and the erosion protection methods applied in the construction site, etc.

Correlation between the turbidity and the disturbed drainage area was also studied with regression analysis. The peak and mean turbidity averaged over all recorded events on each monitored site, and the peak turbidity values of the reconstructed unit runoff turbidity response function are selected for correlation analysis against the disturbed area. None of these turbidity statistics are found to be correlated with the area (P>0.5).
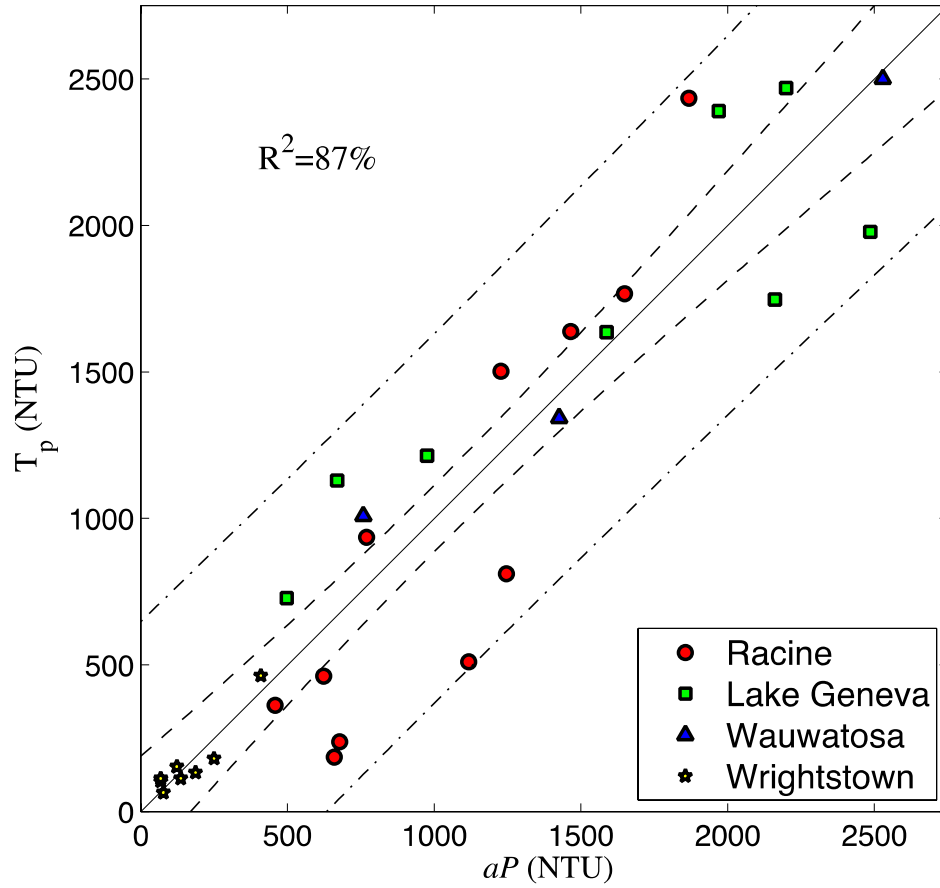
Figure 6.20: Unified linear model $T_p = aP$ for all data measured at four sampling sites, where the solid line (-) represents the one-on-one relation; dashed lines (--) are the 95% confidence intervals; and dash-dotted lines (-.) are the 95% prediction intervals of the linear model.

6.5   Total sediment load

Although the statistical analysis demonstrated a strong correlation between the peak turbidity level and the precipitation depth, this information may not be useful for future stormwater management and regulations. Practically, it is always desirable for managers to have modeling tools to predict the total sediment discharged from a construction site with given or designed storms. Many stormwater management software packages, such as the EPA's SWMM (http://www2.epa.gov/water-research/storm-water-management-model-swmm), are able to estimate the time series and total volume of sediment transport for catchments with well-parameterized properties in terms of erosion. However, few data exist to validate these models, particularly for stormwater runoff from construction sites. As shown in this study, most BMP methods applied on a construction site may help to retain larger solid particles through sedimentation or filtration, but they are not effective at reducing the concentration of fine suspended solids. With automatic turbidity monitoring devices, such as the one designed for this project, valuable data can be obtained to support future modeling design and calibration. Since the turbidity in NTU can be a reasonable surrogate to the suspended solid concentration after careful calibrations, data series acquired can be converted to the total sediment load.

For simplicity, assume a linear relation between turbidity NTU and the suspended solid concentration, the total sediment discharge for a rainfall-runoff event is proportional to the total flux of turbidity in NTU, which is denoted as F_T is this study, and

$$F_T = \int_0^{T_D} Q(t)T(t)dt \qquad (6.11)$$

where T_D is the total duration of stormwater runoff, $Q(t)$ is the time series of flow rate, and $T(t)$ is the time series of the turbidity NTU.

Since the stormwater flow rate $Q(t)$ was not measured in this study, we were not able to provide a direct estimate of the total turbidity flux. Nevertheless, it is noted that the time series of turbidity after precipitation events resembles that of a stormwater discharge hydrograph (cf. Figures 6.7~6.10). Assuming that the discharge $Q(t)$ rises and falls following the same trend as turbidity $T(t)$, the total turbidity flux can be estimated to be proportional to

$$F_T \sim F_{TS} \equiv \int_0^{T_D} T^2(t)dt \qquad (6.12)$$

where F_{TS} is denoted as the surrogate of the total turbidity flux, which is in turn correlated to the total sediment mass flux.

Data obtained from the four sampling sites were processed to calculate the integration of the turbidity squared, i.e., F_{TS}. Statistical analysis was then applied to explore the correlation between F_{TS} and the rainfall parameters, including the total depth, mean and peak intensity, similar to the approach in section 6.4. Similarly, no significant correlation with the mean and

peak intensity was found (not shown in this report), while it seemed that F_{TS} can be correlated with the total rainfall depth following a power law relation:

$$F_{TS} = \lambda P^{\theta} \qquad (6.13)$$

Figure 6.21 shows the linear regression of $\log F_{TS}$ vs $\log P$ for data measured at the four sampling sites.
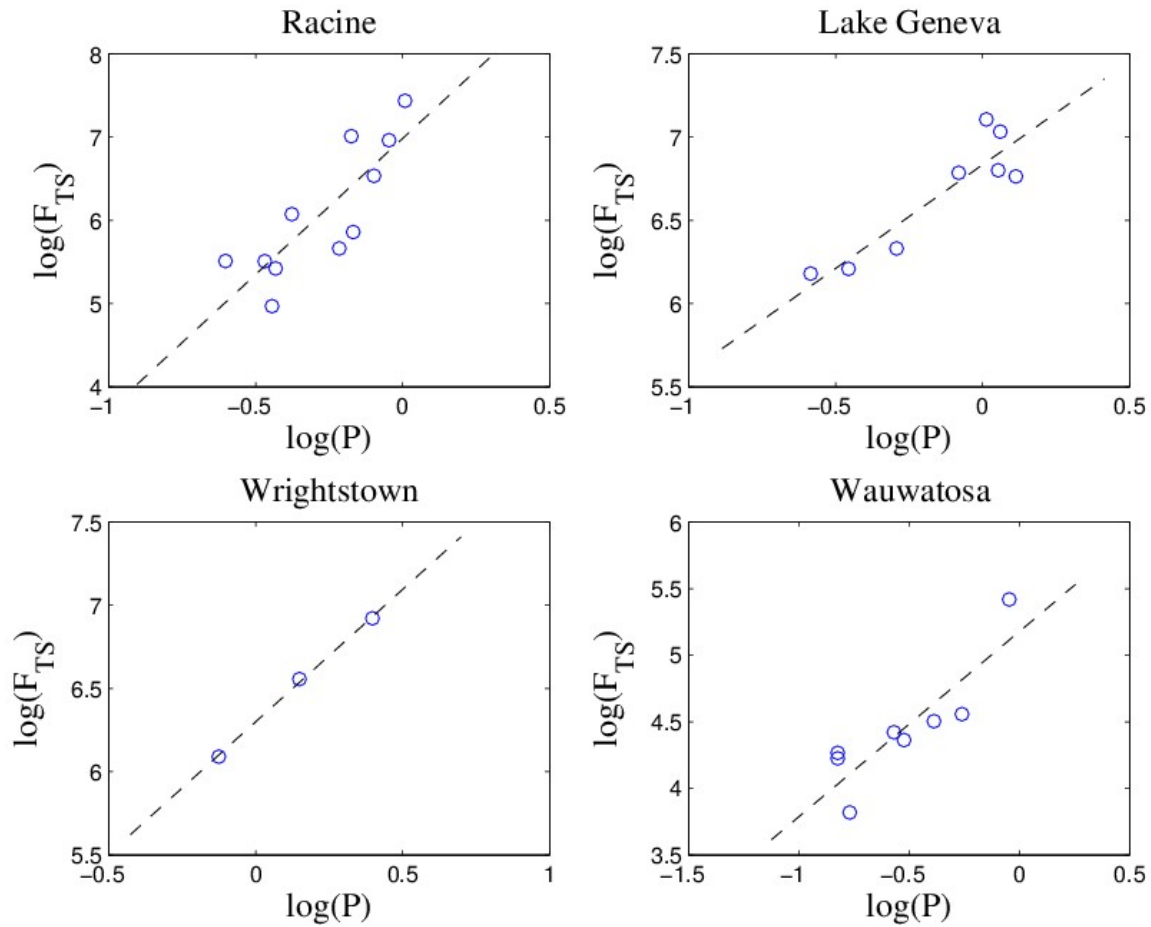
Figure 6.21: Log-linear relation between the surrogate total fine sediment load (F_{TS}) and the total precipitation depth (P).

The coefficients of the log-linear relation according to the regression analysis and the R^2 value of the regression for the four sites are presented in table 6.5. The coefficient λ is only indicative as the total sediment load used here is a surrogate with many uncertainties. The exponent θ for three sites (Lake Geneva, Wrightstown and Wauwatosa) are close, which are 1.25, 1.59 and 1.39, respectively. It is,however, more than two times larger at the Racine site (3.27). These observations suggest that it is possible to use a power-law relation to predict the total fine sediment load according to the total precipitation depth of a storm event, although

uncertainty of the exponent exists which may related to the properties of the soils and other factors associated with the construction activities.

Table 6.5: Coefficients of the power law relation and the coefficient of variation of the log-linear regression between the surrogate sediment load (F_{TS}) and the total precipitation depth (P).

Site Name	λ	θ	R^2
Racine	9.61×10^6	3.27	72%
Lake Geneva	6.82×10^6	1.25	84%
Wrightstown	1.99×10^6	1.59	99%
Wauwatosa	1.50×10^5	1.39	78%

Chapter 7
Conclusions

This research designed and conducted laboratory and field sampling experiments to measure and monitor the turbidity of stormwater runoff from WisDOT construction sites with significant earth work and disturbance.

Five ongoing WisDOT project sites were identified for this study. Field grab samples were collected from four of the five sites at various locations where stormwater drained from disturbed soil and at major outfall locations. Measured parameters included: turbidity level in NTU, mass concentration of total suspended solids, pH value and conductivity.

Measured turbidity in grab samples during or after storms ranged from 20 to 2,300 NTU, which are generally lower than previous reported values from construction sites, e.g., up to 28,000 NTU at North Carolina sites according to McLaughlin (2002, 2007), and up to 23,000 NTU at Texas site according to McFalls (2014). The measurements, however, agreed well with the 500~2,000 NTU range reported by NCHRP (2012), for sites with conventional BMP implementations. In addition, many of the samples were collected near the outfalls of the site, where the effluent was usually a mixture of direct runoff from the disturbed soil and nearby vegetated/covered land.

Some samples measured immediately at both sides of BMP controls, such as straw roll ditch checks and silt fences, did not show significant difference in turbidity. It should also be emphasized that conventional BMP measures are able to effectively protect soil from erosion, reduce runoff volume and speed, and enhance infiltration, thereby reducing the total sediment into the receiving water body. If future EPA regulations specify any form of numeric limitation, the mixing ratio of runoff with the receiving water body should be taken into consideration. For example, turbidity monitoring devices installed at a specified distance away from outfall may provide a more reasonable and comprehensive evaluation of the impact of turbidity runoff. Turbidity measured immediately from outfalls will likely be extremely high despite extensive BMP coverage. Sedimentation basins or ponds with flocculation treatment are likely to be the only known methods to effectively settle out fine clay or silt sediments, thus reducing the turbidity level.

The measured pH values of grab samples ranged from 7.2 to 9.2, and the conductivity values were between 380 and 3,200 μS/cm. No correlations were found among the pH value, conductivity and turbidity for grab samples. Several State DOTs/agencies have some level of numeric effluent limits and sampling procedures for runoff from construction sites. For example, according to California's permitting regulation, a pH value exceeding the 6.5~8.5 range and turbidity above 250 NTU would require sampling for sites categorized as risk level 2.

Laboratory experiments were conducted to investigate the relation between the TSS concentration and the turbidity NTU with both grab samples and laboratory simulated runoff. Good correlations were found between the variables, and a nonlinear power-law based relation performed better compared with a linear correlation. Parameters obtained through a least square fitting with the synthetic laboratory samples described the TSS-turbidity relation found in field grab samples well. This result suggested that the TSS-turbidity relation for runoff from construction sites can be well characterized and predicted by analyzing soil samples collected on-site following a simple laboratory testing. The relation, once well calibrated, can be used to estimate the suspended solids concentration with a much simpler turbidity measurement. This allows continuous monitoring of the TSS concentration of effluents from construction sites.

Five automated turbidity sampling devices were developed and deployed at outfalls of four selected sites to monitor the time series of turbidity where the effluent discharged into the receiving water body (streams and rivers). Thirty rainfall-turbidity runoff events were recorded by these automated sampling devices. It was demonstrated that a unit runoff turbidity function, which represents the response function of turbidity time series with respect to a unit precipitation depth, can be developed with these time series, following a least-square fit approach. The reconstructed unit runoff turbidity response functions were able to reasonably describe all recorded turbidity runoff events, as relative errors were generally less than 15% of the peak turbidity level (cf Figure 6.11). These unit runoff turbidity response functions were characterized by a rapid rise to the peak value at the start of rainfall, and followed by a gradual decrease to the background level. The peak arrival time range from 2 to 5 hours for the four sites monitored. A secondary peak was also observed, about 3~5 hours after the first peak. The secondary peak could be attributed to the subsurface interflow, while the first peak was due to the surface runoff. The secondary peak can also be found in some of the field observations conducted by McFalls et al. (2014).

Statistical correlations were examined between the runoff turbidity and the precipitation. The statistics of turbidity calculated from the observed time series included: the mean, peak values, as well as the daily maximum (i.e., the maximum value of a running average with a 24-hour averaging window). The daily maximum is an important parameter, as the EPA's 2009 C&D rule did recognize the variability of effluent turbidity and stated:

> "… *the numeric turbidity limitation is a daily maximum, meaning an owner or operator will not be in violation of the limitation if individual samples of their discharges exceed the limitation, as long as the average of the samples taken over the course of a day are below the limitation*. …"

At the Wauwatosa construction site, where the sampling device was installed in a creek 50 feet downstream from the outfall, the daily maximum was lower than the 280 NTU limit for all events recorded. At the Racine construction site, where the sensor was installed at the outfall, 5 out of 11 events had a daily maximum lower than 280 NTU. For the other two sites all recorded events exceeded the limit.

Both the peak turbidity and the daily maximum were found to be linearly correlated with the total precipitation depth for all sampling sites, while they were not correlated with either the average or the peak rainfall intensity. Although a power law can also describe their correlation, it is not statistically better than the linear relation, and the exponent varied between 0.6 and 1.6.

Turbidity averaged over the entire runoff period, however, did not seem to be correlated with any precipitation statistics.

With the time series of turbidity, it is possible to estimate the total load of fine sediments discharging into receiving waters. Since the hydrography of runoff was not measured in this study, the total sediment load could not be calculated. However, a surrogate of total load was estimated as the integral of the turbidity value squared with respect to time, with the observation that the series of turbidity resembles that of a typical runoff hydrograph. The surrogate total load was found to scale with the total precipitation depth following a power law relation. For three of the four sites, the exponents were close: 1.25~1.6, while it was much higher for the remaining site, equal to 3.27.

The reconstruction of the turbidity response function and the observed statistical correlations suggest that it is possible to develop models to predict the daily maximum turbidity and the total turbidity load of effluent from construction site for designed storm events. Models of this type are valuable for future BMP managements of WisDOT construction projects as well as for the U.S. EPA to evaluate new regulation policies.

References

Battelle. (1999) Test/QA Plan for Verification of On-Line Turbidimeters . In *Environmental Technology Verification Program Advanced Monitoring Systems Pilot*.

Campbell Scientific, Inc. (2014) OBS-3+ and OBS300 Suspended Solids and Turbidity Monitors. *Instruction Manual*.

Daniel, T. C., McGuire, P.E., Stoffel, D. and Miller, B. (1979) Sediment and Nutrient Yield from Residential Construction Sites. *Journal of Environmental Quality,* **8(3):** 304-308.

Daphne, L. H. X., Utomo, H. D., and Kenneth, L. Z. H. (2011). Correlation between turbidity and total suspended solids in Singapore rivers. *Journal of Water Sustainability*, 1(3): 313-322.

Downing, J. (2008) Turbidity calibration of OBS sensors. App. *Note Code: 2Q-Z, Campbell Scientific*

EPA. (2009) 40 CFR Part 141 Expedited Approval of Alternative Test Procedures for the Analysis of Contaminants Under the Safe Drinking Water Act; Analysis and Sampling Procedures (Final rule). *Federal Register* **Volume 74**, **Number 147**. http://www.gpo.gov/fdsys/pkg/FR-2009-08-03/html/E9-18361.htm

EPA. (2012) *Water: Monitoring and Assessment*: 5.5 Turbidity http://water.epa.gov/type/rsl/monitoring/vms55.cfm.

EPA. (2012) *Water: Monitoring and Assessment*: 5.8 Total Solids. http://water.epa.gov/type/rsl/monitoring/vms58.cfm.

Hannouche, A., Chebbo, G., Ruban, G., Tassin, B., Lemaire, B. J., and Joannis, C. (2011) Relationship between turbidity and total suspended solids concentration within a combined sewer system. *Water Science Technology*, 64(12):2445-52. Doi: 10.2166/wst.2011.779

Harbor, J.M., Snyder, J., and Storer, J. (1995) Reducing nonpoint source pollution from construction sites using rapid seeding and mulching. *Physical Geography*, **16(5):**371-378.

Hayes, S.A., McLaughlin, R.A., Osmond, D.L. (2005). Polyacrylamide use for erosion and turbidity control on construction sites. *Journal of Soil and Water Conservation* 60:193-199.

Holliday, C.P., Rasmussen, T.C. (2003) Establishing the relationship between turbidity and total suspended sediment concentration. *Georgia Water Resources Conference. Athens, GA: Georgia Water Center Publications*.

Jastram, J. D., Zipper, C. E., Zelazny, L. W., and Hyer, K. E. (2009) Increasing precision of turbidity-based suspended sediment concentration and load estimates. *Journal of Environmental Quality*, **39:** 1306-1326.

Magruder C., Waldmer, E., and Wardius K. (2006) Honey Creek Bacteria Investigation Survey, July-August, 2006. *Milwaukee Metropolitan Sewage District (MMSD) Technical Report*, 06-092

McFalls, J. Yi, Y.J., Storey, B. Barrett, M., Lawler, D., Eck B. Rounce, D., Cleveland, T. Murphy, H., Dalton, D., Morse, A., Herrmann, G. (2014) Performance testing of coagulants to reduce stormwater runoff turbidity. *TxDOT Project 0-6638, Final Report*.

McLaughlin, R. (2002). Measures to Reduce Erosion and Turbidity in Construction Site Runoff. *Technical Report*. Washington, D.C.: U.S. Department of Transportation.

McLaughlin, R.A., Bartholomew, N., (2007). Soil factors influencing suspended sediment flocculation by polyacrylamide. *Soil Science Society of America Journal* 71:537-544.

McLaughlin, R. and Jennings. G.(2007) Minimizing Water Quality Impacts of Road Construction Projects. *Technical Report*. Raleigh, NC: North Carolina State University.

Memon, S., Paule, M. C., Lee, B. Y., Umer, R., Sukhbaatar, C., & Lee, C. H. (2015). Investigation of turbidity and suspended solids behavior in storm water run-off from different land-use sites in South Korea. *Desalination and Water Treatment*, 53(11): 3088-3095.

NCHRP (2012) Turbidity reduction and monitoring strategies for highway construction projects. *NCHRP Project 25-25(74) Final Report*.

O'Dell, J. W. (Ed.). (1993) *Method 180.1 Determination of Turbidity by Nephelometry (Rev 2.0.)*. Cincinnati, OH: USEPA.

Ohio Environmental Protection Agency (Ohio EPA). (1998a) Biological and Water Quality Study of Blacklick Creek and Selected Tributaries. *Ohio EPA Technical Report MAS/1997-12-7*.

Ohio Environmental Protection Agency (Ohio EPA) (1998b) Biological and Water Quality Study of Little Beaver Creek and Big Beaver Creek - 1997. *Ohio EPA Technical Report MAS/1998-5-1*.

Ohio Environmental Protection Agency (Ohio EPA) (1999) Biological and Water Quality Study of the Cuyahoga River and Selected Tributaries. *Ohio EPA Technical Report MAS/1997-12-4*.

Rasmussen, P.P., Gray, J.R., (2009) Guidelines and procedures for computing time-series suspended-sediment concentrations and loads from in-stream turbidity-sensor and stream flow data. Reston, VA. Geological Survey.

Rounce, D.R., Lawler, D. F., and Barrett, M. E. (2012). Reducing turbidity of construction site runoff via coagulation with polyacrylamide and chitosan. *Project Report*. University of Texas at Austin.

Perkins, R. Hansen, B., Wilson, B., and Gulliever J. (2014) Development and evaluation of effective turbidity monitoring methods for construction projects. *Minnesota department of transportation Final Project Report 2014-24*.

Reed, L. A. (1980) Suspended-Sediment Discharge, in Five Streams near Harrisburg, Pennsylvania, Before, During, and After Highway Construction. *Geological Survey Water-Supply Paper* 2072.

Ross, C. W., Sojka, R.E., and Foerster, J.A. (2003) Scanning electron micrographs of polyacrylamide-treated soil in irrigation furrows. Journal of Soil and Water Conservation. 58(5): 327-331

Sadar, M. (2005) Introduction to Laser Nephelometry: An Alternative to Conventional Particulate Analysis Methods. Hach Company. Loveland, CO.

Sawyer, C. B. (2009) Characterization of *Escherichia coli* Related to Construction Site Sediment Basins. *Ph.D. Thesis, Clemson University*.

Sojka, R.E., and Lentz, R. D. (1997) Reducing furrow irrigation erosion with polyacrylamide (PAM). *Journal of Production Agriculture* , 10:1-2, 47-52.

Susfalk, R. B., Fitzgeradl, B., and Knust, A. M. (2008) Characterization of turbidity and total suspended solids in the Upper Carson River, Nevada, *Project report, Nevada Division of Environmental Protection Contract Award #DEP 04-039*.

Trempel, E. A. (2011) Fate and Transport of *Escherichia coli* Within Sediment Basins on Active Construction Sites. *M.S. Thesis, Clemson University*.

USEPA (2004) Development Document for Final Action for Effluent Guidelines and Standards for the Construction and Development Category. *EPA-821-B-04-001*.

USEPA (1999) Standard operating procedure for the analysis of residue, non-filterable (suspended solids), water, method 160.2 NS (Gravimetric, 103-105oC)

Vice, R.B., Guy, H.P., and Ferguson, G.E., (1969) Sediment Movement in an Area of Suburban Highway Construction, Scott Run Basin, Fairfax County, Virginia, 1961-64, *USGS Water Supply Paper,* **1591-E**: E1-E41.

Washington State Department of Ecology, (2006) How to Do Stormwater Monitoring: A guide for construction sites, Washington State Department of Ecology, March 2006, Publication # 06-1-020

Wolman, M. C., and Schick, A. P. (1967) Effects of Construction on Fluvial Sediment, Urban and Suburban Areas of Maryland. *Water Resources Research* **3(2)**: 451-464.